TRANSLATION

DYNAMIC AND FLUCTUATION ERRORS IN GUIDED VEHICLES

By

A. N. Shchukin

FOREIGN TECHNOLOGY DIVISION

AIR FORCE SYSTEMS COMMAND

WRIGHT-PATTERSON AIR FORCE BASE

OHIO

UNEDITED ROUGH DRAFT TRANSLATION

DYNAMIC AND FLUCTUATION ERRORS IN GUIDED VEHICLES

BY: A. N. Shchukin

English Pages: 201

S/5838

PREPARED BY:

TRANSLATION SERVICES BRANCH
FOREIGN TECHNOLOGY DIVISION
WP-AFB, OHIO.

A. N. Shohukin

DINAMICHESKIYE I FLYUKTUATSIONNYYE OSHIBKI UPRAVLYAYEMYKH OB"YEKTOV

Izdatel'stvo "Sovetskoye Radio"
Moskva - 1961

Pages: 1-214

FTD-TT-62-1087/1+2

TABLE OF CONTENTS

Preface 2

Introduction 3

Chapter 1. Operational Method for Solution of Linear Differential Equations 16
1. The Laplace Transformation 16
2. Properties of the Laplace Transformation 18
3. Solution of Linear Differential Equations by Means of Laplace Transformations 21

Chapter 2. The Spectral Method of Analyzing Processes in Linear Systems 29
1. The Fourier Transformation. Spectra of Functions. Spectral Distributions of Signal Energy 29
2. Passage of Harmonic Waveforms Through Linear Systems. Amplitude and Phase Curves. Equivalent Frequency Bandwidth 40

Chapter 3. Circuits with Feedback 47

Chapter 4. The Guided Missile as a Loop with Feedback 52
1. General Considerations 52
2. The Control Function $\varphi_{vkh}(t)$ 58
3. Transfer Function $Y(p)$ 65
4. Other Types of Equivalent Closed-Loop Control Diagram 81

Chapter 5. Form of Control Functions and Dynamic Errors for Various Control Methods 89
1. Motion of Missile in Response to Commands 89
2. Homing Guidance 102

Chapter 6. Errors Due to Discontinuous Information 127

Chapter 7. Fluctuation Noise and its Effect Upon Errors in Determining Coordinates of an Object 135

Chapter 8. Fluctuation Errors in Bearing Determination . . . 145
1. Area-Comparison Method 145
2. The Equisignal Method 155
3. Phase Method of Bearing Determination 157

Chapter 9. Fluctuation-Noise Errors in Ranging 163

1. Pulse Method 163
2. Continuous-Wave Method 163

Chapter 10. Probable Values of Coordinates, Velocities, and Accelerations 167
1. Probable Values of Object Coordinates in the Presence of Fluctuation Noise 167
2. Fluctuation Errors in Determining Velocity and Acceleration 172

Chapter 11. Errors Due to Signal Fluctuations 178

Chapter 12. Equivalent Control-Loop Bandwidth 188

Appendix 1 194

Appendix 2 194

References 199

The book "Dynamic and Fluctuation Errors in Guided Vehicles," as the name indicates, deals with the determination of the physical nature, character, and magnitude of deviation of guided vehicles from idealized motion trajectories expected on the basis of design considerations.

The guided objects, together with the complex of devices used to control them, are in this case considered as unified systems possessing a limited number of parameters that characterize error magnitudes under various conditions of object motion. The book aims to give an approximate qualitative evaluation of the basic factors affecting the accuracy of guided objects. At the same time, the book presents in the simplest and clearest possible form the basic physical processes occurring in systems containing controlled members.

The book is designed for readers who are engineers or students with a broad technical background, acquainted with higher mathematics and the fundamentals of theoretical mechanics. To simplify studying, the first portion of the book presents briefly the mathematical apparatus used in the subsequent sections.

PREFACE

This book represents a formalization of many notes and examples produced by the author while becoming acquainted with a field new to him. The chief aim of the author was to cover the behavior of a guided device as a whole, without going into detail, and at the same time, to arrive at numerical results, even though very approximate.

Without doubt, the process of mastering any new field of knowledge is a highly individual one, and what is "intelligible" to one may be unclear or unnecessarily confusing for another. Nonetheless, the author hopes that this book may prove useful to the reader who has a general engineering background, and who wishes to gain an idea of the fundamentals of guided-vehicle behavior, without delving into the special theoretical or descriptive scientific or engineering literature.

At the end of the book, we have given a brief list of references that have been used by the author, and which he recommends to the reader who wishes to become better acquainted with various aspects of the problems touched upon in the book.

The author wishes to express his deep gratitude to his comrades who have taken the trouble to become acquainted with the manuscript, and who have made several valuable suggestions and comments.

INTRODUCTION

Under actual conditions, it is never possible to direct a guided missile to a given point with perfect accuracy. A whole group of factors cause the guided missile to stray from the target. These deviations may be classified into two categories in accordance with the factors responsible for them.

The first category includes deviations, or errors, due to the fact that the missile carries out the commands given inaccurately and, in particular, with a finite lapse of time. These deviations occur since the missile itself and the various types of devices included in the control facilities of the unit possess inertia, and react with a delay to the necessary changes in missile motion condition; deviations of this type are called dynamic deviations or errors.

The second category includes deviations caused by the fact that the commands themselves are processed inaccurately with errors caused by the presence of noise in the information on motion of target and missile, and in the transmission of the instructions. Owing to random noise of irregular nature, these deviations and errors are called fluctuation deviations or errors.

As in the case of any other classification, the separation of errors into dynamic and fluctuation errors is to some degree arbitrary. In actuality, these deviations, as well as the factors causing them, are intimately connected, and interact with each other. For the analysis of the processes occurring in the motion of guided vehicles, however, this classification is extremely useful, since it permits

a deeper understanding of these processes, and a better control over them, if we have available information as to the minimum resultant total error, containing, dynamic and fluctuation portions.

If we were able to determine the magnitude of the dynamic and fluctuation deviations for each instant of time, and to introduce appropriate corrections to the trajectory along which the missile actually moves, a so-called "kinematic trajectory" would be obtained. Thus, the kinematic trajectory takes the form of a curve along which the missile would move if there were no random fluctuation noise in the determination of the position and motion of target and missile, there were no response delays in the missile or in the entire set of devices used to develop and execute the control commands.

In addition to the kinematic trajectory, it is also possible to construct the dynamic trajectory, which takes the form of the curve along which the missile would move if an allowance were made for the effect of response delay in the entire system, but in the absence of noise causing fluctuation deviations.

The distance between points on the kinematic and dynamic trajectories corresponding to precisely the same time instants will give the magnitude of the dynamic deviations or errors. The dynamic error at the instant that corresponds to the intersection of the kinematic trajectory and the target gives the magnitude of the dynamic component involved in the miss.

The distance between points on the dynamic and actual trajectories corresponding to precisely the same time instants will give the magnitude of the fluctuation deviations or errors and, at the instant that corresponds to the intersection of the kinematic trajectory and the target, determines the fluctuation component of the miss.

While the cause or source of dynamic errors is the lagging response of the missile and all links entering into the control system, the source of fluctuation errors is primarily interference of the noise type, appearing in electrical resistances, electronic devices, and other electrical circuit elements that are superposed upon the useful signals that supply information as to target and missile

motion, and upon the control signals. In addition to noise-type fluctuation disturbances that appear in the receiving devices themselves, there is also fluctuation noise due to variation in the signals created by the objects themselves – the target and the missile.

The characteristics of the dynamic and fluctuation errors will also differ in accordance with the various factors giving rise to them.

The sign of the dynamic error is determined by the type of kinematic trajectory, since the dynamic error itself is caused by a response delay of the missile and the entire control system in reacting to changes in motion conditions. The flatter the kinematic trajectory, and the lower the speed of the missile, the smaller the dynamic errors will be.

A characteristic feature of fluctuation errors is the randomness of the deviations created by them. Thus, in the absence of systematic errors, the deflection from the target due to the fluctuation error may with identical probability lie to the right or left of the target or above or below it.

The response characteristics of a system containing a guided missile will affect the magnitude of the dynamic and fluctuation errors in various ways.

The faster the system response, the less will be the magnitude of the dynamic errors appearing in this system, but the more sharply and rapidly the missile will react to random fluctuation perturbations.

And, conversely, the better random perturbations are smoothed out in the system, the greater the delay in missile reaction to control commands, and the larger the dynamic errors.

The need to reconcile these opposing effects leads to the fact that the freedom to choose the parameters determining system response

characteristics will normally be curtailed. In addition, the need for providing stability of the entire system as a whole, as well as for its individual elements, has a great effect upon the choice of system parameters.

It would be extremely undesirable if the missile were to perform damping oscillations about its new direction of motion when it changed this direction under the influence of an applied command. And it is also completely inadmissible for conditions to appear such that the delay in reaction of the object to control commands would lead to oscillation and to a loss of motion stability along the trajectory. Thus, it is normally not possible to vary system parameters over broad limits in order to decrease dynamic or fluctuation errors.

To some extent, a decrease in the dynamic errors can be attained by proper choice of the control function that connects the target motion with the missile position and its velocity vector at corresponding instants of time, and determines the kinematic trajectory of motion for the missile.

Any modern automatic guided vehicle is a complex chain of elements that are linked together. These elements are of very different types. Here we will have: the moving object itself, interacting during the process of movement with the ambient medium, electrical, hydraulic, or pneumatic controls for the object's direction of motion, consisting of electromechanical systems, gyroscope instruments, electronic equipment on board the missile serving to receive information as to target motion and processing the commands, electrical and mechanical elements serving for automatic target tracking, etc. Sometimes, all of the control-system elements are concentrated on board the missile: for example, where the missile homes on the target

with the aid of a radar, infrared, or other device that tracks the target, or where the missile moves independently in accordance with a predetermined program. In other cases, a portion of the complex is not associated with the moving object. This portion obtains information as to target and missile coordinates, or the position of one of these, processes this information, and transmits commands to the missile in accordance with the control function used for the given complex.

In all cases, it is characteristic of automatic missile-movement control that signals originating in the instantaneous positions of the moving missile and target pass through the entire chain of elements forming the complex, and are converted from electrical into mechanical information and back again.

For example, where an antiaircraft missile is guided to an aerial target with the aid of ground radar equipment, this equipment measures the target and missile coordinates, and determines their relative position. Using this data as a basis, the ground apparatus processes and transmits to the missile commands intended to cause the missile to move in a kinematic trajectory, of which we have spoken previously. The commands, when received aboard the missile, are transformed into control signals, and act upon the control surfaces of the missile, which assumes a new position with respect to the target. This position serves as a source that causes new commands to appear at the ground, new control signals on board the missile, etc.

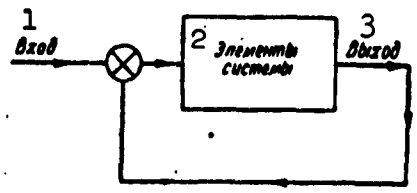

Fig. 1. 1) Input; 2) system elements; 3) output.

When a missile is homing on a target, in many cases the control commands are processed as a function of the angle formed by the axis of the missile and the target bearing.

Systems are also possible in which the control commands are developed solely from the motion of the target, observations of the missile's position are made only at intervals, and additional commands are given only if the missile has deviated from its proper kinematic trajectory.

Despite the well-known variety of principles underlying the construction of systems consisting of a missile and facilities for automatic control of its movement, the diagram shown in Fig. 1 is basic for such systems.

Other versions of this arrangement will be examined in the future; here we shall examine the arrangement of Fig. 1 in somewhat greater detail, since it permits a very clear idea to be gained as to the processes occurring in the circuits of automatically guided missiles, and an understanding of the basic relationships of the phenomena that occur here.

To the input of the two-port of Fig. 1 are applied time-varying values of the differences in the actual linear or angular coordinates of the missile, and the values that these coordinates should have if the missile were moving along the kinematic trajectory. At the output of the two-port there appear missile coordinates, also time-varying obtained as a result of the effect of commands produced in accordance with the coordinate differences for the actual and kinematic trajectories. The new missile coordinate values are again compared with the corresponding kinematic-trajectory coordinates, and the difference in these values is applied to the input of the two-port, etc.

Such a system, shown conventionally in Fig. 1, is called an automatic control system with feedback. For example, in the simplest case of homing, where the control function requires that the missile axis coincide with the target bearing, at the output of the two-port that represents the missile and the complex of instruments found aboard it, there is produced an angle that characterizes the direction of the missile axis. At the input to the two-port, there appear simultaneously the angles characterizing the target bearing and the direction of the missile axis. The difference in these angles, i.e.,

the magnitude of the angle between the missile axis and the target bearing are applied to the input of the two-port in the form of electrical or other magnitudes; here, depending upon the magnitude and sign of the difference, control commands are developed that tend to reduce this difference to zero, i.e., to direct the missile axis toward the target.

Disturbances that create random irregular deviations of the object from the mean motion path may be considered to be random fluctuations in the magnitude of the coordinate differences between corresponding points on the kinematic trajectory and the object coordinates caused by the fact that in the presence of disturbances, the target and object coordinates are not determined accurately.

In order to give a mathematical formulation to the processes occurring in the system shown in Fig. 1, and to find the magnitude by which the coordinates of the actual path deviate from those of the kinematic trajectory, it is first necessary to have the equation of the kinematic trajectory itself and, second, to find the relationship between the coordinates of the actual trajectory and the "control function" $\varphi_{vkh}(t)$, which is the difference between the corresponding points on the kinematic and actual trajectories. This portion of the problem amounts to determining the reaction of the complex of system elements to the magnitude of the coordinate differences for the kinematic and actual trajectories at the input.

In order to determine how the entire complex will react to the control function appearing at its input, it is necessary to find mathematical expressions that connect the magnitudes at the input of each system element with the magnitudes at the output of this element, and to consider in turn all elements forming the guided-missile system. The straightforward direct method of analyzing such

a system consists in formulating the relationship among the quantities at the input and the output of the individual elements forming the system in the form of differential equations.

In the general case, these equations may be either linear or nonlinear with constant or variable multipliers. The differential equations taken in turn for all elements of the complex form a system of equations that must be solved in order to find the instantaneous value of the coordinate differences between the kinematic and actual trajectories of the object.

Thus, the direct method of analysis for guided-missile systems consists in setting up and solving a large number of differential equations.

Even the simplest guided vehicles contain more than ten different series-connected links in the system or, so to speak, in the control loop. Thus, the mathematical-analysis problem reduces to solving a system of ten-fifteen or even more differential equations.

Despite the promising possibilities of numerical integration of high-order equations made available by the development of mathematical computers, there is a need for simpler approximation methods that would permit analysis of the behavior of such complicated complexes as guided missiles without requiring that we solve each time an entire group of differential equations. With such an approximate analysis, the actual system whose behavior is described by the system of many differential equations, would be replaced by a considerably simpler equivalent diagram described by low-order differential equations; here the basic features of the behavior of the real and equivalent systems should approach each other both qualitatively and quantitatively.

Naturally, in the general case it is impossible to demonstrate

that it is possible to replace systems of eighth-tenth order differential equations by second-order equations. Several considerations, however, indicate that for an actual guided-missile system, despite the whole complicated set of elements entering into the system, such a substitution is possible. There is the following support for this possibility.

Numerous links entering into the guided missile and the elements serving to stabilize it and to move it in the given direction, to a considerable degree operate in widely separated portions of the frequency spectrum. In view of the fact that these links are series-connected in the system so as to form a closed control loop, it is natural that the high-frequency signals used, for example, in such elements as the target-detection radars, radio-control command links, exactly as in the case of signals with frequencies corresponding to sections of the system that operate in the pulse mode, are filtered out, and have no effect on the behavior of such system elements with long time constants as the missile itself, its controls, mechanical automatic-tracking systems, etc.

As a result, in examining the entire set of guided-missile elements as a single entity, it is possible to avoid considering those equations and those portions of the spectrum that correspond to these high-frequency elements. This simplification permits a considerable decrease in the number of equations that characterize system behavior. Thus, although in designing and constructing systems it is necessary to consider all links, in analyzing the behavior as a whole it is possible to consider only the low-frequency elements.

The second argument in favor of the possibility of replacing an actual system described by high-order equations by a considerably simpler equivalent system consists in the fact that motion of the

missile in any real system suitable for practical purposes depends solely upon the coordinates themselves and their first and second derivatives. It is impossible to imagine a system in which the missile would react in the same way to changes in acceleration as to the acceleration itself or to the velocity. This follows from the need to provide for system operation under conditions of natural fluctuation disturbances and perturbations. If system reaction to the higher-order derivatives of input magnitudes were considerable, the system, including the missile, would be subject to sharp shocks in the presence of fluctuations having large values of the high-order derivatives, which would forbid the practical application of such a system.

The third argument consists in the fact that the input magnitudes themselves that affect the functioning of the entire complex take the form of functions that vary slowly and smoothly in time, and for which the higher-order derivatives are negligible.

This also makes it possible for us to confine ourselves to low-order differential equations, and in particular second-order equations, in describing mathematically the behavior of the entire set of elements forming the closed missile control loop.

The possibility of such a simplified representation of the missile closed control loop is presupposed by us in the following discussion. As far as the equivalent-loop parameters are concerned, i.e., the values of the numerical coefficients in the corresponding simplified differential equations, in the course of the discussion we shall give one possible method for determining them from experimental data resulting from tests of the system as a whole.

The following statements are basic for our handling of the problem of determining the magnitude of guided-missile dynamic

errors appearing owing to the finite response time of elements forming the control loop:

1. The dynamic errors are completely determined by the parameters of the missile kinematic trajectory and the response of the missile itself and the control-loop elements.

2. The behavior of the guided missile can be described by a system of linear differential equations covering all links in the control loop.

3. The system of linear differential equations that characterize the properties of the missile control loop can be simplified substantially and replaced by no worse than a second-order equation with coefficients chosen on the basis of experimental data. In many cases, the solution to the complete system of equations can be simplified if we confine ourselves solely to the steady motion of the missile along the path after perturbations due to transient processes have died out.

In order to determine the magnitude of random fluctuation errors, we shall assume that these errors are due to inaccurate determination of data on the motion parameters of target and missile, owing to the fact that these data are observed against a background of random noise.

The noise sources are the measurement and receiving equipment, the properties of the medium in which the electromagnetic or acoustical signals propagate, and the properties of the moving target.

One of the most important factors limiting the accuracy with which coordinates are determined by radio methods is fluctuation noise. The accuracy of coordinate determination depends also upon instrumental errors, and upon the curvature of the radio wave propagation paths. We shall not dwell upon these error sources, however,

but shall concentrate our attention precisely upon the errors due to fluctuation phenomena.

In additional to thermal noise caused by fluctuations of charges in resistances and nonuniformities of electron current in radio tubes and semiconductor devices, signal fluctuations can also cause errors in coordinate measurements. Such fluctuations occur either as a result of the nonconstant emission or reflection of signals by the object whose coordinates are being measured, or owing to random irregular variations in propagation conditions.

Numerous investigations in the field of fluctuation processes and their mathematical analysis at present permit a quite accurate evaluation of measurement error due to fluctuations, and indicate possible ways of constructing circuits that are the most efficient from the point of view of decreasing fluctuation errors. The rigorous analysis method, however, frequently requires the application of a quite complicated and cumbersome mathematical apparatus. In addition, the results of rigorous and accurate calculations differ from the results yielded by an approximate but far simpler analysis by amounts that are of no great importance in engineering design, or in the analysis of experimental data. Thus, we shall henceforth discuss a simplified analysis of the effect of fundamental factors upon the magnitude of fluctuation errors, on the basis of the physics of the phenomena occurring here, and we shall derive approximate, quite simple mathematical functions associating the accuracy of coordinate determination with the fluctuation energy, signal energy, and characteristics of the radio devices.

In view of the fact that to determine coordinates with practically acceptable accuracy it is necessary to have a useful-signal strength considerably greater than the mean fluctuation-noise level,

we shall consider precisely this case in the following discussion. The very interesting and complicated problem of determining the existence or absence of a weak signal against a fluctuation-noise background, i.e., the problem of initial detection, shall not be touched upon here.

In analyzing the factors that affect dynamic errors in determining their magnitude, we shall henceforth employ the operational method of differential-equation solution based upon the Laplace transformation.

The analysis of problems associated with a determination of the effect of fluctuations upon the magnitude of random errors for guided missiles will be based upon an examination of the spectrum of oscillations entering into the disturbance and the useful signal, and the frequency responses of the missile control loop. Methods of spectral or frequency analysis of processes in the loops will be based upon the use of the Fourier transformation. Despite the fact that the analysis of system behavior, where the system is described by linear differential equations, by means of operators and frequency methods based upon the Laplace and Fourier transformations is well known, and that these problems are dealt with in many places in the literature, we shall give a brief presentation of the basic concepts of both methods.

This is done in order to make it possible in what is to follow to refer to individual formulas and statements without forcing the reader to refer to other sources.

Manuscript Page No.

[List of Transliterated Symbols]

9 BX = vkh = vkhodnoy = input

Chapter 1

OPERATIONAL METHOD FOR SOLUTION OF LINEAR DIFFERENTIAL EQUATIONS

1. THE LAPLACE TRANSFORMATION

The operational method for solution of linear differential equations is based upon the so-called Laplace transformation. To each sectionally smooth function $\varphi(t)$ (considered only for positive times $t \geq 0$), which we call the "original," there is a Laplace "transform" $L|\varphi(t)| = F(p)$, which is the integral

$$L|\varphi(t)| = F(p) = \int_0^\infty \varphi(t) e^{-pt} dt, \tag{1}$$

where $\underline{p}$ is a complex number $\alpha + j\omega$, called the "operator," whence the name of the method.

The Laplace transformation is single-valued, i.e., for any "original" there is only one "transform," while for any "transform" there is only one "original."

We give the following examples of the Laplace transformation:

Step function

Let a function $\varphi(t)$ satisfy the condition (Fig. 2)

$$\varphi(t) = 0 \text{ for } t < 0,$$
$$\varphi(t) = A \text{ for } t > 0,$$

then

$$L|\varphi(t)| = F(p) = A\int_0^\infty e^{-pt} dt = \frac{A}{p}, \tag{2}$$

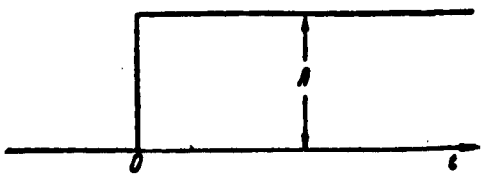

Fig. 2

or $e^{-pt} \to 0$ when $t \to \infty$.

If $A = 1$, then

$$F(p) = \frac{1}{p}.$$

Harmonic functions

$\varphi(t) = \sin \Omega t$ in the region $t > 0$.

$$\sin \Omega t = \frac{e^{j\Omega t} - e^{-j\Omega t}}{2j}.$$

Consequently

$$L[\sin \Omega t] = F(p) = \frac{1}{2j}\left[\int_0^\infty e^{-(p-j\Omega)t}\,dt - \int_0^\infty e^{-(p+j\Omega)t}\,dt\right] =$$

$$= \frac{1}{2j}\left[\frac{1}{p-j\Omega} - \frac{1}{p+j\Omega}\right] = \frac{\Omega}{p^2+\Omega^2}. \qquad (3)$$

$\varphi(t) = \cos \Omega t$ in the region $t > 0$.

$$\cos \Omega t = \frac{e^{j\Omega t} + e^{-j\Omega t}}{2},$$

thus

$$L[\cos \Omega t] = F(p) = \frac{1}{2}\left[\int_0^\infty e^{-(p-j\Omega)t}\,dt + \int_0^\infty e^{-(p+j\Omega)t}\,dt\right] =$$

$$= \frac{1}{2}\left[\frac{1}{p+j\Omega} + \frac{1}{p-j\Omega}\right] = \frac{p}{p^2+\Omega^2}. \qquad (4) \qquad (4)$$

Linearly increasing variable

$\varphi(t) = Ct$ in the region $t > 0$.

$$L[Ct] = F(p) = C\int_0^\infty t e^{-pt}\,dt = \frac{C}{p}\left[-te^{-pt}\right]_0^\infty +$$

$$+ \frac{C}{p}\int_0^\infty e^{-pt}\,dt = \frac{C}{p^2}. \qquad (5)$$

The exponential function $\varphi(t) = e^{\beta t}$ (for $\beta < \alpha$).

$$L\left|e^{\beta t}\right| = F(p) = \int_0^{\infty} e^{-(p-\beta)t}\,dt = \frac{1}{p-\beta}. \qquad (6)$$

Tables of Laplace "transforms" for various functions with "originals" more complicated than those shown above are given in special handbooks.* Appendix I of this book shows some of the most frequently encountered varieties.

2. PROPERTIES OF THE LAPLACE TRANSFORMATION

It follows from the definition of the Laplace transformation (1) that it is a linear transformation. When the "original" is multiplied by a constant, the transform is multiplied by the same factor, i.e., if

$$\varphi_1(t) = C\varphi(t), \text{ where } C = \text{const}$$

and

$$L\left|\varphi(t)\right| = F(p) = \int_0^{\infty} \varphi(t)\,e^{-pt}\,dt,$$

then

$$L\left|C\varphi(t)\right| = F_1(p) = \int_0^{\infty} \varphi_1(t)\,e^{-pt}\,dt = CF(p). \qquad (7)$$

The transform of a sum of originals is the sum of their transforms.

If

$$L\left|\varphi_1(t)\right| = F_1(p) \text{ и } L\left|\varphi_2(t)\right| = F_2(p),$$

then

$$L\left|\varphi_1(t) + \varphi_2(t)\right| = \int_0^{\infty} \left[\varphi_1(t) + \varphi_2(t)\right] e^{-pt}\,dt = F_1(p) + F_2(p). \qquad (8)$$

The transform of a derivative

If F(p) is the transform of an original $\varphi(t)$, then

$$L\left|\frac{d\varphi}{dt}\right| = \int_0^{\infty} \frac{d\varphi}{dt}\,e^{-pt}\,dt = \left|\varphi(t)\,e^{-pt}\right|_0^{\infty} + p\int_0^{\infty} \varphi(t)\,e^{-pt}\,dt =$$

$$= -\varphi(+0) + pF(p). \qquad (9)$$

The notation $\varphi(+0)$ indicates that the value of the function should be taken infinitely close to zero on the side of the positive t.

Reasoning similar to that shown above indicates that the transform of a second derivative $d^2\varphi/dt^2$ is equal to

$$L\left|\frac{d^2\varphi}{dt^2}\right| = pL\left|\frac{d\varphi}{dt}\right| - \frac{d\varphi(+0)}{dt} = p^2 L|\varphi(t)| - p\varphi(+0) - \frac{d\varphi(+0)}{dt}. \qquad (10)$$

The transform of an integral

$$L\left|\int\varphi(t)\,dt\right| = \frac{1}{p}L|\varphi(t)| + \frac{1}{p}\int_{\text{for } t=0}\varphi(t)\,dt = \frac{F(p)}{p} + \frac{1}{p}\int_{t=0}\varphi(t)\,dt, \qquad (11)$$

where $F(p) = L\,|\varphi(t)|$.

The validity of Formula (11) can be demonstrated by means of the formula

$$\int u\,dv = uv - \int v\,du,$$

where $u = e^{-pt}$, $dv = \varphi(t)\,dt$.

Then

$$L|\varphi(t)| = \int_0^\infty \varphi(t)e^{-pt}\,dt = \left|e^{-pt}\int\varphi(t)\,dt\right|_0^\infty + p\int_0^\infty\left[\int\varphi(t)\,dt\right]e^{-pt}\,dt = -\int_{t=0}\varphi(t)dt + pL\left|\int\varphi(t)\,dt\right|,$$

whence follows Formula (11).

Similarly, we find that a double integral has the transform

$$L\left|\int\int|\varphi(t)\,dt|\,dt\right| = \frac{F(p)}{p^2} + \frac{1}{p^2}\int_{\text{for } t=0}\varphi(t)\,dt + \frac{1}{p}\int_{\text{for } t=0}dt\int\varphi(dt)\,dt. \qquad (12)$$

Limits

If $F(p) = L\,|\varphi(t)|$ is the transform of a function $\varphi(t)$ that approaches a limit as $t \to \infty$, this limit may be found as

$$\lim_{t\to\infty}\varphi(t) = \lim_{p\to 0} pF(p). \qquad (13)$$

By the definition of the Laplace transformation, for a derivative

$$L\left|\frac{d\varphi(t)}{dt}\right| = \int_0^\infty \frac{d\varphi(t)}{dt}e^{-pt}\,dt = pF(p) - \varphi(+0).$$

when $p \to 0$, e^{-pt} approaches 1. Consequently

$$\int_0^\infty \frac{d\varphi(t)}{dt}\,dt = \lim_{p\to 0}[pF(p) - \varphi(+0)].$$

Rewriting this equation as

$$\lim_{t\to\infty}\int_0^t \varphi'(\tau)\,d\tau = \lim_{t\to\infty}[\varphi(t) - \varphi\ +0)] =$$
$$= \lim_{p\to 0}[pF(p) - \varphi(+0)],$$

we are led to Formula (13).

Formula (13) permits us to find the limit of a function $\varphi(t)$ from its transform without complete evaluation of the function.

For example, if the transform of a function $\varphi(t)$ is

$$F(p) = \frac{1}{p[(p+\alpha)^2 + \omega^2]},$$

the value of $\lim_{t\to\infty}\varphi(t)$, by (13), will be

$$\lim_{t\to\infty}\varphi(t) = \lim_{p\to 0} pF(p) = \frac{p}{p[(p+\alpha)^2 + \omega^2]}\Big|_{p\to 0} = \frac{1}{\alpha^2 + \omega^2}.$$

The validity of this expression may be demonstrated by finding the complete original of the transform

$$F(p) = \frac{1}{p[(p+a)^2 + \omega^2]},$$

in Table 2 of the Appendix and setting $t \to \infty$ in the original.

Initial value

If $F(p) = L\,|\varphi(t)|$ is the transform of a function $\varphi(t)$ that has a finite initial value at $t = 0$, this initial value may be found as

$$\lim_{t \to 0} \varphi(t) = \lim_{p \to \infty} pF(p). \qquad (14)$$

From the definition of the transform of a derivative (9) it follows that

$$\lim_{p \to \infty} L\left|\frac{d\varphi(t)}{dt}\right| = \lim_{p \to \infty} \int_0^\infty \frac{d\varphi(t)}{dt} e^{-pt}\,dt =$$

$$= \lim_{p \to \infty} [pF(p) - \varphi(+0)].$$

If the derivative is finite, $e^{-pt} \underset{p \to \infty}{\to} 0$ at any finite time t. Consequently, the left side of the equation is equal to zero or

$$\lim_{p \to \infty} [pF(p) - \varphi(+0)] = 0.$$

whence follows Formula (14).

3. SOLUTION OF LINEAR DIFFERENTIAL EQUATIONS BY MEANS OF LAPLACE TRANSFORMATIONS

Consider an element of any mechanical, electrical or hybrid system at whose input a time-varying external force (in the case of a mechanical system) or voltage (in the case of an electrical system) $\varphi_{vkh}(t)$ is applied. At the output of the element, the applied force results in a mechanical force, displacement, current, voltage, or some other magnitude $\varphi_{vykh}(t)$, that also varies with time (Fig. 3). In this case, a mechanical force at the input may result in an electrical voltage at the output, or, conversely, an electnical voltage at the input may result in a mechanical force or displacement at the output, and

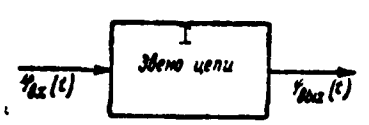

Fig. 3. 1) Circuit element.

so forth.

When the circuit element under discussion consists of linear elements only, the connection between the input variable $\varphi_{vkh}(t)$ and the output variable $\varphi_{vykh}(t)$ can, in the general case, be expressed as a differential equation

$$a_n \frac{d^n \varphi_{вых}}{dt^n} + a_{n-1} \frac{d^{n-1} \varphi_{вых}}{dt^{n-1}} + \ldots . a_0 \varphi_{вых} =$$

$$= b_m \frac{d^m \varphi_{вх}}{dt^m} + b_{m-1} \frac{d^{m-1} \varphi_{вх}}{dt^{m-1}} + \ldots b_0 \varphi_{вх},$$

where φ_{vykh} is an abbreviation for $\varphi_{vykh}(t)$, and, correspondingly, φ_{vkh} for $\varphi_{vkh}(t)$.

Let the circuit element be in the quiescent condition at instant t = 0; as a result, the variable $\varphi_{vykh}(t)$ and all of its derivatives are equal to zero at this time. The input variable $\varphi_{vyk}(t)$ begins to act at time t = 0, so that it and all of its derivatives will equal zero at this instant. Then, using the expressions for the Laplace transforms of functions and their derivatives [Formulas (9) and (10)], we find the transforms of the right and left sides of Equation (15)

$$(a_n p^n + a_{n-1} p^{n-1} + \ldots . a_0) L |\varphi_{вых}(t)| =$$
$$= (b_m p^m + b_{m-1} p^{m-1} + \ldots . b_0) L |\varphi_{вх}(t)|. \qquad (15)$$

or, we may write

$$Y(p) = \frac{b_m p^m + b_{m-1} p^{m-1} + \ldots . b_0}{a_n p^n + a_{n-1} p^{n-1} + \ldots . a_0}; \qquad (16)$$

$$L |\varphi_{вых}(t)| = Y(p) L |\varphi_{вх}(t)|. \qquad (17)$$

Expression (17) shows that if we know the transform of the input variable $L |\varphi_{vkh}(t)|$, we can find the transform of the output variable $L |\varphi_{vykh}(t)|$ by multiplying the transform of the input variable by a factor Y(p) that is the algebraic fraction (16) and which is called the "transfer function" of the circuit or its section.

The transfer function, as we can see from Expressions (16) and

(17) is independent of the input and output variables $\varphi_{vkh}(t)$ and $\varphi_{vykh}(t)$ and is, therefore, characteristic of the mechanical, electrical, or hybrid circuit itself.

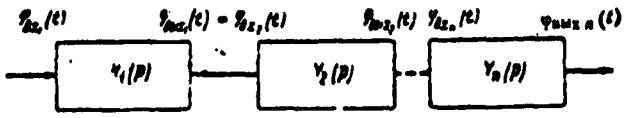

Fig. 4

When the circuit contains several sections connected in series, the transfer function for the entire circuit is the product of the transfer functions for the individual sections (Fig. 4).

Actually, by definition

$$\frac{L|\varphi_{вых1}(t)|}{L|\varphi_{вх1}(t)|} = \frac{\varphi_{вых1}(p)}{\varphi_{вх1}(p)} = Y_1(p); \frac{\varphi_{вых2}(p)}{\varphi_{вх2}(p)} = Y_2(p),$$

from which, if we substitute the value

$$\varphi_{вых1}(p) = Y_1(p)\varphi_{вх1}(p),$$

for $\varphi_{vykh1}(p)$, we find

$$\frac{\varphi_{вых2}(p)}{\varphi_{вх1}(p)} Y_{12}(p) = Y_1(p) Y_2(p).$$

In this formula, $Y_{12}(p)$ is the transfer function for sections 1 and 2, which are connected in series.

In like manner, we obtain

$$\frac{\varphi_{вых\,n}(p)}{\varphi_{вх1}(p)} = Y_{12\ldots n}(p) = Y_1(p) Y_2(p) \ldots Y_n(p). \qquad (18)$$

for the other sections.

Solution of a linear differential equation by means of a Laplace transformation consists, as is clear from what we have said, in the following.

Starting with the differential equation for the circuit under consideration we find, from Formula (16), the transfer function $Y(p)$ by substituting $p^n L\varphi(t)$ for the derivatives $d^n\varphi(t)/dt^n$ and

$L|\varphi(t)|/p^m$ for the integrals $\iint\ldots\int\varphi(t)dt^m$.

The Laplace transform of the input function $L|\varphi_{vkh}(t)|$ is found from the tables of "originals" and "transforms." The transfer functions and the transform of the output function are multiplied together, and the original of $\varphi_{vykh}(t)$ is found, by table, from their product, which is the transform of the output function $L|\varphi_{vykh}(t)|$.

We shall give several simple examples to illustrate the technique of solving linear differential equations by the method of Laplace transformations.

Example 1

Consider a very simplified – schematic – method of controlling the movement of an aircraft or rocket along its course (about the vertical axis), and let the control take the following form:

$$\frac{d^2\psi}{dt^2}+M\frac{d\psi}{dt}=-N\theta,$$

where ψ is the turn angle of the aircraft or rocket, θ is the rudder-deflection angle, M is the aerodynamic yaw constant, N is the aerodynamic efficiency of the rudder.

By (16), the transfer function of the system under discussion is given by the equation

$$Y(p)=-\frac{N}{p^2+Mp}.$$

Let us now assume that the rudder-deflection angle $\theta(t)$ abruptly changes from $\theta(t) = 0$ at $t = 0$ to $\theta(t) = \theta_0$ at $t \geq 0$. In this case, the transform of the input function $\theta(t)$ is the transform of a step function and, by (2),

$$L|\theta(t)|=\frac{\theta_0}{p};$$

the transform of the output variable which, in this case, is the turn angle for the aircraft or rocket $\psi(t)$, will be

$$L|\psi(t)| = Y(p)\,L|\theta(t)| = -\frac{\theta_0 N}{p^2(p+M)}.$$

Using the tables of originals and transforms given in Appendix 1, we find that the original of the transform L $|\psi(t)|$ is

$$\psi(t) = -\frac{N\theta_0}{M^2}(-1 + e^{-Mt} + Mt).$$

The minus sign in front of the right side indicates that the change in the turn angle $\psi(t)$ of the object occurs in a direction opposite to that of the rudder-deflection angle.

Example 2

An electromotive force u_{vkh} from a source having zero internal resistance is applied to a circuit (see Fig. 5) that consists of two tuned circuits having the same inductances L, capacitances C, and resistances r; the two circuits are inductively coupled by the mutual inductance M.

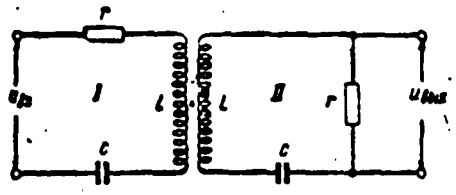

Fig. 5

We must find the output voltage u_{vykh} that appears across the terminals of resistor r in the second circuit.

We write the differential equations for the voltages in the tuned circuits I and II:

$$\text{I. } L\frac{di_1}{dt} + ri_1 + \frac{1}{C}\int i_1 dt + M\frac{di_2}{dt} = u_{вх};$$

$$\text{II. } L\frac{di_2}{dt} + ri_2 + \frac{1}{C}\int i_2 dt + M\frac{di_1}{dt} = 0.$$

We now apply the Laplace transformation to Equations I and II:

$$\text{I. } \left(Lp + r + \frac{1}{Cp}\right)\mathcal{L}|i_1(t)| + Mp\,\mathcal{L}|i_2(t)| = \mathcal{L}|u_{вх}(t)|;$$

$$\text{II. } \left(Lp + r + \frac{1}{Cp}\right)\mathcal{L}|i_2(t)| + Mp\,\mathcal{L}|i_1(t)| = 0,$$

where $\mathcal{L}|i_1(t)$ is the transform of the current i_1 in the first tuned

circuit; $\dot{L}|i_2(t)$ is the transform of the current i_2 in the second tuned circuit; and $\dot{L}|u_{vkh}(t)|$ is the transform of the applied electromotive force u_{vkh}.

Eliminating $\dot{L}|i_1(t)|$ from Equations I and II, we find

$$\mathcal{L}|i_2(t)| = -\frac{Mp\,\mathcal{L}|u_{ex}(t)|}{\left[(L+M)p + r + \frac{1}{Cp}\right]} \times$$

$$\times \frac{1}{\left[(L-M) + r + \frac{1}{Cp}\right]} = \frac{1}{2}\mathcal{L}|u_{ex}(t)| \times$$

$$\times \left\{\frac{1}{(L-M)p + r + \frac{1}{Cp}} - \frac{1}{(L+M)p + r + \frac{1}{Cp}}\right\} =$$

$$= \frac{p}{2(L-M)} \frac{\mathcal{L}|u_{ex}(t)|}{p^2 + \frac{r}{L-M}p + \frac{1}{(L-M)C}} -$$

$$- \frac{p}{2(L+M)} \frac{\mathcal{L}|u_{ex}(t)|}{p^2 + \frac{r}{L+M}p + \frac{1}{(L+M)C}}.$$

We rewrite the denominators of both terms as

$$p^2 + \frac{r}{L-M}p + \frac{1}{(L-M)C} = (p+\alpha_1)^2 + \omega_1^2;$$

$$p^2 + \frac{r}{L+M}p + \frac{1}{(L+M)C} = (p+\alpha_2)^2 + \omega_2^2,$$

where

$$\alpha_1 = \frac{1}{2} \cdot \frac{r}{L-M}; \quad \alpha_1^2 + \omega_1^2 = \frac{1}{(L-M)C};$$

$$\alpha_2 = \frac{1}{2} \cdot \frac{r}{L+M}; \quad \alpha_2^2 + \omega_2^2 = \frac{1}{(L+M)C},$$

and, using the fact that $u_{vykh}(t) = ri_2(t)$ and $\dot{L}|u_{vykh}(t)| = r|i_2(t)|$, we find the transfer function Y(p) from the condition

$$\mathcal{L}|u_{vykh}(t)| = Y(p)\mathcal{L}|u_{ex}(t)| = \left[\frac{r}{2(L-M)} \cdot \frac{p}{(p+\alpha_1)^2 + \omega_1^2} -\right.$$

$$\left. - \frac{r}{2(L+M)} \cdot \frac{p}{(p+\alpha_2)^2 + \omega_2^2}\right]\mathcal{L}|u_{ex}(t)|.$$

Let us consider the special case in which the electromotive force $u_{vkh}(t)$ at the instant $t = 0$ jumps from $u_{vkh}(t) = 0$ at $t < 0$

to the constant u_0, i.e., $u_{vkh}(t) = u_0$ when $t \geq 0$. In this case, as we have seen, $L|u_{vkh}(t)| = u_0/p$.

Thus, for the conditions given,

$$\mathcal{L}|u_{вых}(t)| = \left[\frac{r}{2(L-M)} \cdot \frac{u_0}{(p+\alpha_1)^2+\omega_1^2} - \right.$$
$$\left. - \frac{r}{2(L+M)} \cdot \frac{u_0}{(p+\alpha_2)^2+\omega_2^2}\right].$$

Using the tables of originals and transforms given in Appendix 2, we find that to the transform

$$\frac{1}{(p+\alpha)^2+\omega^2}$$

there corresponds the original

$$\frac{1}{\omega} e^{-\alpha t} \sin \omega t.$$

Thus, the voltage at the output will equal

$$u_{вых}(t) = \frac{r u_0}{2(L-M)} \cdot \frac{1}{\omega_1} e^{-\alpha_1 t} \sin \omega_1 t -$$
$$- \frac{r u_0}{2(L+M)} \cdot \frac{1}{\omega_2} e^{-\alpha_2 t} \sin \omega_2 t,$$

i.e., it is the difference of two damped sinusoidal oscillations with different damping factors α_1 and α_2, and different periods $T_1 = 2\pi/\omega_1$ and $T_2 = 2\pi/\omega_2$.

As these examples show, in order to find the original of the output variable, it is necessary to find the roots of the denominator in the fraction $Y(p)L|\varphi_{vkh}(t)|$, and to write it as a product of a series of binomials of the form $(p - \alpha_1)$ or $(p^2 + \gamma_1^2)$, or polynomials of the form

$$[(p+\alpha_i)^2+\omega_i^2].$$

It is generally quite difficult to find the roots of an equation of degree higher than three. Consequently, although the Laplace-transformation technique greatly facilitates the solution of linear differential equations, it becomes extremely cumbersome when the

circuit under consideration contains more than ten series-connected sections, each of which is described by an equation of first or second order, while the entire circuit is described by an equation of degree ten or higher. In addition, the Laplace transformation is suited only to solution of linear differential equations. At the same time nonlinear elements or elements whose operation is time-dependent, are frequently encountered in guided-missile practice. These elements include, for example, the flying craft itself when it flies in a medium of varying density or flies at a changing speed, owing to which, for example, the coefficients M and N in our first example cease to be constant and become time-dependent. An example of a nonlinear element is a flying craft in which the deflection of the control surfaces is proportional, within certain limits, to the applied torque, while beyond these limits, stops are hit.

Thus, despite the considerable simplification gained by using the Laplace transformation in solving linear differential equations, this method does not eliminate the difficulties encountered during discussion of complex circuits or circuits containing nonlinear elements. On the other hand, the Laplace-transformation method is a very convenient and intuitive means of analyzing processes occurring in simple circuits.

Manuscript Page No.	[List of Transliterated Symbols]
21	ВХ = vkh = vkhodnoy = input
21	ВЫХ = vykh = vykhodnoy = output

Manuscript Page No.

[Footnote]

18 See, for example, V.A. Ditkin and P.I. Kuznetsov, Spravochnik po operatsionnomu ischisleniyu [A Handbook for Operational Calculus], GTTI, 1951, or M.F. Gardner and Dzh. L. Berns, Perekhodnyye protsessy v lineynykh sistemakh [Transient Processes in Linear Systems], GTTI, 1951.

Chapter 2

THE SPECTRAL METHOD OF ANALYZING PROCESSES IN LINEAR SYSTEMS

1. THE FOURIER TRANSFORMATION. SPECTRA OF FUNCTIONS. SPECTRAL DISTRIBUTIONS OF SIGNAL ENERGY

The spectral method is based upon the so-called Fourier transformation. From the physical viewpoint, the essence of the spectral method lies in replacing a function $\varphi(t)$ that depends upon time in some complicated fashion by the sum of harmonic waveforms that have a continuous frequency spectrum covering a bounded or unbounded region, and that have amplitudes varying continuously over the spectrum. In the general case, then, the function $\varphi(t)$ can be written in the form of an integral over the spectrum of frequencies from $\omega = 0$ to $\omega = \infty$ with amplitude densities a_ω and b_ω varying over the spectrum:

$$\varphi(t) = \frac{1}{\pi} \int_0^\infty (a_\omega \cos \omega t + b_\omega \sin \omega t)\, d\omega. \tag{19}$$

In Expression (19) $\varphi(t)$ is the value of the function under consideration at time t, a_ω and b_ω are real coefficients that characterize the process under discussion, and ω is the angular frequency of the waveform.

Formula (19) may also be written as

$$\varphi(t) = \frac{1}{\pi} \int_0^\infty \sqrt{a_\omega^2 + b_\omega^2} \cos(\omega t + \psi_\omega)\, d\omega, \tag{20}$$

where

$$\psi_\omega = \operatorname{arctg} \frac{-b_\omega}{a_\omega}.$$

Here

$$\sqrt{a_\omega^2 + b_\omega^2} = |\varphi_\omega|$$

is the amplitude density of the waveforms at frequency ω; ψ_ω is the waveform phase at this frequency. The waveform amplitude itself at the frequency ω equals $|\varphi(\omega)|\, d\omega$ and is an infinitely small quantity.

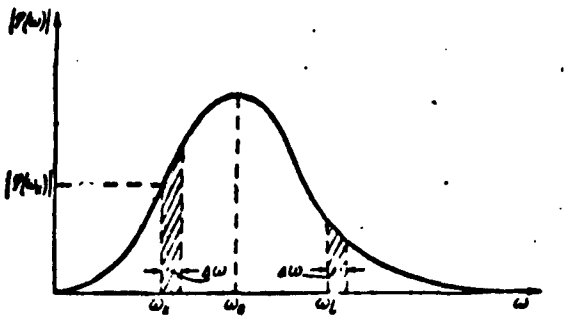

Fig. 6

Integral (20) can be written in a more convenient form.

Let, for example, the amplitude-density distribution $|\varphi_\omega|$ for some function $\varphi(t)$ be given by the curve of Fig. 6, and the phase distribution for ψ_ω by the curve of Fig. 7.

Then the mean waveform amplitude between frequencies ω_k and $\omega_k + \Delta\omega$ is represented by the hatched area $\varphi_{\omega k}\Delta\omega$ of Fig. 6, while the phase $\psi_{\omega k}$ can be found from the curve of Fig. 7.

Integral (20) may be represented as the projection of the sum of an infinite number of vectors having amplitudes $\varphi_{\omega k}\, d_\omega$, and forming angles $\omega_{kt} + \psi_{\omega k}$ with the real axis.

At time $t = 0$, for example, the vector positions will be characterized by Fig. 8, where the dashed line shows the location of the end points for the vectors $\varphi_\omega\, \Delta\omega$, and the projection of their sums on the real axis is the instantaneous value of the function $\varphi(t = 0)$.

In order to find the instantaneous value of the function $\varphi(t)$ at time t, it is necessary while retaining their absolute magnitudes to locate the vectors $\varphi_{\omega k}\, \Delta\omega$, $\varphi_{\omega 0}\, \Delta\omega$, $\varphi_{\omega i}\, \Delta\omega$, etc., at angles to the

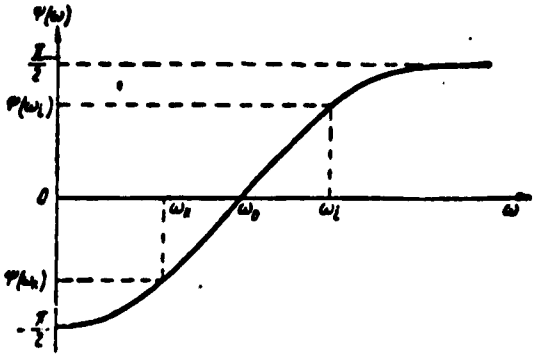

Fig. 7

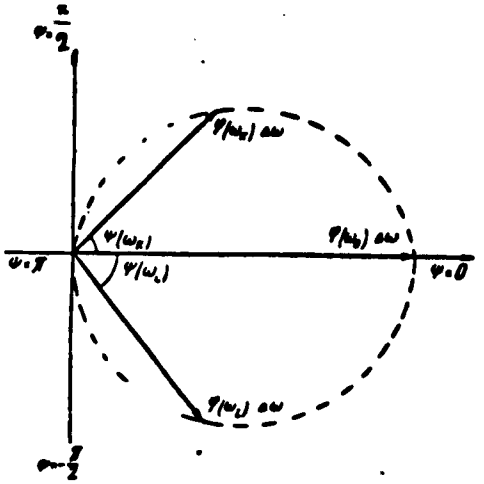

Fig. 8

real axis equal respectively to $\omega_k t + \psi_{\omega k}$, $\omega_0 t + \psi_{\omega 0}$, $\omega_1 t + \varphi_{\omega 1}$, etc., and then to find the sum of their projections upon the real axis. The smaller the increments $\Delta\omega$, i.e., the greater the number of parts into which the band of frequencies ω is divided, the more closely the sum of the projections of the individual vectors $\varphi_{\omega k}\,\Delta\omega$, $\varphi_{\omega 1}\,\Delta\omega$, etc., will be to the precise value of $\varphi(t)$ given by Integral (20).

The values of the coefficients a_ω and b_ω in Formulas (19) and (20) equal

$$a_\omega = \int_{-\infty}^{+\infty} \varphi(t)\cos\omega t\,dt \text{ and } b_\omega = \int_{-\infty}^{+\infty} \varphi(t)\sin\omega t\,dt. \qquad (21)$$

Making use of the fact that $a_{-\omega} = a_{\omega}$, since $\cos(-\omega t) = \cos \omega t$ and $b_{-\omega} = -b_{\omega}$ in view of the fact that $\sin(-\omega t) = \sin \omega t$, and thus $a_{\omega} \cos \omega t = a_{-\omega} \cos(-\omega t)$ and $b_{\omega} \sin \omega t = b_{-\omega} \sin(-\omega t)$, we can extend the limits of integration in (19) to $\pm\infty$. The Expression (19) will take the form

$$\varphi(t) = \frac{1}{2\pi} \int_{-\infty}^{+\infty} (a_{\omega} \cos \omega t + b_{\omega} \sin \omega t)\, d\omega. \tag{22}$$

Integral (19) may also be written as

$$\varphi(t) = \frac{1}{2\pi} \int_{-\infty}^{+\infty} \varphi_{\omega} e^{j\omega t}\, d\omega. \tag{23}$$

Such a representation is possible owing to the fact that when we take (20) into account, the value of the vector φ_{ω} equals

$$\varphi_{\omega} = a_{\omega} - j b_{\omega},$$

and since

$$e^{j\omega t} = \cos \omega t + j \sin \omega t,$$

then

$$\int_{-\infty}^{+\infty} \varphi_{\omega} e^{j\omega t} d\omega = \int_{-\infty}^{+\infty} (a_{\omega} - j b_{\omega})(\cos \omega t + j \sin \omega t)\, d\omega =$$

$$= \int_{-\infty}^{+\infty} (a_{\omega} \cos \omega t + b_{\omega} \sin \omega t)\, d\omega +$$

$$+ j \int_{-\infty}^{+\infty} (a_{\omega} \sin \omega t - b_{\omega} \cos \omega t)\, d\omega.$$

The second integral on the right side equals zero, since

$$a_{-\omega} \sin(-\omega t) = -a_{\omega} \sin \omega t,$$

while

$$b_{-\omega} \cos(-\omega t) = -b_{\omega} \cos \omega t,$$

which leads to Expression (23).

Substituting the values given by (21) for a_{ω} and b_{ω} into the

expression for the vector $\varphi_\omega = a_\omega - jb_\omega$ yields

$$\varphi_\omega = \int_{-\infty}^{+\infty} \varphi(t)(\cos \omega t - j \sin \omega t)\, dt =$$

$$= \int_{-\infty}^{+\infty} \varphi(t)\, e^{-j\omega t}\, dt. \qquad (24)$$

Where the function $\varphi(t)$ has nonzero values only for $t \geq 0$,

$$\varphi_\omega = \int_{0}^{\infty} \varphi(t)\, e^{-j\omega t}\, dt. \qquad (25)$$

Comparison of this expression with the "transform" of the function $\varphi(t)$ [Formula (1)] shows that φ_ω is the Laplace transform of the function $\varphi(t)$ for the special case in which $p = j\omega$ and $a = 0$:

$$\varphi_\omega = F(j\omega) = F(p)_{a=0}. \qquad (26)$$

The fact that the Fourier transform (25) of the function $\varphi(t)$ is a special case of its Laplace transform (1) makes it possible to find the spectral amplitude and phase distributions for various functions $\varphi(t)$ by means of tables of Laplace "originals" and "transforms" if we assume that $p = j\omega$ in the "transforms."

As an example, let us find the spectral distribution for the waveform amplitudes and phases for certain of the functions $\varphi(t)$.

Step function

$$\varphi(t) = 0 \quad \text{for } t < 0;$$
$$\varphi(t) = A \quad \text{for } t > 0.$$

The Laplace transform of this function is $F(p) = A/p$.

Substituting p for $j\omega$, we obtain

$$\varphi_\omega = F(j\omega) = \frac{A}{j\omega} = -j\frac{A}{\omega} = -jb_\omega,$$

whence

$$|\varphi_\omega| = \frac{A}{\omega}; \quad \psi = \frac{\pi}{2}. \qquad (27)$$

Thus, a step function may be written in the form

$$\varphi(t) = \frac{A}{\pi}\int_0^\infty \frac{\sin \omega t}{\omega}\, d\omega. \qquad (28)$$

Rectangular pulse of length τ

A rectangular pulse with a height A and length τ (Fig. 9), can be thought of as two steps of height A, one of which (positive) appears at time $t_1 = -\tau/2$ and the second (of opposite sign) appears at time $t_2 = \tau/2$.

Thus,

$$\varphi(t) = \frac{A}{\pi}\int_0^\infty \frac{\sin \omega\left(t+\frac{\tau}{2}\right)}{\omega}\, d\omega -$$

$$-\frac{A}{\pi}\int_0^\infty \frac{\sin \omega\left(t-\frac{\tau}{2}\right)}{\omega}\, d\omega =$$

$$=\frac{A}{\pi}\int_0^\infty \frac{\sin \omega\left(t+\frac{\tau}{2}\right)-\sin \omega\left(t-\frac{\tau}{2}\right)}{\omega}\, d\omega =$$

$$=\frac{2A}{\pi}\int_0^\infty \frac{\sin\left(\omega\frac{\tau}{2}\right)\cos \omega t}{\omega}\, d\omega. \qquad (29)$$

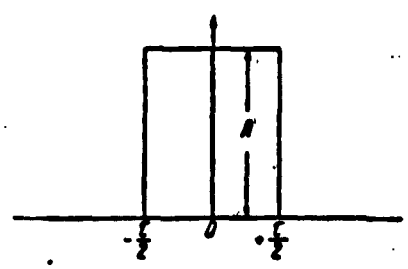

Fig. 9

from which it is clear that

$$|\varphi_\omega| = \frac{2A\tau \sin\left(\omega\frac{\tau}{2}\right)}{\omega\tau};\ \psi_\omega = 0. \qquad (30)$$

The spectral amplitude-density distribution for $|\varphi_\omega|$ is shown in Fig. 10. An important property of the spectrum obtained from a rectangular pulse is the constancy of the amplitude $|\varphi_\omega|$ density at small values of ω.

So far, the following inequality has held:

$$\frac{\omega\tau}{2} \ll \frac{\pi}{2},$$

$$|\varphi_\omega| = \frac{2A\tau \sin\left(\omega\frac{\tau}{2}\right)}{\omega\tau} \approx A\tau \text{ and } \psi_\omega = 0. \qquad (31)$$

In the solution of certain problems, it becomes convenient to use the so-called "unit pulse" or δ function.

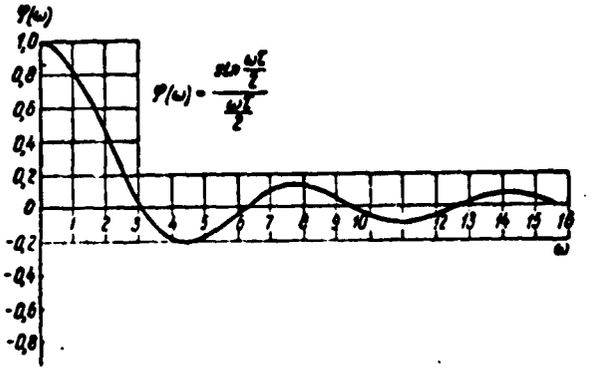

Fig. 10

The unit pulse is that pulse for which the area $A\tau$ equals unity for an infinitely small pulse length, i.e., $A\tau = 1$ where $\tau \to 0$.

It is clear from Expression (31) that for a unit pulse $|\varphi_\omega| = A\tau = 1$ within any finite frequency range. In other words, the spectrum of such a pulse is a straight line parallel to the x axis lying at a distance unity from it, i.e., it represents a uniform amplitude distribution over the entire frequency spectrum.

Exponential decay function $\varphi(t) = e^{-\alpha t}$, where $t \geq 0$.

The Laplace transform for this function is

$$F(p) = \frac{1}{p + a},$$

whence

$$\varphi_\omega = F(j\omega) = \frac{1}{a + j\omega}.$$

Consequently

$$|\varphi_\omega| = \frac{1}{\sqrt{a^2 + \omega^2}}, \quad \psi_\omega = \operatorname{arctg} \frac{\omega}{a}. \tag{32}$$

Cosine curve beginning at time t = 0

$$\varphi(t) = \cos \Omega t \text{ for } t > 0.$$

$$F(p) = \frac{p}{p^2 + \Omega^2}; \quad \varphi_\omega = F(j\omega) = \frac{j\omega}{\Omega^2 - \omega^2};$$

$$|\varphi_\omega| = \frac{\omega}{\Omega^2 - \omega^2}; \quad \psi_\omega = \frac{\pi}{2}. \tag{33}$$

Function of the form $\varphi(t) = te^{-\alpha t}$ at $t \geq 0$

$$\left.\begin{aligned} F(p) &= \frac{1}{(p + a)^2}; \\ \varphi_\omega = F(j\omega) &= \frac{1}{(a + j\omega)^2} = \frac{1}{a^2 - \omega^2 + 2ja\omega}, \\ |\varphi_\omega| &= \frac{1}{\sqrt{(a^2 - \omega^2)^2 + 4a^2\omega^2}} = \frac{1}{a^2 + \omega^2}; \\ \psi_\omega &= \operatorname{arc\,tg} \frac{\pm 2a\omega}{a^2 - \omega^2}. \end{aligned}\right\} \tag{34}$$

Fluctuation noise

The discontinuous – corpuscular – structure of an electric current, representing the motion of individual electrons, the thermal motion of electrons in conductors – all of this leads to variations in electrical voltages at the inputs and outputs of electrical-circuit elements. The statistical nature of the processes occurring in this case are responsible for the fact that currents or voltages are constant only with respect to their mean values, when taken over a sufficiently large time interval. The instantaneous current and voltage values taken over short time intervals deviate from the mean

values. In this case, the probability P(x) that the instantaneous current or voltage values observed at a given time will deviate in the positive (or negative) direction by more than an amount x is determined by the expression

$$P(x) = \frac{1}{\sqrt{2\pi}\sigma}\int_{x}^{\infty} e^{-\frac{x^2}{2\sigma^2}} dx. \tag{35}$$

In this expression, σ is the root-mean-square deviation of the quantity under consideration from its mean value.

In (35) we replace the random deviation x by the ratio of x to the root-mean-square deviation

$$y = \frac{x}{\sigma}$$

and concentrate our attention on the probability for the relative deviation y greater than the predetermined quantity, without taking the sign into consideration, i.e., independent of whether or not this deviation occurs in the positive or negative direction, obtaining

$$\Phi(y) = \sqrt{\frac{2}{\pi}}\int_{y}^{\infty} e^{-\frac{y^2}{2}} dy. \tag{36}$$

The probability distribution characterized by Expression (36) is called the normal Gaussian distribution. A short table of values for $\Phi(y)$ as a function of y is given in Appendix 1.

From the physical viewpoint, fluctuation noise consists of an enormous number of extremely small and very short pulses following each other irregularly.

We have already shown that the spectrum of a single short pulse can be represented by Formula (30) or (31)

$$|\varphi_\omega| = \frac{2A\tau \sin\left(\omega\frac{\tau}{2}\right)}{\omega\tau} \quad (30) \quad \text{or} \quad |\varphi_\omega| \approx A\tau. \tag{31}$$

Since the individual pulses that generate fluctuation noise are ex-

tremely short, the spectrum of such a pulse can be assumed to be uniform for all practical purposes. Consequently, the spectrum of an ensemble of such pulses, creating fluctuation noise, will also be uniform, since the mean noise amplitude density $|\varphi_{\omega i}|$, lying anywhere between the frequencies ω_i and $\omega_i + \Delta\omega$, will equal the noise amplitude density $|\varphi_{\omega k}|$ between the frequencies ω_k and $\omega_k + \Delta\omega$ in any other portion of the spectrum.

For the waveforms of each frequency ω entering into the noise spectrum, the phase angle ψ_ω of the fluctuation noise will be a random variable, since each pulse making up the noise, and appearing at an arbitrary – random – moment in time will cause a jump in the phase angle. There are a number of such jumps, and they appear randomly. Consequently, the resultant phase angle will also be a random magnitude, so that at a given moment in time any value of the angle from 0 to 2π will be equiprobable.

Distribution of Waveform Energy Over the Frequency Spectrum

If the function $\varphi(t)$ is a time-limited function of electrical current or voltage, or of a mechanical force that is balanced by frictional forces, inertial forces, or elastic-deformation forces, then the energy of the current or voltage, as well as the work, will be proportional to the integral

$$\int_{-\infty}^{+\infty} \varphi(t)^2 dt.$$

Let us express the function $\varphi(t)$ in terms of its spectral density $|\varphi_\omega|$. According to Expression (20)

$$\varphi(t) = \frac{1}{\pi} \int_0^\infty |\varphi_\omega| \cos(\omega t + \psi_\omega) d\omega.$$

Using this expression for $\varphi(t)$, we find

$$\int_{-\infty}^{+\infty} \varphi(t)^2 dt = \frac{1}{\pi} \int_0^{\infty} |\varphi_\omega| \cos(\omega t + \psi_\omega) d\omega \int_{-\infty}^{+\infty} \varphi(t) dt.$$

We now change the order of integration. Then

$$\int_{-\infty}^{+\infty} \varphi(t)^2 dt = \frac{1}{\pi} \int_0^{\infty} |\varphi_\omega| d\omega \int_{-\infty}^{+\infty} \varphi(t) \cos(\omega t + \psi_\omega) dt.$$

Since, by (21)

$$\cos \psi_\omega = \frac{a_\omega}{\sqrt{a_\omega^2 + b_\omega^2}} = \frac{a_\omega}{|\varphi_\omega|};$$

$$\sin \psi_\omega = \frac{-b_\omega}{\sqrt{a_\omega^2 + b_\omega^2}} = \frac{-b_\omega}{|\varphi_\omega|};$$

we can transform the integral

$$\int_{-\infty}^{+\infty} \varphi(t) \cos(\omega t + \psi_\omega) dt = \int_{-\infty}^{+\infty} \varphi(t) \cos \psi_\omega \cos \omega t \, dt +$$

$$+ \int_{-\infty}^{+\infty} \varphi(t) \sin \psi_\omega \sin \omega t \, dt = \frac{a_\omega^2 + b_\omega^2}{|\varphi_\omega|} = |\varphi_\omega|.$$

Making use of this expression and substituting, we find

$$\int_{-\infty}^{+\infty} \varphi(t)^2 dt = \frac{1}{\pi} \int_0^{\infty} |\varphi_\omega|^2 d\omega. \qquad (37)$$

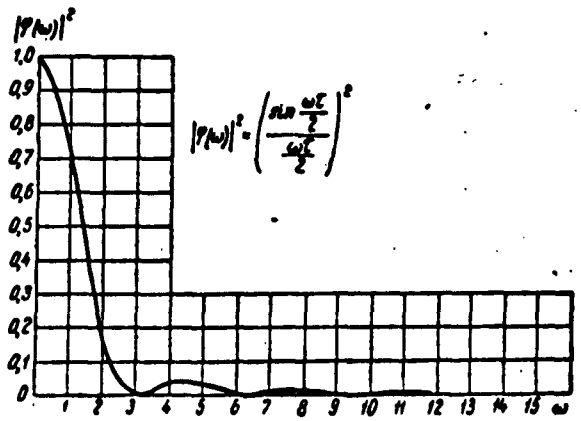

Fig. 11

Formula (37) is a very important relationship in spectral theory. It shows that the energy of any process – single pulse, pulse train,

continuous function – equals the sum of the energies of the individual harmonic-oscillation components of the spectrum forming this function. The energy distribution over the spectrum of waveforms generating the function $\varphi(t)$ is expressed, in some scale, by the spectral distribution of the squares of the amplitudes $|\varphi_\omega|^2$ of these waveforms.

To clarify what we have said, we return to a discussion of our examples.

Step function

$$|\varphi_\omega| = \frac{A}{\omega}; \tag{27}$$

$$|\varphi_\omega|^2 = \frac{A^2}{\omega^2}. \tag{38}$$

Rectangular pulse of length τ

$$|\varphi_\omega| = \frac{2A \sin\left(\omega \frac{\tau}{2}\right)}{\omega}; \tag{30}$$

$$|\varphi_\omega|^2 = \frac{4A^2 \sin^2\left(\omega \frac{\tau}{2}\right)}{\omega^2}. \tag{39}$$

The spectral energy distribution for this case is shown in Fig. 11.

For a very short pulse or a δ function, the energy is distributed uniformly over the spectrum. Consequently, the mean fluctuation-noise energy is also distributed uniformly over the spectrum.

2. PASSAGE OF HARMONIC WAVEFORMS THROUGH LINEAR SYSTEMS. AMPLITUDE AND PHASE CURVES. EQUIVALENT FREQUENCY BANDWIDTH

System Amplitude and Phase Responses

As is well known, the passage of harmonic oscillations through a tuned circuit or a system of tuned circuits is accompanied by variations in their amplitude and phase. This variation can be characterized by the complex quantity $Y(j\omega)$ by which it is necessary to multiply the input signal in order to obtain the signal at the system output. In linear systems, the factor $Y(j\omega)$ is a function of frequency

and the system parameters.

Representing a complex input signal $\varphi_{vkh}(t)$ as a Fourier integral, we can write the output signal of the linear system in the form

$$\varphi_{вых}(t) = \frac{1}{2\pi}\int_{-\infty}^{+\infty} \varphi_{\omega} e^{j\omega t}\, Y(j\omega)\, d\omega. \tag{40}$$

Writing the harmonic waveforms at the system input as the vector $\varphi_{vkh}(t) = u_{vkh}e^{j\omega t}$, and the waveforms at the system output as $\varphi_{vykh}(t) = u_{vykh}e^{j(\omega t + \psi\omega)}$, we can represent the factor $Y(j\omega)$ in the form

$$Y(j\omega) = \frac{\varphi_{вых}(t)}{\varphi_{вх}(t)} = \frac{u_{вых}}{u_{вх}} e^{j\psi\omega}. \tag{41}$$

If the relationship between the input and output variables of a complex circuit is expressed in the form of differential equation (15), substitution of the values for $\varphi_{vkh}(t)$ and $\varphi_{vykh}(t)$ for the case of harmonic waveforms yields

$$\begin{aligned} u_{вых} e^{j(\omega t+\psi\omega)}[a_n(j\omega)^n + a_{n-1}(j\omega)^{n-1} + \dots a_0] = \\ = u_{вх} e^{j\omega t}[b_m(j\omega)^m + b_{m-1}(j\omega)^{m-1} + \dots b_0]. \end{aligned} \tag{42}$$

Consequently,

$$Y(j\omega) = \frac{b_m(j\omega)^m + b_{m-1}(j\omega)^{m-1} + \dots b_0}{a_n(j\omega)^n + a_{n-1}(j\omega)^{n-1} + \dots a_0}. \tag{43}$$

The expression $Y(j\omega)$ is called the complex frequency response of the circuit. The absolute value of this characteristic $|Y(j\omega)$ is the coefficient by which it is necessary to multiply the amplitude or amplitude density of the input signal at frequency ω in order to find the amplitude or amplitude density of the output signal at the same frequency. The argument of the characteristic $Y(j\omega)$ is the additional phase-shift angle

$$\psi_{\omega} = \arg Y(j\omega),$$

that appears when a signal of frequency ω traverses the circuit.

Through the same considerations as were used to show that the transfer function of a group of series-connected elements is the

product of the transfer functions of the individual elements (18), we may show that the frequency response of a group of series-connected elements is the product of the frequency characteristics of these elements:

$$Y_{12\ldots n}(j\omega) = Y_1(j\omega)Y_2(j\omega)\ldots Y_n(j\omega). \tag{44}$$

Thus, multiplication of the moduli of the frequency characteristics for the individual elements will yield the modulus of the frequency characteristic for the system formed by these same elements connected in series.

The argument of the frequency characteristic for a group of series-connected elements is the sum of the arguments of the frequency characteristics for the individual elements:

$$\arg Y_{1,2\ldots n}(j\omega) = \sum_{i=1}^{n} \arg Y_i(j\omega). \tag{45}$$

A comparison of Expression (16) for the transfer function Y(p) and Expression (43) for the frequency characteristic Y(jω) shows that the frequency response may be obtained from the transfer function by substituting jω for the operator p.

As an example, we shall consider the amplitude-frequency and phase-frequency characteristics of a system having the transfer function

$$Y(p) = -\frac{N}{p^2 + Mp}.$$

The frequency characteristic of this circuit is written as

$$Y(j\omega) = -\frac{N}{-\omega^2 + j\omega M} = \frac{N}{\omega} \cdot \frac{\omega + jM}{\omega^2 + M^2}.$$

Consequently,

$$|Y(j\omega)| = \frac{N}{\omega} \frac{1}{\sqrt{\omega^2 + M^2}},$$

$$\arg Y(j\omega) = \operatorname{arctg} \frac{-M}{\omega}.$$

The transfer function for two coupled tuned circuits (Fig. 5) takes the form

$$Y(p) = \frac{r}{2(L-M)} \frac{p}{[(p+\alpha_1)^2+\omega_1^2]} - \frac{r}{2(L+M)} \frac{p}{[(p+\alpha_2)^2+\omega_2^2]}.$$

Thus, the frequency characteristic for these tuned circuits will be

$$Y(j\omega) = \frac{j\omega\alpha_1}{(j\omega+\alpha_1)^2+\omega_1^2} - \frac{j\omega\alpha_2}{(j\omega+\alpha_2)^2+\omega_2^2} =$$

$$= -j\omega\left\{\frac{\alpha_1[(\alpha_1^2+\omega_1^2-\omega^2)-2j\omega\alpha_1]}{(\alpha_1^2+\omega_1^2-\omega^2)^2+4\alpha_1^2\omega^2} - \frac{\alpha_2[(\alpha_2^2+\omega_2^2-\omega^2)-2j\omega\alpha_2]}{(\alpha_2^2+\omega_2^2-\omega^2)^2+4\alpha_2^2\omega^2}\right\}.$$

Transformation of Waveform Spectra in Passing Through a Linear Circuit

The spectrum of a signal passing through a circuit containing tuned elements is transformed, since each of the waveforms forming the spectrum will change in amplitude and phase angle; the latter are multiplied by the complex frequency characteristic of the circuit $Y(j\omega)$. Thus, the spectrum of waveforms at the system output can be written as

$$\varphi_{вых}(\omega) = \varphi_{вх}(\omega) Y(j\omega) = F_{вх}(j\omega) Y(j\omega) = F_{вх}(p)\Big|_{\omega=0} Y(j\omega). \qquad (46)$$

For the special case in which there is applied to the circuit input a unit pulse (δ function) possessing the property that, in accordance with (31), $\varphi(\omega) = 1$ and its spectrum is uniform,

$$\varphi_{вых}(\omega) = Y(j\omega) \quad \text{where } F_{вх}(j\omega) = 1,$$

i.e., the spectrum at the circuit output is numerically equal to the frequency characteristic.

As an example of spectrum transformation, we shall consider the spectrum at the output of a circuit that has the transfer function

$$Y(p) = -\frac{N}{p^2+Mp}.$$

when the step function

$$\varphi(t) = 0 \text{ for } t < 0,$$
$$\varphi(t) = A \text{ for } t > 0.$$

is applied to its input. The Laplace transform of this step function equals

$$F(p) = \frac{A}{p}.$$

Consequently, the spectrum at the circuit output will be

$$\varphi_{вых}(\omega) = F_{вых}(p)_{\omega=0} = F_{вх}(p)_{\omega=0} Y(p)_{\omega=0} = F_{вх}(j\omega) Y(j\omega) =$$
$$= -\frac{AN}{p(p^2 + Mp)}_{\omega=0} = -\frac{AN}{j\omega(j\omega M - \omega^2)} =$$
$$= \frac{AN}{\omega^2} \cdot \frac{\omega - jM}{\omega^2 + M^2}.$$

The amplitude-frequency characteristic for this function will be

$$|\varphi_{вых}(\omega)| = \frac{AN}{\omega^2 \sqrt{\omega^2 + M^2}}.$$

The phase-frequency characteristic is written as

$$\arg |\varphi_{вых}(\omega)| = \operatorname{arc\,tg}\left(\frac{-M}{\omega}\right).$$

Spectral Distribution of Waveform Energy at the Circuit Output. Equivalent Bandwidth

Owing to the fact that the energy of a complex waveform equals the sum of the energies of the individual harmonic waveforms entering into the spectrum, the spectral energy distribution at the circuit output, by (37), will equal

$$\int_{-\infty}^{+\infty} \varphi_{вых}(t)^2 \, dt = \frac{1}{\pi} \int_0^{\infty} |\varphi_{вых}\omega|^2 \, d\omega =$$
$$= \frac{1}{\pi} \int_0^{\infty} |F_{вх}(j\omega) Y(j\omega)|^2 \, d\omega. \qquad (47)$$

Thus, the square of the absolute value of the product $|F_{vkh}(j\omega) \times Y(j\omega)|$ characterizes the spectral energy distribution of the waveforms at the circuit output.

When fluctuation noise acts at the input, the amplitude-density mean values are distributed uniformly over the frequency spectrum at the circuit input. Consequently, the spectral distribution of fluctuation-noise energy at the circuit output depends solely upon the amplitude-frequency response of the circuit itself, $Y(j\omega)$, and is determined by the square of this characteristic.

It is convenient to introduce the notion of the equivalent system bandwidth Ω_{ekv} in order to compare various circuits to see how they transmit fluctuation-noise energy. By the equivalent system bandwidth we mean the bandwidth of an ideal filter that transmits waveforms with frequencies $\omega_0 - (\Omega_e/2) \leq \omega_0 \leq \omega_0 + (\Omega_e/2)$ when the modulus of the amplitude characteristic $Y(j\omega) = 1$, and does not pass waveforms lying outside these limits. In this case, the bandwidth Ω_{ekv} is such that the energy of the fluctuation-noise waveforms at the output of the ideal and the actual circuits is the same.

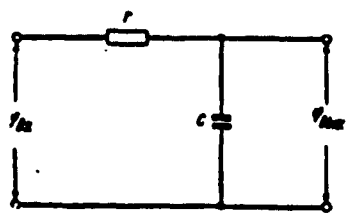

Fig. 12

As an example, let us examine the equivalent bandwidth of the element formed by the capacitance C and resistance r (Fig. 12). The amplitude-frequency characteristic of such an element takes the form

$$|Y(j\omega)| = \frac{1}{\sqrt{1 + r^2 C^2 \omega^2}}.$$

Thus

$$|Y(j\omega)|^2 = \frac{1}{1 + r^2 C^2 \omega^2}.$$

If a signal with a uniform amplitude-density distribution, $|F(j\omega)| = 1$, is applied to the element input, at the ideal-filter bandwidth Ω_{ekv} the energy at the input will be proportional to the factor:

$$\Omega_{ekv} |F(j\omega)|^2 = \Omega_{ekv} 1^2.$$

Energy proportional to the integral

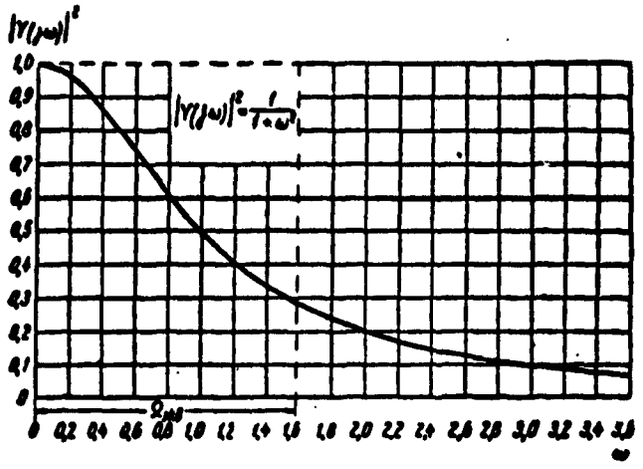

Fig. 13

$$\int_0^\infty |Y(j\omega)|^2 d\omega = \int_0^\infty \frac{d\omega}{1 + r^2C^2\omega^2} =$$

$$= \frac{1}{rC}\left|\operatorname{arctg} rC\omega\right|_0^\infty = \frac{\pi}{2rC}.$$

will appear at the output of the element shown in Fig. 12.

Setting the last equation equal to the product $\Omega_{ekv}\, 1^2$, we find the equivalent bandwidth to be

$$\Omega_{ekv} = \frac{\pi}{2rC}.$$

The graph for the function $|Y(j\omega)|^2$ and the determination of Ω_{ekv} with its aid is shown in Fig. 13.

Manuscript Page No.	[List of Transliterated Symbols]
41	ВХ = vkh = vkhodnoy = input
41	ВЫХ = vykh = vykhodnoy = output
45	ЭКВ = ekv = ekvivalentnyy = equivalent

Chapter 3

CIRCUITS WITH FEEDBACK

Let us turn to the circuit of Fig. 1, which illustrates the entire aggregate of elements entering into a missile control system as a single-loop circuit with feedback. As we have already noted, the coordinates $\varphi_{vkh}(t)$ of the kinematic trajectory, which are compared with the actual missile coordinates $\varphi_{vykh}(t)$ at the same instant in time, are applied to the circuit input. The difference $\varphi_{vkh}(t) - \varphi_{vykh}(t) = \varepsilon(t)$ acts upon the missile and the system for developing, receiving and executing the control commands.

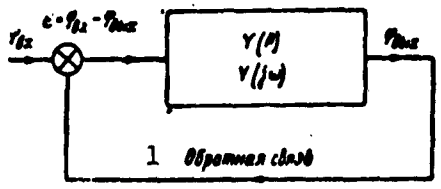

Fig. 14. 1) Feedback.

Let us turn from the originals of the functions $\varphi_{vkh}(t)$, $\varphi_{vykh}(t)$, and $\varepsilon(t)$ to their Laplace transforms, which we shall write in the following abbreviated forms

$$L|\varphi_{вх}(t)| = \varphi_{вх}(p);\ L|\varphi_{вых}(t)| = \varphi_{вых}(p);\ L|\varepsilon(t)| = \varepsilon(p).$$

We shall characterize the entire control loop, together with the missile, by the transfer function Y(p) and the frequency response Y(jω) for an open-loop system, as shown in Fig. 14.

For a closed loop, the relationship between the function at the input φ_{vkh} and the function at the output φ_{vykh} can be written in operator form as

$$\varphi_{вых}(p) = Y(p)\varepsilon(p) = Y(p)[\varphi_{вх}(p) - \varphi_{вых}(p)]. \qquad (48)$$

It follows from Formula (48) that the closed-loop transfer function Y'(p) can be expressed in terms of the open-loop transfer function as

$$Y'(p) = \frac{\varphi_{вых}(p)}{\varphi_{вх}(p)} = \frac{Y(p)}{1+Y(p)}, \qquad (49)$$

and the transform of the error is equal to

$$\varepsilon(p) = \frac{\varphi_{вх}(p)}{1+Y(p)} \text{ or } \frac{\varepsilon(p)}{\varphi_{вх}(p)} = \frac{1}{1+Y(p)}. \qquad (50)$$

Correspondingly, the closed-loop frequency response Y'(jω) may be expressed in terms of the open-loop frequency response as

$$Y'(j\omega) = \frac{\varphi_{вых}(j\omega)}{\varphi_{вх}(j\omega)} = \frac{Y(j\omega)}{1+Y(j\omega)}, \qquad (51)$$

while the error spectrum has the form

$$\varepsilon(j\omega) = \frac{\varphi_{вх}(j\omega)}{1+Y(j\omega)}. \qquad (52)$$

Let us now find an expression for the dynamic error, i.e., for the difference between the coordinates of points on the kinematic and dynamic trajectories corresponding to the same time instants. In this case we shall assume that the motion of the missile and the behavior of all control-system elements may be represented in the form of a system of linear differential equations with constant coefficients.

The form of the open-loop transfer function Y(p) makes it possible to judge how accurately the closed-loop system reproduces the input function $\varphi_{vkh}(t)$ at its output after the transient process has ended.

The open-loop transfer function is given by Formula (16)

$$Y(p) = \frac{b_m p^m + b_{m-1} p^{m-1} + \dots b_0}{a_n p^n + a_{n-1} p^{n-1} + \dots a_0}. \qquad (16)$$

Thus, the transform for the closed-loop error, by (19), is

$$\varepsilon(p) = \frac{1}{1+Y(p)}\varphi_{вх}(p) = \frac{\varphi_{вх}(p)}{1+\dfrac{b_m p^m + b_{m-1} p^{m-1} + \dots b_0}{a_n p^n + a_{n-1} p^{n-1} + \dots a_0}},$$

while after the transient process has ended, i.e., as $t \to \infty$, the error $\varepsilon(t)$, according to (13), has a steady-state value

$$\lim_{t\to\infty} \varepsilon(t) = \lim_{p\to 0} p\,\varepsilon(p) = \lim_{p\to 0} \frac{p\,\varphi_{vx}(p)}{1+\dfrac{b_m p^m + b_{m-1} p^{m-1} + \dots b_0}{a_n p^n + a_n \quad p^{n-1} + \dots a_0}}.$$

If the function $\varphi_{vkh}(t)$, acting at the loop input is a step function, i.e., changes instantaneously from one constant value to another constant value, its transform, by (2), is

$$\varphi_{vx}(p) = \frac{A}{p}.$$

As a result, the limiting – steady-state – error value for such an input function will equal

$$\lim_{t\to\infty} \varepsilon(t) = \lim_{p\to 0} \frac{A}{1+\dfrac{b_m p^m + b_{m-1} p^{m-1} + \dots b_0}{a_n p^n + a_{n-1} p^{n-1} + \dots a_0}}.$$

If the denominator of the open-loop transfer function (16) has a constant term $a_0 \neq 0$, the steady-state error value will be nonzero

$$\lim_{t\to\infty} \varepsilon(t) = \frac{A}{1+\dfrac{b_0}{a_0}} \qquad \text{for } b_0 \neq 0$$

or

$$\lim_{t\to\infty} \varepsilon(t) = A \qquad \text{for } b_0 = 0.$$

Thus, a system having an open-loop transfer function of the form (16) cannot, when $a_0 \neq 0$, accurately reproduce a step-type function applied to its input.

Such a loop possesses, as we say, a "position error" or a "coordinate error."

For the position error to vanish, it is necessary that $a_0 = 0$ and $b_0 \neq 0$.

In this case

$$\lim_{t\to\infty} \varepsilon(t) = \lim_{p\to 0} \frac{A}{1+\dfrac{1}{p}\dfrac{b_m p^m + b_{m-1} p^{m-1} + \dots b_0}{a_n p^{n-1} + a_{n-1} p^{n-2} + \dots a_1}}.$$

The physical interpretation of the fact that the factor 1/p in the

open-loop transfer function compensates the position error lies in the fact that this is an integration factor. Its presence shows that one of the elements forming the control loop integrates the variable $\varepsilon(t)$ that acts at the input of the first element. (1)

The integrating element stores the difference between the input and output quantities, and as a result it ceases to act only when the "margin" that it has accumulated is dissipated.

When a function $\varphi_{vkh}(t) = vt$, which increases continuously and linearly with time, is applied to the loop input, a single integrating element is not sufficient to produce error compensation.

Actually, the transform of a magnitude varying linearly with time is

$$\varphi_{вх}(p) = L\{vt\} = \frac{v}{p^2}.$$

Thus, where there is only a single integrating element in the control loop, when a linearly increasing function is applied to it, the error will tend toward a constant value

$$\lim_{t\to\infty} \varepsilon(t) = \lim_{p\to 0} p \cdot \frac{v}{p^2} \cdot \frac{1}{1 + \frac{1}{p} \frac{b_m p^m + b_{m-1} p^{m-1} + \dots b_0}{a_n p^{n-1} + a_{n-1} p^{n-2} + \dots a_1}}.$$

This error is called a "velocity error." To compensate it, the control loop must contain two integrating elements, i.e., the system must carry out a double integration of the difference between the input and output functions.

In this case, the open-loop transfer function contains $1/p^2$ as a factor, and the limiting error proves to equal zero, since

$$\lim_{t\to\infty} \varepsilon(t) = \lim_{p\to 0} p \cdot \frac{v}{p^2} \cdot \frac{1}{1 + \frac{1}{p^2} \cdot \frac{b_m p^m + b_{m-1} p^{m-1} + \dots b_0}{a_n p^{n-2} + a_{n-1} p^{n-3} + \dots a_2}}.$$

We may show, in precisely the same way, that three integrating elements are necessary to compensate for an "acceleration error" appear-

ing when a function $\varphi_{vkh}(t) = wt^2$, which increases with the square of the time, is applied to the input of the loop shown in Fig. 14, i.e., the factor $1/p^3$ must appear in the open-loop transfer function, and so forth.

These considerations can shed no light on the question of how long a time interval would be necessary to compensate position, velocity, or acceleration errors.

The duration and nature of the transient process depends upon the entire transfer function Y(p). In addition, it must be remembered that guided missiles are frequently in the transient state. In such cases, despite the presence in the control loop of elements designed to compensate errors, the difference between the kinematic and actual missile trajectories, the error, and the magnitude of the miss can be considerable, since there may not be sufficient time for the integrating elements to take effect.

Manuscript Page No.

[List of Transliterated Symbols]

47 BX = vkh = vkhodnoy = input

47 BЫX = vykh = vykhodnoy = output

Chapter 4

THE GUIDED MISSILE AS A LOOP WITH FEEDBACK

1. GENERAL CONSIDERATIONS

An unmanned aircraft, rocket, or homing torpedo is controlled in accordance with a specific law that is selected beforehand when the device is designed.

This law may be, for example, that the angle between the longitudinal axis of the missile or the direction of its velocity vector and the line-of-sight to the target should always be zero (the so-called "pursuit" method). This control law is a special case of the more general law in which the angle between the longitudinal missile axis or its velocity vector and the target direction is held constant.

With external control of missile motion – from a ground or shipboard installation – one of the possible control methods is the so-called "three-point" method in which the missile is held to a line connecting the control point and the target.

It is also possible to use a control law in which the turn angle of the missile axis with respect to a fixed direction in space changes in time in accordance with a specific program, or is set beforehand, or is corrected during flight, depending upon the missile speed and other flight parameters.

With all of the control laws mentioned, as well as with several other possible variants, it is only the direction of motion of the missile that is controlled; here the controls effecting the change

are the rudders, ailerons, steering motors, or other equivalent control devices. Continuous automatic control of missile flight speed is not as yet found as a method of homing on a target.

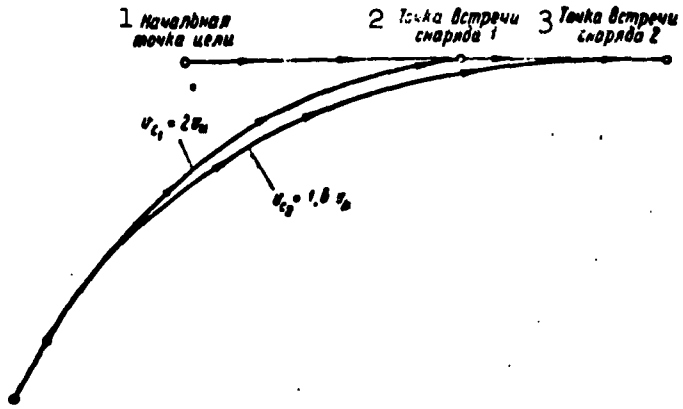

Fig. 15. 1) Initial target position; 2) missile 1 intercept point; 3) missile 2 intercept point.

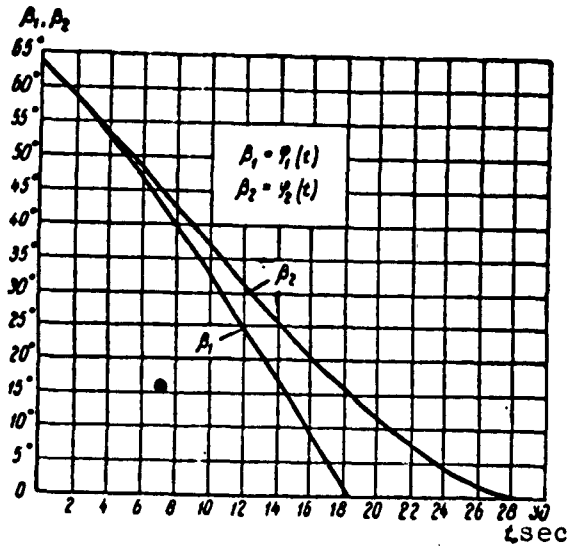

Fig. 16

The control process for missile motion is as follows: depending upon the motion of the target and upon the speed and direction of motion of the missile itself, commands controlling the direction of missile motion are generated in the complex of elements making up

the missile. Thus, for example, given exactly the same target motion path, the trajectory of the missile will differ, depending not only upon the rate at which the target moves along its path, but also upon the speed of the missile. Any change in the speed of the missile during flight will also change its direction of motion, i.e., vary its trajectory.

For the sake of illustration, Fig. 15 shows the motion trajectory of a missile using the "pursuit" method for precisely the same initial conditions, and for the same target path and velocity, but with different missile speeds $v_{s1} = 2v_{ts}$ and $v_{s2} = 1.6v_{ts}$.

Figure 16 shows the way in which missile direction varies with time for the same cases with $v_{s1} = 2v_{ts}$ and $v_{s2} = 1.6v_{ts}$.

The missile path of motion, plotted as a function of the control law for a given target motion, given initial conditions, and a given relationship between the rate of motion of the missile and time, but with no allowance for inertial forces, is the "kinematic" trajectory.

In actuality, the missile reacts to a change in external conditions, and to control commands, with a delay due to its own inertia, and to the inertia of the control devices. The commands themselves are also produced with some delay, since the electrical and mechanical circuits in which they are formed possess electrical and mechanical inertia. Thus, the missile does not move along the kinematic trajectory determined by the control law, but along a dynamic trajectory, provided that fluctuation noise is slight, and that its effect is negligibly small.

The control law determining the missile kinematic trajectory is a function of angular or linear quantities. The latter case occurs, for example, when the missile is controlled by a radio beam that tracks the target. In this case, the control commands are produced

as a function of the distance between the axis of the radio beam and the missile.

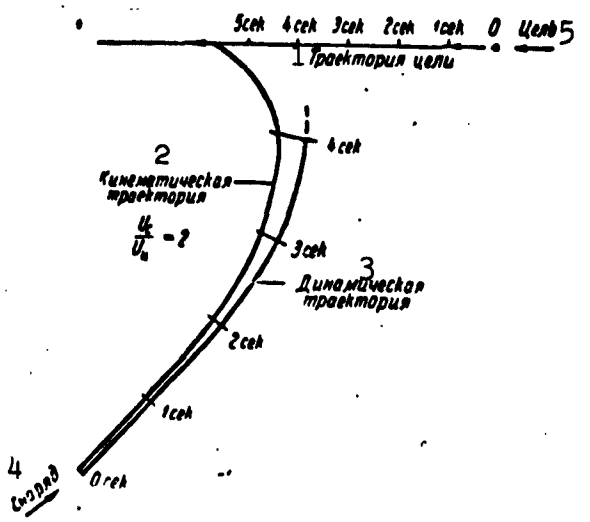

Fig. 17. 1) Target path; 2) kinematic trajectory; 3) dynamic trajectory; 4) missile; 5) target.

As we have already noted, Fig. 14 may be used to represent the basic missile diagram for continuous automatic control, showing all elements involved in obtaining information and producing commands. In this case, the function $\varphi_{vkh}(t)$ is the time function for the angle formed by the missile axis and some stationary direction in space, when the missile moves in strict accordance with a kinematic trajectory, or the time function for the distance of the missile from some fixed line. The function $\varphi_{vykh}(t)$ is the time function of the same quantities, allowing for the response times of the missile and all control-system elements.

The difference $\varepsilon(t) = \varphi_{vkh}(t) - \varphi_{vykh}(t)$ gives the deviation of the dynamic trajectory from the kinematic trajectory or the magnitude of the error.

It is not quite accurate to represent the error $\varepsilon(t)$ as the difference between the functions $\varphi_{vkh}(t) - \varphi_{vykh}(t)$ of changes in

angular or linear quantities at points on the kinematic and dynamic trajectories corresponding to precisely the same instants of time. Actually, the error is the difference between the function $\varphi_{vkh}(t)$ corresponding to the "instantaneous" kinematic trajectory passing through a given point on the dynamic trajectory, and the function $\varphi_{vykh}(t)$ for this same point on the dynamic trajectory. Here by the "instantaneous" kinematic trajectory we mean that kinematic trajectory along which the missile must move if, given the initial conditions corresponding to its motion along the dynamic trajectory at the given instant, it is henceforth to move in precise correspondence with the control law in use.

For example, if the control law calls for the missile velocity vector to coincide with the line-of-sight to the target (pursuit curve), then the tangent to the "instantaneous" kinematic trajectory at the given point would point toward the target. The magnitude of the error $\varepsilon(t)$ in this case would equal the angle between the direction of the missile velocity vector and the line to the target at the given point on the dynamic trajectory.

If we represent the error $\varepsilon(t)$ as the difference in the functions $\varphi_{vkh}(t) - \varphi_{vykh}(t)$, then at the same instant, it will equal the angle between the direction of the missile velocity vector and the tangent to the kinematic trajectory, which is displaced with respect to the dynamic trajectory, and will not intersect it at the given point. This is shown in Fig. 17.

Where beam-rider guidance is used, the actual error $\varepsilon_1(t)$ will equal the distance between the given point on the dynamic trajectory and the line connecting the control point and the target. Taking $\varepsilon(t) = \varphi_{vkh}(t) - \varphi_{vykh}(t)$, we shall assume that this quantity equals the distance between the points corresponding to the same instant of time

on the dynamic and kinematic trajectories.

If the equivalent control-loop diagram takes the form shown in Fig. 14, and $\varphi_{vkh}(t)$ is the input function to a linear system with feedback that has an open-loop transfer function Y(p), then, as we have already noted, the transform of the error $\varepsilon(p)$ will be

$$\varepsilon(p) = \varphi_{ex}(p)\frac{1}{1+Y(p)} = \varphi_{ex}(p) - \varphi_{vyx}(p). \qquad (50)$$

Let us explain this by means of an example. Let us consider a homing-missile system for which we arbitrarily take a control law for which the input function $\varphi_{vkh}(t)$ is the angle θ formed by the longitudinal axis of the missile with a fixed direction. Let us assume that the target moves in such fashion that the missile kinematic trajectory will be a circle. In this case, the angle θ formed by the missile axis and the fixed line, which we take to lie in the plane of the trajectory, will change for constant missile speed, in proportion to the angular velocity Ω. Thus

$$\varphi_{ex}(t) = \theta(t) = \Omega t + \theta_0.$$

If we assume that at the initial time instant $\theta_0 = 0$, we find the transform of the input function

$$\varphi_{ex}(p) = \frac{\Omega}{p^2}.$$

For the sake of the example, we assume that the transfer function Y(p) for the open-loop system formed by the missile and its entire control system, takes the form

$$Y(p) = \frac{1}{p}\frac{B(p)}{A(p)},$$

where

$$B(p) = b_m p^m + b_{m-1}p^{m-1} + \ldots b_0,$$
$$A(p) = a_n p^n + a_{n-1}p^{n-1} + \ldots a_0.$$

Then the transform for the closed control loop error will be

$$\varepsilon(p)=\frac{\varphi_{ust}(p)}{1+Y(p)}=\frac{\Omega}{p^2\left(1+\frac{1}{p}\frac{B(p)}{A(p)}\right)}. \tag{50}$$

In the limit, when $t \to \infty$, the value of the error $\varepsilon(t)$ will equal

$$\lim_{t\to\infty}\varepsilon(t)=\lim_{p\to 0}p\varepsilon(p), \tag{13}$$

i.e.,

$$\lim_{t\to\infty}\varepsilon(t)=\lim_{p\to 0}\frac{p\Omega}{p^2\left(1+\frac{1}{p}\frac{B(p)}{A(p)}\right)}=\frac{a_0}{b_0}\Omega.$$

Thus, in the limit, after the transient has been damped, the missile will also move in a circle, and its axis will form an angle with the fixed direction lying in the plane of the trajectory equal to

$$\varphi_{ust}(t)=\Omega\left(t-\frac{a_0}{b_0}\right).$$

This means that the output function will lag behind the input function $\varphi_{vkh}(t)$ by an angle $\Omega(a_0/b_0)$.

2. THE CONTROL FUNCTION $\varphi_{vkh}(t)$

The approximate representation of the error $\varepsilon(t)$ as the difference in the functions $\varphi_{vkh}(t)$ and $\varphi_{vykh}(t)$

$$\varepsilon(t)=\varphi_{ust}(t)-\varphi_{ust}(t)$$

leads in the majority of cases to complicated equations that are inconvenient to use in calculation or in analysis. Thus, it proves desirable and possible to go still further in our simplifications, and to substitute approximate expressions for the function $\varphi_{vkh}(t)$. Such simplifications are permissible since in practice, the kinematic trajectories prove to be quite smooth, and the accuracy of the results is not affected noticeably when they are replaced piecewise by low-order polynomials. In particular, it is permissible in many cases to replace trigonometric functions by their arguments, or to represent

a section of a kinematic trajectory by a curve of no worse than third or fourth degree, etc.

In order to determine what approximate expression for a kinematic trajectory or control function may be used from the viewpoint of the permissible resulting error in the determination of the $\varepsilon(t)$ error, it is first necessary to see how rapidly the series representing a limited section of the kinematic trajectory or control function converges, i.e., what error is introduced by neglecting each successive term in the expansion.

Here the error in determining the $\varepsilon(t)$ error in accordance with the precise and the approximate control functions will be substantially less than the difference in the coordinates of the kinematic and dynamic trajectories for the given time t.

If the kinematic trajectory or control function takes the form of an infinite power series

$$\varphi_{ki}(t) = A_0 + A_1 t + A_2 t^2 + \ldots A_{k-1} t^{k-1} + \ldots,$$

its transform will take the form

$$\varphi_{ki}(p) = \frac{A_0}{p} + \frac{A_1}{p^2} + \frac{2A_2}{p^3} + \ldots \frac{(k-1)!A_{k-1}}{p^k} + \ldots \qquad (53)$$

The transfer function of the open-loop missile control system will be

$$Y(p) = \frac{1}{p^m} \frac{B(p)}{A(p)}.$$

where there are m integrating elements in the control system.

Thus, the closed control loop error transform will equal

$$\varepsilon(p) = \frac{\varphi_{ki}(p)}{1 + Y(p)} = \left(\frac{A_0}{p} + \frac{A_1}{p^2} + \frac{2A_2}{p^3} + \right.$$

$$\left. + \ldots \frac{A_{k-1}(k-1)!}{p^k}\right) \frac{1}{1 + \frac{1}{p^m} \frac{B(p)}{A(p)}} =$$

$$= C_0(p) + C_1(p) + \ldots C_k(p) \ldots \qquad (54)$$

Let us consider the kth term of this series

$$C_k(p) = \frac{(k-1)!\,A_{k-1}p^{m-k}}{p^m + \frac{B(p)}{A(p)}}.$$

In the limit, where t tends to infinity or is sufficiently large, the kth term will tend toward the value

$$\lim_{t\to\infty} C_k(t) = \lim_{p\to 0} pC_k(p) = \lim_{p\to 0} \frac{(k-1)!\,A_{k-1}p^{m+1-k}}{p^m + \frac{B(p)}{A(p)}}. \qquad (55)$$

Terms for which $m + 1 - k > 0$, will approach zero when $t \to \infty$. A term for which $m + 1 = k$ in the limit will be a constant. Terms for which $m + 1 - k < 0$ will increase, and thus in the general case there will be no limiting value of $\varepsilon(t)$ at $t \to \infty$.

As a rule, as we have already pointed out, the coefficients of terms in the expansion for the control function $\varphi_{vkh}(t)$ that contain high powers of the time are very small. If we assume that controlled motion of the missile takes place, as a rule, over a limited time interval, it is sufficient to have one-two integrating elements in the control loop for the error $\varepsilon(t)$ to lie within permissible limits at the end of the control period. In addition, the insertion of each additional integrating element delays the reaction of the entire control loop to changes in the magnitude of the control function. System response time worsens, and transients become ever longer.

On the basis of all these considerations, we may assume that a missile control loop contains no more than two integrating elements, and that the open-loop transfer function will take the form

$$Y(p) = \frac{1}{p}\frac{B(p)}{A(p)} \qquad (56)$$

or

$$Y(p) = \frac{1}{p^2}\frac{B(p)}{A(p)}, \qquad (57)$$

where B(p) and A(p) are polynomials with constant terms a_0 and b_0; the degree of the polynomial B(p) is less than or equal to the degree of the polynomial A(p).

Thus, if the transfer function Y(p) takes the form represented by Formula (57), a limiting finite value for the $\varepsilon(t)$ error may be found at $t \to \infty$ provided that the number of terms in the polynomial representing the function $\varphi_{vkh}(t)$ is no greater than 3. In this case, the limiting error will be

$$\lim_{t\to\infty} \varepsilon(t) = \lim_{t\to\infty} C_3(t) = \lim_{p\to 0} \frac{2A_2}{\frac{B(p)}{A(p)}} = 2A_2 \frac{a_0}{b_0}. \tag{58}$$

If at m = 2, the number of terms in the expansion for the function $\varphi_{vkh}(t)$ = k = 4, the $\varepsilon(t)$ error will increase linearly with time.

In order to obtain a limiting value for the $\varepsilon(t)$ error, taking the word "limiting" in the sense that it refers to values of the time such that the transients have nearly died out, we find the transform of the derivative $\underline{d}\ \varepsilon(t)/dt$.

As we know [see Formula (9)],

$$L\left|\frac{d\varepsilon(t)}{dt}\right| = pL|\varepsilon(t)| - \varepsilon(t=0) = \left(\frac{A_0}{p} + \frac{A_1}{p^2} + \right.$$
$$\left. + \frac{2A_2}{p^3} + \ldots \frac{(k-1)!A_{k-1}}{p^k} + \ldots\right) \frac{p}{1 + \frac{1}{p^m}\frac{B(p)}{A(p)}} - A_0, \tag{59}$$

the kth term of this series will in the limit have a value

$$\lim_{t\to\infty} \frac{dC_k(t)}{dt} = \frac{(k-1)!A_{k-1}p^{m+2-k}}{p^m + \frac{B(p)}{A(p)}}, \tag{60}$$

where k = 4

$$\lim_{t\to\infty} \frac{dC_4(t)}{dt} = 3!A_3 \frac{A(p)}{B(p)} = 6A_3 \frac{a_0}{b_0}. \tag{61}$$

Thus, for sufficiently large values of t, the "limiting" or steady-state error value will be

$$\varepsilon(t) = 2A_2\frac{a_0}{b_0} + 6A_3\frac{a_0}{b_0}t. \qquad (62)$$

If at m = 2, the number of terms in the expansion for the function $\varphi_{vkh}(t)$ is five, using the same method to find the second derivative $d^2\eta_\varepsilon(t)/dt^2$, and assuming that $d\eta\varepsilon(0)/dt = 0$ and $\varepsilon(0) = 0$, we obtain

$$\frac{d^2C_k(t)}{dt^2} = \frac{(k-1)!A_{k-1}p^{m+2-k}}{p^m + \frac{B(p)}{A(p)}}. \qquad (63)$$

Thus, for sufficiently great values of t, substituting in m = 2 and k = 5,

$$\lim_{t\to\infty}\frac{d^2C_5(t)}{dt^2} = 4!A_4\frac{a_0}{b_0},$$

whence

$$\frac{dC_5(t)}{dt} = 4!A_4\frac{a_0}{b_0}t \text{ и } C_5(t) = \frac{4!}{2}A_4\frac{a_0}{b_0}t^2.$$

Thus, where m = 2 and k = 5

$$\varepsilon(t) = 2A_2\frac{a_0}{b_0} + 3!A_3\frac{a_0}{b_0}t + \frac{4!}{2}A_4\frac{a_0}{b_0}t^2. \qquad (64)$$

In the general case, when the function $\varphi_{vkh}(t)$ contains a finite number of terms, equal to n, and the control loop has two integrating elements, m = 2, the expression for the $\varepsilon(t)$ error, for sufficiently high time values, will equal

$$\varepsilon(t) = 2A_2\frac{a_0}{b_0} + 3!A_3\frac{a_0}{b_0}t + \frac{4!}{2!}A_4\frac{a_0}{b_0}t^2 + \\ + \ldots + \frac{(n-1)!}{(n-3)!}A_{n-1}\frac{a_0}{b_0}t^{n-2}. \qquad (65)$$

By exactly the same method, we may show that where m = 1 the $\varepsilon(t)$ error, for sufficiently great time values (after the transient has died out) will turn out to equal

$$\varepsilon(t) = A_1\frac{a_0}{b_0} + 2A_2\frac{a_0}{b_0}t + \frac{3!}{2!}A_3\frac{a_0}{b_0}t^2 + \ldots \\ \ldots + \frac{(n-1)!}{(n-2)!}A_{n-1}\frac{a_0}{b_0}t^{n-2}. \qquad (66)$$

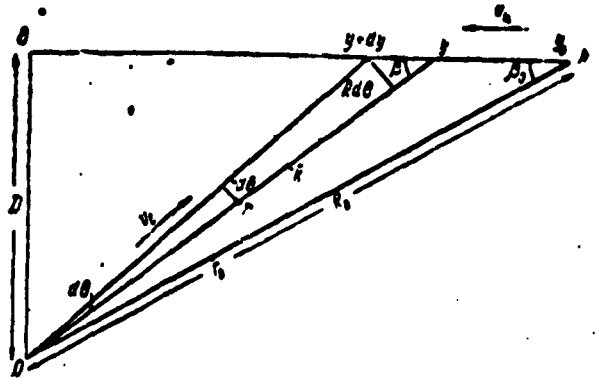

Fig. 18

As an example of the approximate representation of the $\varphi_{vkh}(t)$ control function as a polynomial with a limited number of terms, let us consider the case in which a missile moves at constant speed with beam-rider guidance toward a target that moves in a straight line at constant speed (Fig. 18).

Let the target move at a constant speed v_{ts} along line AB, that lies at a distance D from a fixed point O, which we shall call the control point.

The beam OA, radiated from point O, tracks the target. The missile moves at constant speed v_s; if it were moving in a kinematic trajectory, it would at all times be located on the moving line OA (on the beam), which follows the target.

For the given control method the function $\varphi_{vkh}(t)$ represents the translation of the missile, perpendicular to the control beam. In other words,

$$\varphi_{vkh}(t) = \int v_n\,dt = \int r\,\Omega\,dt, \qquad (67)$$

where v_n is the missile velocity component normal to the beam, and $\Omega = d\theta/dt$ is the angular velocity of the beam that tracks the target.

It follows from Fig. 18 that

$$R d\vartheta = v_n \sin\beta \, dt$$

or

$$\Omega = \frac{d\vartheta}{dt} = \frac{v_n \sin\beta}{R} = \frac{v_n D}{R^2} = v_n \frac{D}{y^2 + D^2} =$$

$$= \frac{v_n D}{(y_0 - v_n t) + D^2}. \qquad (68)$$

The distance r is determined from the condition that the missile velocity v_s is constant

$$v_c \, dt = \sqrt{(dr)^2 + (r\Omega \, dt)^2}$$

or

$$\frac{dr}{dt} = \sqrt{v_c^2 - (r\Omega)^2}. \qquad (69)$$

In all cases, when $v_{ts} < v_s$, $(r\Omega)^2 << v_s^2$. Thus, we may assume without great error that

$$\frac{dr}{dt} \approx v_c \text{ and } r = r_0 + v_c t.$$

It follows from Expressions (67), (68), (69) that the missile normal velocity component v_n will equal

$$v_n = r\Omega = v_n \frac{D(r_0 + v_c t)}{D^2 + y_0^2 - 2y_0 v_n t + (v_n t)^2}. \qquad (70)$$

Letting $R_0^2 = y_0^2 + D^2$,

$$v_n = v_n \frac{D r_0}{R_0} \cdot \frac{1 + \frac{v_c}{r_0} t}{1 - \frac{2y_0 v_n}{R_0^2} t + \frac{v_n^2}{R_0^2} t^2}.$$

We let

$$v_{n0} = v_n D \frac{r_0}{R_0^2}; \; q = \frac{v_c}{r_0}; \; m = \frac{2y_0 v_n}{R_0^2}; \; n = \frac{v_n^2}{R_0^2}.$$

Then

$$v_n = v_{n0} \frac{1 + qt}{1 - mt + nt^2}. \qquad (71)$$

Dividing the numerator of this expression by the denominator, we find

$$v_n = v_{n0}(1 + a_1 t + a_2 t^2 + a_3 t^3 + a_4 t^4 + \ldots), \qquad (72)$$

where

$$a_1 = q + m;\ a_2 = ma_1 - n;\ a_3 = ma_2 - na_1;$$

$$a_4 = ma_3 - na_2 \text{ and in general } a_k = ma_{k-1} - na_{k-2}.$$

Integrating Expression (72), we are able to find the control function $\varphi_{vkh}(t)$, which equals

$$\varphi_{вх}(t) = \int v_в\,dt = \varphi_0 + v_{в0}\left(t + \frac{a_1 t^2}{2} + \frac{a_2 t^3}{3} + \frac{a_3 t^4}{4} + \ldots\right). \qquad (73)$$

where φ_0 is the value of the function $\varphi_{vkh}(t)$ at time t = 0.

As an example, let us consider the special case in which

$$y_0 = 100 \text{ km};\ D = 50 \text{ km};\ r_0 = 35 \text{ km};$$
$$v_ц = 0{,}5 \text{ km/sec};\ v_с = 1{,}0 \text{ km/sec}.$$

Then

$$v_{в0} = 0{,}07 \text{ km/sec};\ q = 2{,}9 \cdot 10^{-2};\ m = 8 \cdot 10^{-3};\ n = 2 \cdot 10^{-5};$$
$$a_1 = 3{,}66 \cdot 10^{-2};\ a_2 = 2{,}73 \cdot 10^{-4};\ a_3 = 1{,}45 \cdot 10^{-6};$$
$$a_4 = 0{,}61 \cdot 10^{-8}.$$

We shall consider the time interval extending from $t_0 = 0$, when the missile is at a distance $r_0 = 35$ km from the control point 0 to $t_{maks} = 50$ sec, when the missile will nearly be at the target.

Setting $t_{maks} = 50$ sec in Formula (73) yields

$$\varphi_{вх}(t_{макс}) = \varphi_0 + v_{в0}(50 + 45{,}8 + 11{,}4 + 2{,}3 + 0{,}4 + \ldots).$$

It is clear from this expression that for practical calculations, within the time interval from $t_0 = 0$ to $t_{maks} = 50$ sec, we need consider only the first three terms within the parentheses, i.e., we assume that

$$\varphi_{вх}(t) = \varphi_0 + v_{в0}\left(t + \frac{1}{2} a_1 t^2 + \frac{1}{3} a_2 t^3\right). \qquad (74)$$

3. TRANSFER FUNCTION Y(p)

The transfer function Y(p) includes the characteristics of all elements forming the control loop, including the missile itself with its aerodynamic response. The extremely large number of elements in the control loop, which contains radiofrequency units, electrical,

electromechanical units, various types of drive mechanisms, automatic pilots, control surfaces and devices, etc., many themselves representing systems with feedback, leads, as we have already said, to exceptional complexity and cumbersomeness in the transfer function expression Y(p), even for the case in which the entire system and its individual elements are linear. The most accurate possible knowledge of the transfer function Y(p) for the entire control loop, and the transfer functions of its individual elements, is an absolute necessity in examining stability questions. The ensurance of stability, i.e., the exclusion of the possibility for the appearance of ever increasing oscillations in the entire system or in any individual element as a result of a random shock, as well as the suppression of free undamped oscillations in individual elements is an absolutely necessary condition for normal functioning of the control system. Thus, in the formation of the control loop, i.e., when its parameters are chosen, on the basis of the attempt to provide optimum design and the necessary stability, it is necessary to use an entire set of complicated expressions characterizing the properties of the individual system elements.

In order to determine the magnitude of the errors that appear in the control system, however, there is no need to consider the characteristics of all the elements. For example, the characteristics of the radiofrequency elements have no noticeable effect upon the magnitude of dynamic errors in a guided missile, since the processes occurring in these elements are so fleeting that they cannot affect the behavior of those elements having long time constants, such as the missile itself. The same applies to other system elements whose natural frequencies are sufficiently large, and time constants sufficiently small in comparison with the frequencies and time constants

of the control loop as a whole.

In this connection, in considering problems of accuracy, i.e., the magnitude of dynamic errors and especially the "limiting" values of these errors that remain after transients have been damped, there is no need to use the full cumbersome expression for the transfer function of the entire control loop, $Y(p)$, but it is possible to replace it with the comparatively simpler equivalent transfer-function expression $Y_e(p)$.

The primary property required of the equivalent transfer function $Y_e(p)$ is that the loop possessing this function have the same "limiting" – steady-state – dynamic error as the actual loop for the guided missile.

The second condition that the equivalent transfer function should satisfy is that the natural oscillation period or time required for transients to be damped be roughly identical for the actual and equivalent control loops.

Both of these requirements can be satisfied with the aid of simple expressions for the equivalent transfer function; these expressions make it possible not only to determine accurately the steady-state values of the dynamic errors, but also to find them quite well under the conditions of transient – steady-state – processes.

Formulas (65) and (66) indicate that the value of dynamic error established after the transient process has ended, for a control function $\varphi_{vkh}(t)$ that has the form of a polynomial with a finite number of terms, depends solely upon two quantities entering into the transfer function $Y(p) = (1/p^m)\,[B(p)/A(p)]$ – on the number of integrating elements $\underline{m}$ in the control loop, and upon the ratio of the constant terms a_0/b_0. All the remaining terms in the polynomials

B(p) and A(p) have no effect upon the magnitude of the steady-state dynamic error and, from this viewpoint, they may be neglected.

Thus, the simplest type of equivalent transfer function may be, where m = 1,

$$Y_э(p) = \frac{1}{p}\frac{b_0}{a_0} = \frac{k}{p}, \tag{75}$$

where k is a coefficient selected on the basis of experiment. More frequently, however, the transfer function will in this case take the form

$$Y_э(p) = \frac{\omega_0^2}{p(p+2\alpha)}. \tag{76}$$

For the case in which m = 2, the simplest form of equivalent transfer function will be

$$Y_э(p) = \frac{2\alpha p + \omega_0^2}{p^2}, \tag{77}$$

where α and ω_0^2 are coefficients, also selected on the basis of experimental data.

The simpler expression for the equivalent transfer function (75) will be unsuitable here, since it leads to the appearance of a factor having the form $1/[p^2 + (b_0/a_0)]$ in the error transform $\varepsilon(p)$, characterizing the presence in the error $\varepsilon(t)$ of terms corresponding to undamped oscillations, which contradicts the actual motion conditions for the guided missile.

Expression (77) contains two arbitrary constants: α and $\omega_0^2 = b_0/a_0$. Only the second of these constants affects the magnitude of the steady-state dynamic error $\varepsilon(t)$. As far as the constant α is concerned, it may be so chosen that not only the steady-state value of the error $\varepsilon(t)$, but even its variations during transients correspond very closely to the movement of an actual missile given the precise value of the transfer function Y(p).

The numerical coefficients entering into Expressions (75), (76), and (77), for the equivalent transfer function are chosen on the basis of experimental data. These data may be quite different in form; the simplest and clearest method for obtaining them, however, is to study the behavior of the entire control loop, including the missile, when the control function $\varphi_{vkh}(t)$ is applied to the loop as a step function

$$\varphi_{vkh}(t)\begin{cases}=0 \text{ for } t<0\\=A \text{ for } t>0.\end{cases}$$

This step function is obtained by applying for the briefest possible period of time, almost instantaneously, a discrete command of constant magnitude.

Affected by the control function $\varphi_{vkh}(t)$, the missile changes its direction. If it initially moved along some straight line, then after application of $\varphi_{vkh}(t)$, and after conclusion of the transient process, the missile will move along another straight line: this line will either be parallel to the first line, displaced by an amount A, or it will form an angle A with the initial direction. In which way the motion of the missile will change depends upon the control method chosen.

The transient process involved in going from one direction of motion to another, i.e., the variation in distance of the missile from the line along which it had first been moving, or the change in its direction, most frequently takes the form of an oscillatory damped process.

The shape of this process is shown in Fig. 19. The difference $\varphi_{vkh}(t) - A = \varepsilon(t)$ represents the error in the closed missile control loop when a step function with amplitude A is applied to the loop. A transient curve of the type shown in Fig. 19 makes it possible for us

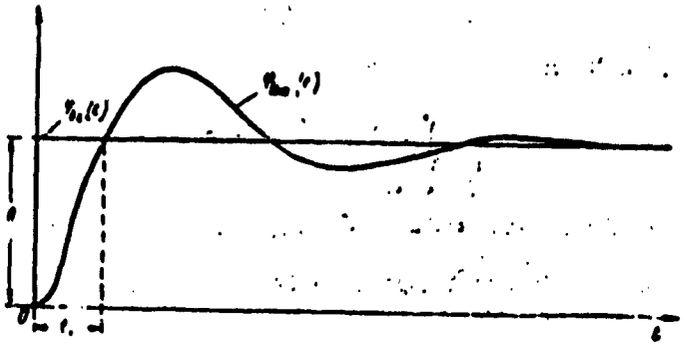

Fig. 19

to obtain all of the data needed to determine the equivalent transfer function. In addition, it enables us to plot the system transients occurring when the control function $\varphi_{vkh}(t)$ is not a step function, but a polynomial with a limited number of terms.

To find the curve for a transient occurring in the system when a step function is applied, we must first determine the number of integrating elements in the control loop.

The transform of a step function having a single amplitude $A_m = 1$ is [Formula (2)]

$$\varphi_m(p) = \frac{1}{p}.$$

Thus, if the control loop contains m integrating elements, and its transfer function takes the form

$$Y(p) = \frac{1}{p^m}\frac{B(p)}{A(p)},$$

then the transform of the error $\varepsilon(t)$ will be

$$\varepsilon(p) = \varphi_m(p)\frac{1}{1+Y(p)} = \frac{p^{m-1}}{p^m + \frac{B(p)}{A(p)}},$$

and its limiting value at $t \to \infty$ will be

$$\lim_{t\to\infty}\varepsilon(t) = \varepsilon_1(t) = \lim_{p\to 0} p\,\varepsilon(p) = \left(\frac{p^m}{p^m + \frac{B(p)}{A(p)}}\right)_{p\to 0}.$$

Thus, if the error found experimentally and referred to a unit step function at the input

$$\varepsilon_1(t) = 1 - \varphi_{ex}(t),$$

tends to zero in the course of time, then $m \geq 1$, since where $m = 0$

$$\lim_{t\to\infty} \varepsilon(t) = \frac{1}{1 + \lim_{p\to 0} \frac{B(p)}{A(p)}} = \frac{a_0}{a_0 + b_0}. \tag{78}$$

Let us consider the limits of the integral

$$\int_0^t \varepsilon(\tau)\, d\tau \text{ for } t \to \infty.$$

The integral $\int_0^t \varepsilon(\tau)\, d\tau = Q_1(t)$ represents the area under the curve for the error $\varepsilon(t)$ as a function of time.

Figure 20 shows both the curve for $\varepsilon(t)$ corresponding to Fig. 19, and the curve for $\int_0^t \varepsilon(\tau)\, d\tau$. The transform of the curve $\int_0^t \varepsilon(\tau)\, d\tau$ is*

$$\frac{1}{p}\varepsilon(p) = \frac{1}{p^2} \frac{p^m}{p^m + \frac{B(p)}{A(p)}}. \tag{79}$$

Thus, if in the course of time the function $\int_0^t \varepsilon(\tau)\, d\tau$ tends to zero, then

$$\lim_{p\to 0} L\,|\varepsilon(t)| = \lim_{p\to 0} \left(\frac{p^{m-1}}{p^m + \frac{B(p)}{A(p)}} \right) = 0, \tag{80}$$

which is possible only where $m \geq 2$.

Integrating the error $\varepsilon(t)$ once again, plotting the curve

$$\int\int \varepsilon(\tau)\, d\tau_1\, d\tau_2 = \int_0^t Q_1(\tau)\, d\tau = Q_2(t)$$

and finding the limiting value of $Q_2(t)$ where $t \to \infty$, making use of considerations similar to those cited above, we find that $m \geq 3$ provided that the limit of $Q_2(t)$ as $t \to \infty$ is zero.

The error $\varepsilon(t)$ should be integrated repeatedly until the limit-

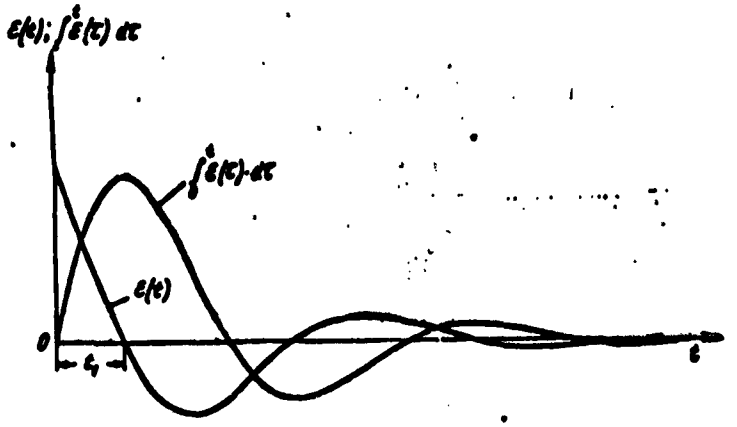

Fig. 20

ing value of the integral $Q_n(t)$, as $t \to \infty$, does not yield a constant. In this case, m = n. In practice, as a rule, m never exceeds two, and thus no more than three integrations are necessary.

The first result of integrating $\varepsilon(t)$, yielding in the limit a nonzero quantity, makes it possible for us to find the ratio of the constant terms a_0/b_0 entering into the expression for the transfer function.

In order to scale the step function $\varphi_{vkh}(t)$ so that it will have a magnitude of unity, $\varphi_{vkh}(t) = 1$, the first multiple integral, which in the limit yields a nonzero result, will equal

$$\int_0^t \int_0^t \dots \int_0^t \varepsilon(\tau)\, d\tau_1\, d\tau_2 \dots d\tau_n = \frac{a_0}{b_0}. \tag{81}$$

This permits us to find the coefficient k in Expression (75) for the equivalent transfer function at m = 1

$$Y_э(p) = \frac{1}{p}\frac{b_0}{a_0}$$

where the magnitude $\omega_0^2 = b_0/a_0$ in Formula (77) when m = 2.

Thus, multiple successive integration of the curve for the error $\varepsilon(t)$ that appears when the function $\varphi_{vkh}(t)$ is applied to the guided-missile loop as a unit step function, permits us to find the

quantities $\underline{m}$ and a_0/b_0, which then permits us to use Formulas (66) and (65) or similar formulas to find, when $m > 2$, the "limiting" steady-state expression for the error $\varepsilon(t)$ when the control function $\varphi_{vkh}(t)$ acting on the loop takes the form of a step series with a limited number of terms.

If $m = 2$, the curve for the transient process, of the type shown in Figs. 19 or 20, enables us to select a value of α, entering into Expression (77) for the equivalent transfer function $Y(p)$, such that the error $\varepsilon(t)$ for the equivalent and real systems will not only be identical in the limit where $t \to \infty$, but in addition, the error curves for both systems will also be similar during the existence of transients.

The simplest and most natural condition restricting the choice of α is that the function $\varepsilon(t)$ for the equivalent system should pass through zero for the first time at the same instant of time following application of $\varphi_{vkh}(t) = 1$ as in the actual system, i.e., the time segments t_1 (Figs. 19 and 20) for the real and equivalent systems should be equal.

If the transfer function takes the form

$$Y_0(p) = \frac{2\alpha p + \omega_0^2}{p^2} \tag{77}$$

and the $\varphi_{vkh}(t)$ acting on the closed control loop takes the form of a unit step function, and has a transform

$$\varphi_{вх}(p) = \frac{1}{p},$$

then the transform for the error $\varepsilon(t)$ will equal

$$\bar{\varepsilon}(p) = \frac{1}{p}\frac{1}{1+Y_0(p)} = \frac{p}{p^2 + 2\alpha p + \omega_0^2} = \frac{p}{(p+\alpha)^2 + (\omega_0^2 - \alpha^2)}. \tag{82}$$

The original of this transform is

$$\varepsilon(t) = \frac{\omega_0}{\omega} e^{-\alpha t} \sin(\omega t + \psi). \qquad (83)$$

where

$$\omega^2 = \omega_0^2 - \alpha^2, \text{ a } \psi = \operatorname{arctg} \frac{\omega}{-\alpha}.$$

According to Formula (83) the function $\varepsilon(t)$ will pass through zero for the first time when $\omega t_1 = -$ arc tan $(\omega/-\alpha)$, which enables us to find α if we know $\omega_0^2 = b_0/a_0$ and t_1.

In order to illustrate the technique used to determine the coefficients of the equivalent transfer function from experimental data, let us consider the following example.

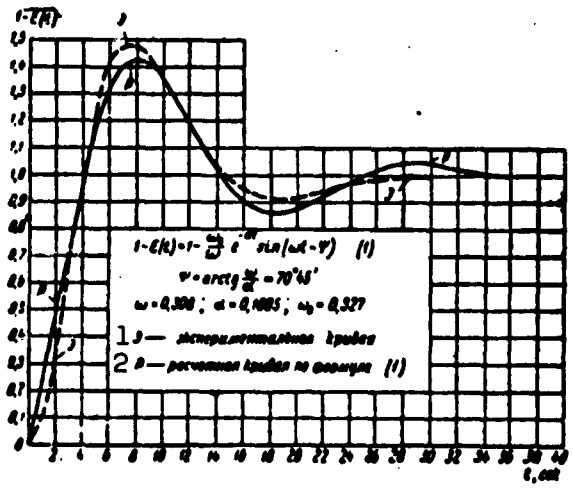

Fig. 21. 1) e – experimental curve; 2) r – curve calculated from Formula (1).

The curves of Figs. 21, 22 and 23 represent: the corresponding curve shown in Fig. 20, which we shall arbitrarily consider to be the curve obtained experimentally for the variation in the error upon application to the loop of the unit step function, the integral $\int_0^t \varepsilon(\tau)\,d\tau = Q_1(t)$ (Fig. 22), and the integral $\int_0^t \int_0^t \varepsilon(\tau)\,d\tau_1\,d\tau_2 = Q_2(t)$ (Fig. 23).

In the course of time, the curve of Fig. 21 tends to unity, i.e.,

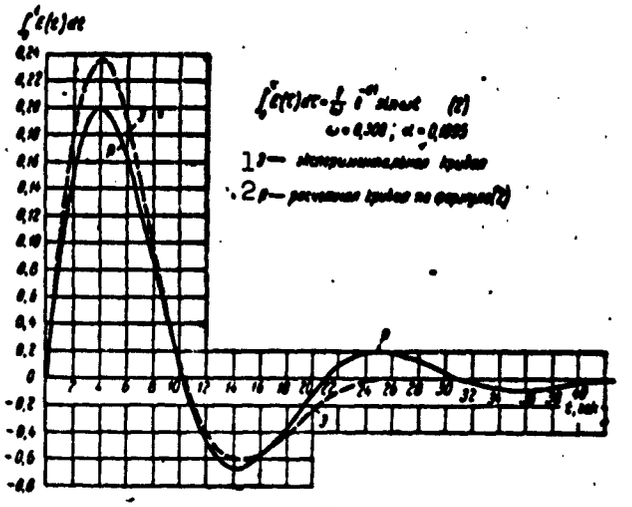

Fig. 22. 1) e – experimental curve; 2) r – curve calculated from Formula (2).

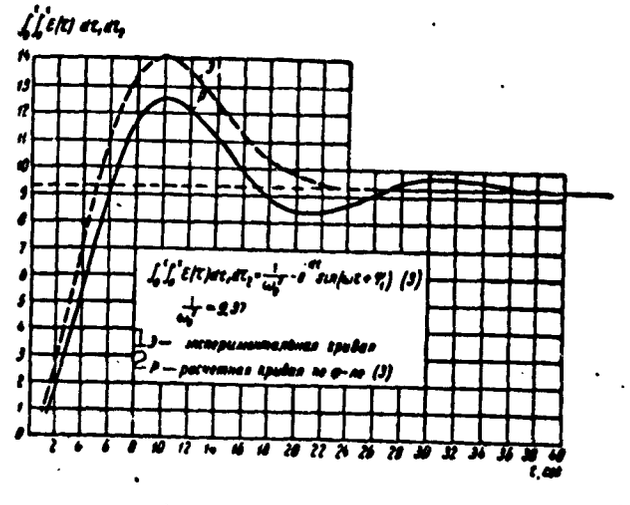

Fig. 23. 1) e – experimental curve; 2) r – curve calculated from Formula (3).

$\lim_{t\to\infty} \varepsilon(t) = 0$, and consequently the closed control loop contains at least a single integrating element, $m \geq 1$.

The curve of Fig. 22 approaches the x axis in the course of time. Thus, $\lim_{t\to\infty} \int_0^t \varepsilon(\tau)\,d\tau = 0$, from which it is clear that the closed control loop contains at least two integrating elements, $m \geq 2$.

Finally, the curve of Fig. 23 tends to a limit of 9.37 with time,

i.e.,

$$\lim_{t\to\infty}\int_0^t\int_0^t \varepsilon(\tau)\,d\tau_1\,d\tau_2 = \frac{a_0'}{b_0'} = 9{,}37.$$

Thus, the number of integrating elements in the control loop is m = = 2 and the quantity ω_0^2 in the expression for the equivalent transfer function

$$V_e(p) = \frac{2\alpha p + \omega_0^2}{p^2}$$

will equal

$$\omega_0^2 = \frac{1}{9{,}37} \quad \text{or} \quad \omega_0 = 0{,}327.$$

In order to determine the value of α in Formula (77), we use the curve of Fig. 21 to find the time at which the function ε(t) first passes through zero at t_1 = 4 sec.

Then according to Formula (83)

$$4\omega = -\psi = \operatorname{arctg}\frac{\omega}{\alpha}$$

or, going from the inverse trigonometric functions to the normal functions,

$$\sin 4\omega = \sin\left(\operatorname{arctg}\frac{\omega}{\alpha}\right) = \frac{\omega}{\sqrt{\omega^2+\alpha^2}} = \frac{\omega}{\omega_0} =$$
$$= 3{,}06\,\omega = 0{,}763\cdot 4\,\omega.$$

Solving the transcendental equation

$$\sin x = 0{,}763\,x, \text{ where } x = 4\omega,$$

we obtain

$$x = 70^\circ 45' = 1{,}23 \text{ rad}$$

whence

$$\omega = 0{,}308 \text{ rad/sec}; \alpha = \sqrt{\omega_0^2 - \omega^2} = 0{,}1095, \psi = -70^\circ 45'.$$

Thus, the equivalent loop transfer function for the transient shown in Fig. 21 can be represented as

$$Y_0(p)=\frac{0,215p+0,1095}{p^2}.$$

The error $\varepsilon_1(t)$ as a function of time, obtained experimentally for the case in which the control function $\varphi_{vkh}(t)$ acting on the system takes the form of a unit step function, enables us to find the error $\varepsilon(t)$ when a control function $\varphi_{vkh}(t)$ in the form of a power series with a finite number of terms acts upon the system.

The transform of the kth term $A_{k-1}t^{k-1}$ in the expansion for the control function $\varphi_{vkh}(t)$ is [see Formula (53)]

$$L|A_{k-1}t^{k-1}|=\frac{(k-1)!A_{k-1}}{p^k}. \qquad (84)$$

From the basic property of the Laplace transformation (see the footnote to Russian page 74)

$$L\left|\int_0^t \varepsilon_1(\tau)\,d\tau\right|=\frac{1}{p}L|\varepsilon_1(t)|.$$

If an experimentally obtained curve for $\varepsilon_1(t)$ is available, the expression $A_0\varepsilon_1(t)$ is the first term in the expansion for the error $\varepsilon(t)$ when a control function of the form

$$\varphi_{0n}(t)=A_0+A_1t+\ldots A_kt^k+A_nt^n. \qquad (85)$$

acts on the system. The expression

$$\frac{A_1}{p}L|\varepsilon_1(t)|=\frac{A_1}{p^2}\frac{1}{1+Y(p)}=L\left|A_1\int_0^t\varepsilon_1(\tau)\,d\tau\right|$$

is the transform of the second term of the expansion for $\varphi_{vkh}(t)$. Thus, the second term in the expansion for the error $\varepsilon_2(t)$ will equal

$$A_1\int_0^t\varepsilon(\tau)\,d\tau.$$

when the control function $\varphi_{vkh}(t)$ acts on the system.

In like manner, we find that the third term in the error expansion $\varepsilon_3(t)$ will equal

$$A_2 2! \int_0^t \int_0^t \varepsilon_1(\tau)\, d\tau_1\, d\tau_2$$

and so forth. Thus, if we obtain experimentally a function $\varepsilon_1(t)$, we can find not only the steady-state error $\varepsilon(t)$ when a control function of the type (85) acts upon the system, but we are also able to construct the entire transient process represented by the formula

$$\varepsilon(t) = A_0 \varepsilon_1(t) + A_1 \int_0^t \varepsilon_1(\tau)\, d\tau + 2! A_2 \int_0^t \int_0^t \varepsilon_1(\tau)\, d\tau_1\, d\tau_2 +$$

$$+ \ldots (k-1)! A_{k-1} \int_0^t \int_0^t \ldots \int_0^t \varepsilon_1(\tau)\, d\tau_1\, d\tau_2 \ldots d\tau_{k-1} +$$

$$+ \ldots n! \int_0^t \int_0^t \ldots \int_0^t \varepsilon_1(\tau)\, d\tau_1\, d\tau_2 \ldots d\tau_n. \qquad (86)$$

In practice, by making use of the experimental function obtained, $\varepsilon_1(t)$, and Formula (86), we are able to plot the curve $\varepsilon(t)$ with acceptable accuracy only when $\varphi_{vkh}(t)$ is a polynomial that is not of too high degree. If this is not the case, the errors accumulating in multiple successive graphical integration of the curve $\varepsilon_1(t)$ distort the results substantially.

The transient process can also be constructed with the aid of the equivalent transfer function $Y_e(p)$, by finding the originals for the transforms of the individual terms in the series forming $L\,|\varepsilon(t)|$, and using the expression

$$L|\varepsilon(t)| = \frac{1}{1 + Y_e(p)} \left[\frac{A_0}{p} + \frac{A_1}{p^2} + \ldots \frac{(k-1)! A_{k-1}}{p^k} + \right.$$

$$\left. + \ldots \frac{n! A_n}{p^{n+1}} \right]. \qquad (87)$$

for this purpose.

In order to illustrate these considerations, let us find the steady-state – "limiting" – error $\varepsilon(t)$ when a control function $\varphi_{vkh}(t)$, represented by Formula (74) acts upon a system in which the transient

$\varepsilon_1(t)$ for a unit step function takes the form shown in Figs. 19 and 20. Let us find the error $\varepsilon(t)$ at time t = 50 sec

$$\varphi_{вх}(t) = \varphi_0 + v_{вх0}\left(t + \frac{1}{2}a_1 t^2 + \frac{1}{3}a_2 t^3\right). \qquad (74)$$

As we have already shown by analyzing the curves of Figs. 21, 22, and 23, the closed loop having the transient shown in Figs. 19 and 20 has two integrating elements, m = 2, and the ratio of the constant terms in the polynomials A(p) and B(p), that form the open-loop transfer function, is

$$Y(p) = \frac{1}{p}\frac{B(p)}{A(p)}, \quad \frac{a_0}{b_0} = 9{,}37.$$

The steady-state error $\varepsilon(t)$ for time t = 50 sec, according to Formula (65), will equal

$$\varepsilon(t)_{\substack{t=50\\ \text{sec}}} = \frac{a_0}{b_0}(2A_2 + 3!A_3 t) = \frac{a_0}{b_0}(v_{вх0}a_1 + 2v_{вх0}a_2 t),$$

or, substituting in the numerical values of the coefficients

$$v_{вх0} = 0{,}07\ \text{km/sec};\ a_1 = 3{,}66\cdot10^{-2};\ a_2 = 2{,}73\cdot10^{-4},$$

$$\varepsilon(t)_{\substack{t=50\\ \text{sec}}} = 9{,}37\,(0{,}07\cdot3{,}66\cdot10^{-2} + 2\cdot0{,}07\cdot2{,}73\ 10^{-4}50) =$$

$$= 26\cdot2\cdot10^{-3}\ \text{km or } 26{,}2\ \text{m}.$$

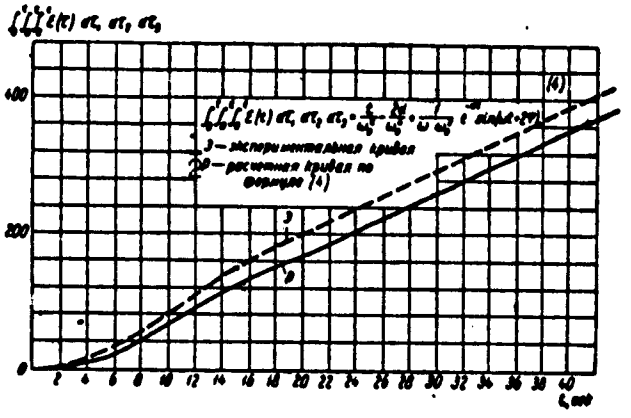

Fig. 24. 1) e – experimental curve;
2) r – curve calculated from Formula (4).

Figures 21, 22, 23, 24 and 25 show, in turn: the unit error

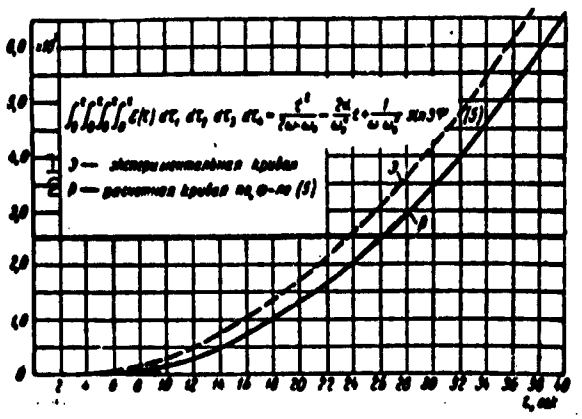

Fig. 25. 1) e – experimental curve;
2) r – curve calculated from Formula (5).

$\varepsilon_1(t)$, its integral $\int_0^t \varepsilon_1(\tau)\,d\tau$, the double integral $\int_0^t\int_0^t \varepsilon_1(\tau)\,d\tau_1\,d\tau_2$, the triple and quadruple integrals plotted from the "experimental" transient curve for the closed loop, Fig. 19 (or 21), labeled with the letter e, and the same integrals, calculated for a closed loop with equivalent parameters for which

$$Y_0(p)=\frac{2\alpha p+\omega_0^2}{p^2}=\frac{0{,}215\,p+0{,}1095}{p^2},$$

labled with the letter r.

By using these curves, we can find the error at an instant in time at which the transient in the closed loop has not yet died out.

Assuming, for example, that a control function $\varphi_{vkh}(t)$ defined by Expression (74) acts on the loop, and that

$$\varphi_0=0 \quad \text{and} \quad t=10 \text{ sec},$$

we find from Formula (86)

$$\varepsilon(t)_{t=10\,\text{sec}}=v_{\infty}\int_0^t \varepsilon_1(\tau)\,d\tau+2!\,v_{\infty}a_1\int_0^t\int_0^t \varepsilon_1(\tau)\,d\tau_1\,d\tau_2+$$

$$+3!\,v_{\infty}\int_0^t\int_0^t\int_0^t \varepsilon_1(\tau)\,d\tau_1\,d\tau_2\,d\tau_3.$$

Substituting into this formula, as before, the numerical values

$$v_{x_0} = 0{,}07 \text{km/sec}; \; a_1 = 3{,}66 \cdot 10^{-3}; \; a_2 = 2{,}73 \cdot 10^{-4}$$

and finding from the curves of Figs. 22, 23, and 24 the values of the ordinates at t = 10 sec, we obtain the following error values:

$$\varepsilon(t)_{t=10\,\text{sec}} = 0{,}07 \cdot 0{,}1 + 2 \cdot 0{,}07 \cdot 3{,}66 \cdot 10^{-3} \cdot 14 +$$
$$+ 3 \cdot 0{,}07 \cdot 2{,}73 \cdot 10^{-4} \cdot 80 = 7 \cdot 10^{-3} + 71{,}7 \cdot 10^{-3} + 9 \cdot 10^{-3} \approx 88 \text{ m}.$$

A determination of $\varepsilon(t)$ at t = 10 sec from the corresponding calculated curves gives

$$\varepsilon_e(t)_{t=10\,\text{sec}} \approx 79 \text{ m}.$$

Thus, in the case given, the difference in the errors found directly from experimental data, and found with the aid of the equivalent transfer function $Y_e(p)$ turns out to be small.

4. OTHER TYPES OF EQUIVALENT CLOSED-LOOP CONTROL DIAGRAM

As we have already noted, Figs. 1 and 14 illustrate the basic equivalent diagram for a guided missile with a continuous closed loop; this is not the only possible arrangement, however.

The loop of Fig. 26 is a development of the control loop shown in Fig. 14; it contains additional means for compensating dynamic errors.

The operating principle of the loop of Fig. 26 consists in the following.

If the open control loop transfer function $Y_e(p)$ is known, it is possible to find the magnitude of the error in the closed loop $\varepsilon(p)$ or $\varepsilon(t)$. Knowing the error, it is possible to produce control commands that will correspond to the kinematic trajectory corrected for the error. This is shown in Fig. 27, where curve a represents the kinematic trajectory, curve b the dynamic trajectory, and curve c the kinematic trajectory corrected for the error.

If the missile is required to move as close as possible to the kinematic trajectory a, if the control function $\varphi_{1vkh}(p)$, which cor-

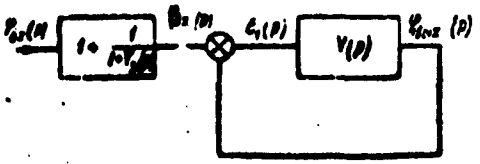

Fig. 26

responds to the corrected kinematic trajectory c, is applied to the closed-loop input, the missile can be forced to move almost precisely along path a.

Let us find the error for this case.

According to (49), the function $\varphi_{1vykh}(p)$ at the loop output will equal

$$\varphi_{1\,вых}(p) = \varphi_{вх}(p)\frac{Y(p)}{1+Y(p)}. \qquad (49)$$

In turn, the input function $\varphi_{1vkh}(p)$ equals the function $\varphi_{vkh}(p)$ corresponding to the kinematic trajectory, corrected for the error, which equals in accordance with (50)

$$\varepsilon_e(p) = \varphi_{вх}(p)\frac{1}{1+Y_e(p)}. \qquad (50a)$$

The subscript "e" in Formula (50) indicates that the transfer function $Y_e(p)$ may not be known accurately, and may not completely correspond to the actual transfer function Y(p).

Fig. 27

Inserting in front of the closed loop an element having a transfer function equaling 1 + + [1/1 + $Y_e(p)$], we obtain

$$\varphi_{1\,вх}(p) = \varphi_{вх}(p)\left(1+\frac{1}{1+Y_e(p)}\right) = \varphi_{вх}(p)+\varepsilon_e(p).$$

Thus, the function $\varphi_{1vykh}(p)$ at the loop output turns out to equal, on the basis of Expression (49),

$$\varphi_{1вых}(p) = \varphi_{вх}(p)\frac{Y(p)}{1+Y(p)} =$$
$$= \varphi_{вх}(p)\left(1+\frac{1}{1+Y_e(p)}\right)\frac{Y(p)}{1+Y(p)}.$$

or

$$\varphi_{1\,вых}(p) = \varphi_{вх}(p)\frac{2Y(p)+Y(p)Y_e(p)}{(1+Y_e(p))(1+Y(p))}. \qquad (88)$$

The difference between $\varphi_{vkh}(p)$ and $\varphi_{1vykh}(p)$ or the transform of the empirical error $\varepsilon_k(p)$ will equal

$$\varepsilon_k(p) = \varphi_{ex}(p) - \varphi_{1\,exx}(p) = \\ = \varphi_{ex}(p)\left[1 - \frac{2Y(p) + Y(p)Y_e(p)}{(1+Y_e(p))(1+Y(p))}\right] = \\ = \varphi_{ex}(p)\frac{1+Y_e(p)-Y(p)}{(1+Y_e(p))(1+Y(p))}. \qquad (89)$$

For the special case in which the supposed loop transfer function $Y_e(p)$ equals the actual transfer function $Y(p)$, the error $\varepsilon_k(p)$ will equal

$$\varepsilon_k(p) = \varphi_{ex}(p)\frac{1}{(1+Y(p))^2}. \qquad (90)$$

Expression (90) indicates that where the transfer functions are equal, $Y_e(p) = Y(p)$, the error in the "compensated" circuit of Fig. 26 is incomparably less than the error in the circuit of Fig. 14. Actually, the error transform in the loop of Fig. 26 equals, by Formula (90),

$$\varepsilon_k(p) = \varphi_{ex}(p)\frac{1}{(1+Y(p))^2} = \varepsilon(p)\frac{1}{1+Y(p)}, \qquad (91)$$

where $\varepsilon(p)$ is the error transform in the uncompensated loop of Fig. 14.

Using the error transform $\varepsilon(p)$, by Formula (54), we find that

$$\varepsilon_k(p) = \varepsilon(p)\frac{1}{1+\frac{1}{p^m}\cdot\frac{B(p)}{A(p)}} = \\ = \left(\frac{A_0}{p} + \frac{A_1}{p^2} + \frac{2A_2}{p^3} + \ldots \frac{A_{k-1}\cdot(k-1)!}{p^k}\right)\times \\ \times \frac{1}{\left[1+\frac{1}{p^m}\cdot\frac{B(p)}{A(p)}\right]^2}. \qquad (92)$$

In the limit, when $t \to \infty$, the kth term of Expression (92) approaches the value

$$\lim_{t\to\infty} C_k(t) = \lim_{p\to 0}\frac{(k-1)!\,A_{k-1}p^{2m+1-k}}{\left(p^m + \frac{B(p)}{A(p)}\right)^k}. \qquad (93)$$

Thus, if $2m + 1 = k$, $C_k(t)$ tends to a constant value. If $2m + 1 - k > 0$, then $C_k(t)$ tends toward zero.

It follows from this that if the control function $\varphi_{vkh}(t)$ can be represented by a polynomial of degree k, then when $k < 2m + 1$, the dynamic error will tend to zero in the limit.

In particular, where $m = 1$, the dynamic error tends to zero when $k < 3$. Where $m = 2$, the dynamic error tends to zero when $k < 5$.

When $k = 5$ and the transfer function Y(p) has the form represented by Formula (57),

$$\lim_{t\to\infty} \varepsilon(t) = \lim_{t\to\infty} C_5(t) = \lim_{p\to 0} \frac{4! A_4}{\left(p^2 + \frac{B(p)}{A(p)}\right)^5} = 24 A_4 \left(\frac{a_0}{b_0}\right)^5 \qquad (94)$$

etc.

For example, for the case in which the control function can be represented by Formula (90) when $m = 2$, the dynamic error turns out to equal zero in the limit, instead of having the values that were found on page 65, and in the succeeding examples.

The transient resulting in the circuit of Fig. 26 when a unit step function is applied to the input will differ from a transient process in the circuit of Fig. 14.

For example, if the open-loop transfer function equals

$$Y(p) = \frac{2\alpha p + \omega^2}{p^2}, \qquad (77)$$

the error transform, according to Formulas (82) and (92), will equal

$$\varepsilon_k(p) = \varepsilon(p) \frac{1}{1 + Y(p)} = \frac{p^3}{[(p+\alpha)^2 + (\omega_0^2 - \alpha^2)]^3}. \qquad (95)$$

The original of this transform is

$$\varepsilon_k(t) = \frac{\omega_0^2}{2\omega^2} e^{-\alpha t}\left[\frac{1}{\omega_0^2}\sqrt{\frac{\alpha^2}{\omega^2}(\omega_0^2 + \omega^2)^2 + 4\omega^4} \times \right.$$
$$\left. \times \sin(\omega t + \varphi_1) + \omega_0 t \cos(\omega t + \psi_2)\right], \qquad (96)$$

where $\omega_0^2 = \omega^2 + \alpha^2$, instead of the $\varepsilon(t)$ found from Formula (83) for the uncompensated loop of Fig. 14.

In view of the fact that, as we shall show later, the kinematic trajectories can normally be represented by curves of degree five or higher, for which the error in the fully compensated loop is either zero or negligibly small, there is no point in a more detailed examination of Formula (96).

Actually, however, total compensation cannot be achieved in the circuit of Fig. 26, since it is impossible to ensure that $Y_e(p) = Y(p)$. The coefficients in the transfer function Y(p) of a real control loop containing a missile are not constants. They depend upon missile speed, the density of the medium in which it moves, and upon many other parameters that vary while the missile is moving.

Thus, even if it were possible for $Y_e(p) = Y(p)$, for some single flight regime or portion of the trajectory, it is impossible to ensure this equality for other sections of the path. In addition, the transfer function for a real control loop Y(p) is considerably more complicated than the equivalent function $Y_e(p)$ that can be formulated diagramatically.

Let us see how a compensated loop makes it possible to decrease the dynamic errors when $Y_e(p) \neq Y(p)$.

Let the transfer functions of the real and equivalent control loops be, respectively,

$$Y(p) = \frac{1}{p^m}\frac{B(p)}{A(p)} \text{ and } Y_e(p) = \frac{1}{p^m}\frac{B_1(p)}{A_1(p)},$$

where A(p), B(p), $A_1(p)$ and $B_1(p)$ are polynomials of various degrees with constant terms.

According to Formula (89), the error in a compensated loop may be represented as follows:

$$\varepsilon_k(p) = \varphi_{ex}(p)\frac{1 + Y_e(p) - Y(p)}{(1 + Y_e(p))(1 + Y(p))} =$$

$$= \varepsilon_0(p) + \varepsilon(p)\frac{Y_e(p) - Y(p)}{1 + Y_e(p)}, \qquad (97)$$

where $\varepsilon_0(p)$ is the dynamic error for ideal compensation [Formula (90)], and $\varepsilon(p)$ is the dynamic error in the uncompensated control loop.

Substituting the values of Y(p) and $Y_e(p)$ into Formula (97), we find

$$\varepsilon_k(p) = \varepsilon_0(p) + \varepsilon(p)\frac{\frac{B_1(p)}{A_1(p)} - \frac{B(p)}{A(p)}}{p^m + \frac{B_1(p)}{A_1(p)}}. \qquad (98)$$

Let us find the limit to which the error $\varepsilon_k(t)$ tends when $t \to \infty$,

$$\varepsilon_{k\,t\to\infty} = \varepsilon_{0\,t\to\infty} + \varepsilon_{t\to\infty}\frac{\frac{b_1}{a_1} - \frac{b}{a}}{\frac{b_1}{a_1}}, \qquad (99)$$

and if we represent the difference in the ratio of the constant terms by means of the ratio of the constant terms in the equivalent transfer function

$$\frac{b_1}{a_1} - \frac{b}{a} = \frac{1}{k}\cdot\frac{b_1}{a_1},$$

then

$$\varepsilon_{k\,t\to\infty} = \varepsilon_{0\,t\to\infty} + \varepsilon_{t\to\infty}\frac{1}{k}.$$

As we have already shown, the dynamic error in a fully compensated loop normally is zero, $\varepsilon_0(t) \to 0$. Thus, the steady-state error in a loop that is not fully compensated will equal the error in an uncompensated loop divided by a factor of $\underline{k}$.

Thus, as we can see from Expression (99), the decrease in the steady-state error remaining after a transient has died out will depend solely upon the magnitude of the constant terms in the polynomials A(p), B(p), $A_1(p)$, and $B_1(p)$, and will be independent of all the remaining terms in these polynomials.

For example, if the transfer functions for the real and equivalent

control loops are represented by Formula (77) and the difference $(\omega_{0e}^2 - \omega_0^2)/\omega_{0e}^2) = 0.1$, the dynamic error, calculated from the example of page 65 will be 2.62 m, rather than 26.2 m, regardless of how the coefficients α and α_e may differ or whether or not there are terms in the numerators of Formula (77) with powers greater than $\underline{p}$.

Thus, it is possible to construct compensated diagrams of the type of Fig. 26, in which the transfer function $Y_e(p)$ is considerably simpler than the transfer function $Y(p)$ of the actual loop, and that, nonetheless, under steady-state conditions will have completely satisfactory compensation of dynamic errors.

A transient process depends heavily upon the relationships of all of the terms in the polynomials $A(p)$, $B(p)$, $A_1(p)$, and $B_1(p)$, and thus the dynamic errors in the transient state will be determined by all of the terms in Expression (98).

Errors in a compensated loop are damped more slowly than in an uncompensated loop. Thus, in some cases, compensation may prove to be unsuitable from the point of view of the size of fluctuation errors.

Manuscript Page No.

[Footnotes]

71 Formula (79) follows from the basic definition

$$L\left|\int s_1(\tau)\,d\tau\right| = \frac{1}{p}L|s_1(t)| + \frac{1}{p}\int_{t=0} s_1(\tau)\,d\tau,$$

whence

$$L\left|\int_{\tau=t} s_1(\tau)\,d\tau - \int_{t=0} s_1(\tau)\,d\tau\right| = L\left|\int_0^t s_1(\tau)\,d\tau\right| = \frac{s_1(p)}{p}.$$

Manuscript Page No.

[List of Transliterated Symbols]

54 Ц = ts = tsel' = target

54 С = s = snaryad = missile

55 сек = sek = sekundy = seconds

63 Н = n = normal'nyy = normal

65 макс = maks = maksimal'nyy = maximal

68 э = e = ekvivalentnyy = equivalent

Chapter 5

FORM OF CONTROL FUNCTIONS AND DYNAMIC ERRORS FOR VARIOUS CONTROL METHODS

1. MOTION OF MISSILE IN RESPONSE TO COMMANDS

The three-point method

In the preceding chapter, we obtained an expression for the control function $\varphi_{vkh}(t)$ for a missile using beam-rider control (the three-point method) with the missile and target moving at constant speed, and the target moving in a straight line toward the control point, i.e., where the missile is fired to meet the target [Fig. 18 and Formula (73)]. For examples of this case, we computed the dynamic errors for certain arbitrarily selected control-loop data.

We continue our examination of control functions, and calculate the dynamic errors for the case in which the missile is controlled in accordance with the three-point method, but with somewhat different target and missile motion conditions.

Target moving away from control point (pursuit course)

For this case (Fig. 18), the signs before v_{ts} and $\underline{m}$ in Formulas (70) and (71) should be reversed.

Thus, as in the case of a collision course,

$$v_s = v_{s0}(1 + a_1 t + a_2 t^2 + a_3 t^3 + \ldots) \qquad (72)$$

and the control function will take the form (73)

$$\varphi_{sk}(t) = \int v_s\, dt = \varphi_0 + v_{s0}\left(t + \frac{1}{2} a_1 t^2 + \frac{1}{3} a_2 t^3 + \right.$$

$$+\frac{1}{4}a_3t^4+\dots\Big)=A_0+A_1t+A_2t^2+A_3t^3+A_4t^4+\dots \qquad (73)$$

Owing to the change in signs of $\underline{m}$ and v_{ts}, the values of the coefficients in Formulas (72) and (73) prove to be somewhat different

$$a_1=q-m;\ a_2=-ma_1-n;\ a_3=-ma_2-na_1;$$
$$a_4=-ma_3-na_2 \text{ etc.}$$

Let us examine a numerical example (Fig. 18)

$$y_0=60\ км;\ D=50\ км;\ r_0=35\ км;$$
$$v_n=0{,}5\ \text{km/sec};\ v_c=1\ \text{km/sec}.$$

The target moves away from the control point along the line BA.

In this case

$$v_{n0}=-0{,}144\ \text{km/sec};\ q=2{,}86\cdot10^{-2};$$
$$m=9{,}9\cdot10^{-3};\ n=4{,}1\cdot10^{-5};$$
$$a_1=1{,}87\cdot10^{-2};\ a_2=-2{,}26\cdot10^{-4};$$
$$a_3=1{,}47\cdot10^{-6};\ a_4=5{,}29\cdot10^{-9}.$$

The time of impact of the missile with the target can be roughly estimated to be

$$t_0\approx\frac{R_0-r_0}{v_c-v_n\cos\beta}=70\ \text{sec}.$$

At this time, the value of the control function will equal

$$\underset{t=70\text{sec}}{\varphi_{vkh}(t)}=\varphi_0+v_{n0}(70+45{,}8-25{,}8+8{,}8+1{,}8+\dots).$$

Thus, in Expression (73), at least four terms of the function $\varphi_{vkh}(t)$ should be taken (including φ_0).

If we assume, as we did in the preceding examples, that the missile control loop contains two integrating elements, m = 2, and that $a_0/b_0 = 9.37$ for it, then from Formula (65)

$$\underset{t=70\text{sec}}{\varepsilon(t)}=\frac{a_0}{b_0}v_{n0}(a_1+2a_2t+3a_3t^2)=$$

$$= 1{,}35(1{,}87\cdot10^{-2} + 2\cdot2{,}26\cdot10^{-4}\cdot70 + \\ + 3\cdot1{,}47\cdot10^{-6}\cdot4{,}9\cdot10^{-3}) \approx 8{,}7\ м.$$

Uniformly accelerated or retarded motion of missile

If the rate of motion of the missile is not constant, but increases linearly with time, i.e.,

$$v_c = v_{c0} + w_c t, \tag{99}$$

then Formula (70), corresponding to the constant missile-speed case will take the form

$$v_u = v_{u0}\frac{Dr_0}{R_0^2}\cdot\frac{1 + \frac{v_{c0}}{r_0}t + \frac{w_c}{r_0}t^2}{1 - \frac{2y_0v_{u0}}{R_0^2}t + \frac{v_{u0}^2}{R_0^2}t^2}. \tag{100}$$

retaining the notation used in Formula (71), and, in addition, letting $w_s/r_0 = u$, we find

$$v_u = v_{u0}\frac{1 + qt + ut^2}{1 - mt + nt^2}, \tag{101}$$

or

$$v_u = v_{u0}(1 + a_1t + a_2t^2 + a_3t^3 + \ldots), \tag{102}$$

where

$$a_1 = q + m;\quad a_2 = ma_1 + u - n;\quad a_3 = ma_2 - na_1;$$
$$a_4 = ma_3 - na_2 \text{ etc.}$$

Example.

$$y_0 = 100\ км;\quad D = 50\ км;\quad r_0 = 35\ км;\quad v_c = 0{,}5\ \text{km/sec};$$
$$v_{c0} = 0{,}7\ \text{km/sec};\quad w_c = 0{,}01\ \text{km/sec}^2.$$

then

$$v_{u0} = 0{,}07\ \text{km/sec};\quad q = 2\cdot10^{-2};\quad m = 8\cdot10^{-2};$$
$$n = 2\cdot10^{-3};\quad u = 2{,}9\cdot10^{-4};\quad a_1 = 2{,}8\cdot10^{-2};$$
$$a_2 = 5{,}1\cdot10^{-4};\quad a_3 = 3{,}5\cdot10^{-6}.$$

According to Formula (73)

$$\varphi_m(t) = \varphi_0 + v_{m0}\left(t + \frac{1}{2}a_1 t^2 + \frac{1}{3}a_2 t^3 + \ldots\right).$$

If we assume, as in the preceding examples, that m = 2 and $a_0/b_0 = 1/\omega_0^2 = 9.37$, we find for the steady-state error value

$$\varepsilon(t) = \frac{a_0}{b_0} v_{m0}(a_1 + 2a_2 t + 3a_3 t^2 + \ldots).$$

Substituting into this formula, for example, t = 50 sec, we obtain

$$\varepsilon(t)_{t=50\,\text{sec}} = 0{,}66(2{,}8\cdot 10^{-2} + 2\cdot 5{,}1\cdot 10^{-4}\cdot 50 + 3\cdot 35\cdot 10^{-6}\cdot 2{,}5\cdot 10^{3}) \approx 41\ м.$$

We shall not examine in detail the case of uniformly retarded missile motion, for which the corresponding expression can be obtained from Formulas (101) and (102) by changing the sign of u; instead, we examine the case in which the missile acceleration changes in an instantaneous jump. In particular, this corresponds to missile motor burnout, when accelerated motion or motion at constant speed changes instantaneously to retarded motion owing to the braking effect of the medium.

If the missile moves with uniform acceleration until time t_1, and its speed at $t < t_1$ equals

$$v_c = v_{c0} + w_{1c}t,$$

and then, from time $t = t_1$, it moves with deceleration at a speed

$$v_c = v_{c0} + w_{1c}\cdot t_1 - w_{2c}(t - t_1),$$

we may represent this as a continuation of uniformly accelerated motion, to which at time t_1 there is added the negative acceleration $(w_{1s} + w_{2s})$.

In other words,

$$v_c = v_{c0} + w_{1c} t - (w_{2c} + w_{1c})(t - t_1).$$

For this case, Formula (99) can be rewritten:

$$v_u = v_u \frac{D r_0}{R_0^2} \cdot \left[\frac{1 + \frac{v_{c0}}{r_0} t + \frac{w_{1c}}{r_0} t^2}{1 - \frac{2 y_0 v_u}{R_0} t + \frac{(v_u t)^2}{R_0^2}} - \right. \\ \left. - \frac{\frac{w_{2c} + w_{1c}}{r_0} (t - t_1)^2}{1 - \frac{2 y_0 v_u}{R_0} t + \frac{(v_u t)^2}{R_0^2}} \right], \tag{103}$$

or

$$v_u = v_{u0} \frac{1 + q t + u t^2}{1 - m t + n t^2} - v_{u0} \frac{u_1 \tau^2}{1 - m(t_1 + \tau) + n(t_1 + \tau)^2}. \tag{104}$$

we let

$$v'_{u0} = \frac{v_{u0}}{1 - m t_1 + n t_1^2}; \quad m_1 = \frac{m - 2 n t_1}{1 - m t_1 + n t_1^2};$$

$$n_1 = \frac{n}{1 - m t_1 + n t_1^2};$$

Then the second term in the right side of Formula (104) can be written as

$$\Delta v_u = v_{u0} \frac{u_1 \tau^2}{1 - m(t_1 + \tau) + n(t_1 + \tau)^2} = \\ = v'_{u0} \frac{u_1 \tau^2}{1 - m_1 \tau + n_1 \tau^2}$$

or, approximately,

$$\Delta v_u = v'_{u0} [u_1 \tau^2 + m_1 u_1 \tau^3 + (m_1^2 - n_1) u_1 \tau^4 + \ldots].$$

Thus, the increment in the control function $\varphi_{vkh}(t)$ proves to equal

$$\Delta \varphi_{vkh}(t) = v'_{u0} u_1 \left(\frac{\tau^3}{3} + \frac{m_1 \tau^4}{4} + \frac{(m_1^2 - n_1) \tau^5}{5} + \ldots \right). \tag{105}$$

The pertubation, i.e., the additional change in the error $\varepsilon(t)$, due to the instantaneous change in missile acceleration, can be found for the transient process during the first seconds after the jump has

taken effect by Formula (86), using multiple integration of the experimental curve $\varepsilon_1(t)$.

In view of the fact that the lowest power of the time in Formula (105) is τ^3, in the right side of Formula (86), it is necessary to start with the triple integrals, i.e.,

$$\Delta\varepsilon(t) = 2 v_{\text{в}}'_0 a_1 \int_0^t \int_0^t \int_0^t \varepsilon_1(\tau)\, d\tau_1\, d\tau_2\, d\tau_3 +$$

$$+ 3 v_{\text{в}}'_0 a_1 m_1 \int_0^t \int_0^t \int_0^t \int_0^t \varepsilon_1(\tau)\, d\tau_1\, d\tau_2\, d\tau_3\, d\tau_4 .$$

As an illustration, let us make a slight change in the conditions of the preceding example; we will assume that prior to time t_1 = = 45 sec, the missile moves with uniform acceleration at w_s = = 0.01 km/sec^2, while after the 45th second, the missile moves with uniform deceleration at w_{2s} = -0.02 km/sec^2. Thus,

$$y_0 = 100 \text{ км};\quad D = 50 \text{ км};\quad r_0 = 35 \text{ км};\quad t_1 = 45 \text{ sec};$$
$$v_{\text{в}} = 0{,}5 \text{ km/sec};\quad v_{\text{с.с}} = 0{,}7 \text{ km/sec};\quad w_{1c} = 0{,}01 \text{ km/sec}^2;$$
$$w_{2c} = -0{,}02 \text{ km/sec}^2;\quad 1 - m t_1 + n t_1^2 = 0{,}68;\quad v_{\text{в}}'_0 = 0{,}103;$$
$$m_1 = 9{,}1\ 10^{-3};\quad n_1 = 2{,}94 \cdot 10^{-5};\quad a_1 = 8{,}6 \cdot 10^{-4}.$$

Let us find the additional error $\Delta\varepsilon(t)$ 5 sec after the instantaneous change in acceleration, i.e., at t = 50 sec, as in the preceding example.

Then, using the curves of Figs. 24 and 25, we obtain

$$\Delta\varepsilon(t) = 2 \cdot 0{,}103 \cdot 8{,}6 \cdot 10^{-4} \cdot 24 +$$
$$+ 6 \cdot 0{,}103 \cdot 8{,}6 \cdot 10^{-4} \cdot 9{,}1 \cdot 10^{-3} \cdot 40 \approx 4{,}4 \text{ м}.$$

Thus, in the case given, the change in missile acceleration leads to a decrease in the error.

It is interesting to note that a step-type change in the longitudinal acceleration of the missile causes a perturbation in the direction perpendicular to the path.

Target evasive action

In the simplest case in which the target moves in a curved path, the trajectory will be a circle, along which the target moves with a constant speed $v_{ts} = \Omega\rho$, where ρ is the radius of the circle. At the initial instant, the target is at point a, where the tangent to the trajectory forms angle β_0 with the line joining point a and the control point 0 (Fig. 28).

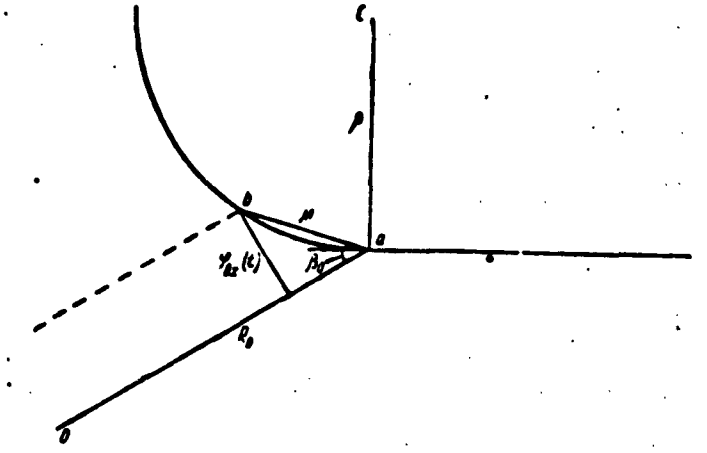

Fig. 28

Let the distance R_0 be so large in comparison with ρ, the radius of curvature of the target path, that the lines Oa and Oc, joining the two points a and c on this path with the control point 0 can be assumed to be parallel.

The control function $\varphi_{vkh}(t)$ will in this case represent the distance between the lines R_0 and R as a function of time, and may be expressed as

$$\varphi_{vkh}(t) = M \sin\left(\beta_0 + \frac{\Omega t}{2}\right),$$

where

$$M = 2\rho \sin\frac{\Omega t}{2}.$$

Then,

$$\varphi_{ex}(t) = 2\rho \sin\frac{\Omega t}{2}\sin\left(\beta_0 + \frac{\Omega t}{2}\right) =$$
$$= \rho(\cos\beta_0 - \cos\beta_0\cos\Omega t + \sin\beta_0\sin\Omega t). \qquad (106)$$

The control function (106) cannot be represented as a power series with a finite number of terms. Thus, in order to find the error in the case given, it is more convenient to use its transform

$$\varepsilon(p) = \varphi_{ex}(p)\frac{1}{1+Y_0(p)},$$

substituting into it the equivalent transfer function obtained from experimental data. In particular, when there are two integrating elements in the control loop, we may take as the transfer function

$$Y_0(p) = \frac{2\alpha p + \omega^2}{p^2}. \qquad (77)$$

The transform of Function (106) equals

$$\varphi_{ex}(p) = \rho\left[\frac{\cos\beta_0}{p} - \frac{\cos\beta_0 p}{p^2+\Omega^2} + \frac{\sin\beta_0\Omega}{p^2+\Omega^2}\right], \qquad (107)$$

while the error transform is

$$\varepsilon(p) = \frac{\rho\Omega}{(p^2+2\alpha p+\omega^2)(p^2+\Omega)}\cdot[\Omega\cos\beta_0 p + \sin\beta_0 p^2]. \qquad (108)$$

Considering the error transform $\varepsilon'(p)$ as the sum of two terms $\varepsilon_1(p) + \varepsilon_2(p)$, we find the originals of these terms

$$\varepsilon_1(t) = \frac{\rho\Omega^2\cos\beta_0}{\sqrt{(\omega_0^2-\Omega^2)^2+4\alpha^2\Omega^2}}\times$$
$$\times\left[\sin(\Omega t+\psi_1) + \frac{\omega_0}{\omega}e^{-\alpha t}\sin(\omega t+\psi_2)\right];$$
$$\varepsilon_2(t) = \frac{\rho\Omega\sin\beta_0}{\sqrt{(\omega_0^2-\Omega^2)^2+4\alpha^2\Omega^2}}\times \qquad (109)$$
$$\times\left[-\Omega\sin(\Omega t+\psi_3) + \frac{\omega_0^2}{\omega}e^{-\alpha t}\sin(\omega t+\psi_4)\right],$$

where

$$\psi_1 = \frac{\pi}{2} - \operatorname{arctg}\frac{2\alpha\Omega}{\omega_0^2 - \Omega^2};$$

$$\psi_2 = \operatorname{arctg}\frac{\omega}{-\alpha} - \operatorname{arctg}\frac{-2\alpha\omega}{-(\omega^2 - \alpha^2 - \Omega^2)};$$

$$\psi_3 = -\operatorname{arctg}\frac{2\alpha\Omega}{\omega_0^2 - \Omega^2};$$

$$\psi_4 = \operatorname{arctg}\frac{-2\alpha\omega}{-(\omega^2 - \alpha^2)} - \operatorname{arctg}\frac{-2\alpha\omega}{-(\omega^2 - \alpha^2 - \Omega^2)}.$$

In order to get a clear idea of the change in the error (miss distance) as a function of the time of missile-target impact after the latter has begun to take evasive action, let us examine the following numerical example

$$\rho = 10 \text{ km}; \quad v_u = \rho\Omega = 0{,}5 \text{ km/sec}; \quad \Omega = 5\cdot 10^{-2} \text{ rad/sec};$$
$$\beta_0 = 45°; \quad \omega_0 = 0{,}707 \text{ rad/sec}; \quad \alpha = 0{,}25; \quad \omega = 0{,}6614 \text{ rad/sec}.$$

Substituting the appropriate values into Formula (109) and carrying out trigonometric manipulations, we find

$$\varepsilon(t) = 5{,}02\cdot 10^{-2}\cos(\Omega t + 42°) + 0{,}534\, e^{-\alpha t}\sin(\omega t - 4°6').$$

This would be the magnitude of the error for the case in which the missile moved first along a fixed beam, and then at time t=0 began to move along the target-tracking beam in a circle, as shown in Fig. 28.

A more natural case is that in which the target first moves in a straight line, and then executes a turn of radius ρ. In this case, prior to t = 0, the function $\varphi_{0vkh}(t)$ will act at the missile loop input; this corresponds to straight-line target flight, and for very large values of the distance R_0 will equal

$$\varphi_{0\,ex}(t) = v_u \sin\beta_0 t.$$

Owing to the presence in the control loop of integrating elements, the error will equal zero during this extended motion. From time t =

= 0, a transient will appear in the loop due to the control-function difference

$$\varphi_{\Sigma вх}(t) = \varphi_{вх}(t) - \varphi_{0 вх}(t). \qquad (110)$$

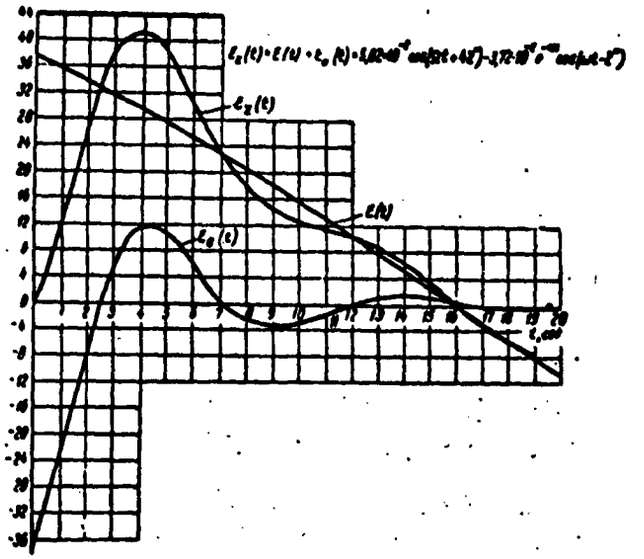

Fig. 29

Keeping the data of the preceding example, we find that in this case, the error will equal

$$\varepsilon_{\Sigma}(t) = \varepsilon(t) - \varepsilon_0(t) = 5{,}02 \cdot 10^{-3} \cos(\Omega t + 42°) +$$
$$+ 0{,}534\, e^{-\omega t} \sin(\omega t - 4°\,6') - 0{,}534\, e^{-\omega t} \sin \omega t =$$
$$= 5{,}02 \cdot 10^{-3} \cos(\Omega t + 42°) - 3{,}72 \cdot 10^{-3} e^{-\omega t} \cos(\omega t - 2°).$$

Figure 29 shows the total error and its components: one, corresponding to the steady-state process, and a second, corresponding to the transient process.

If the target executes an "inside" rather than an "outside" turn, as shown in Fig. 28, then in place of Formula (106), we will have for the function $\varphi_{vkh}(t)$

$$\varphi_{ex}(t) = 2\rho \sin\frac{\Omega t}{2} \sin\left(\beta_0 - \frac{\Omega t}{2}\right) = \quad (111)$$
$$= \rho\left[\cos\beta_0(1-\cos\Omega t) - \sin\beta_0 \sin\Omega t\right].$$

Thus

$$\varepsilon(t) = \varepsilon_1(t) - \varepsilon_2(t), \quad (112)$$

where $\varepsilon_1(t)$ and $\varepsilon_2(t)$ have the values shown in Formula (109).

Using the same numerical data as for the preceding example, we find that

$$\varepsilon(t) = 5{,}02\cdot 10^{-3}\cos(\Omega t + 42°) - 0{,}534\, e^{-\omega t}\sin(\omega t - 4°6') -$$
$$- 0{,}534\, e^{-\omega t}\sin\omega t.$$

Motion toward instantaneously predicted point

When missile movement is controlled by the three-point method, straight-line motion of the target with constant target and missile speeds v_s and v_{ts} gives rise to a dynamic error $\varepsilon(t)$ due to the fact that the beam along which the missile rides is not fixed, but tracks the target. The dynamic error can be eliminated if with straight-line and uniform target motion and constant missile speed, missile motion is directed toward a previously computed target impact point. Then missile motion will take place along a fixed line, which eliminates the possible appearance of a dynamic error.

If the target does not move in a straight line, while the speeds of target and missile are not constant, one method of controlling missile motion is that in which the missile, moving along the kinematic trajectory, will always be pointed at the instantaneously predicted impact point. By the instantaneously predicted point, we mean that point in space at which the missile and target would meet if their velocities would retain the magnitude and direction that they have at the instant of time under consideration.

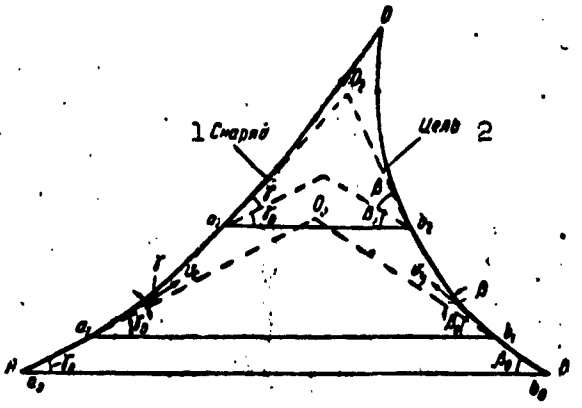

Fig. 30. 1) Missile; 2) target.

Figure 30 shows a plot of the kinematic trajectory for the case in which the missile moves toward the instantaneously predicted point of impact with the target.

It follows from simple geometric considerations that when the missile moves toward the predicted impact point, the condition

$$v_c \sin(\gamma + \gamma_0) = v_{ts} \sin(\beta + \beta_0), \qquad (113)$$

should be observed, where the angle β is the moving angle between the vector corresponding to the target speed v_{ts} and the straight line AB joining the target and the missile at the initial instant of time.

Condition (113) is satisfied for any values of the angle $(\beta + \beta_0)$ if the missile velocity v_s is greater than the target velocity v_{ts}.

A property of the missile path when it moves toward an instantaneously predicted point follows from Condition (113), namely, the fact that the lines a_0b_0, a_1b_1, a_2b_2 connecting together the corresponding points on the target and missile paths are parallel to each other. Thus, the control method in which the missile is directed toward the instantaneously predicted point of impact with the target is also called the "parallel-approach method" [constant bearing naviga-

tion method].

The lateral displacement of the missile relative to the position that it occupied at the initial time, when it was at point a_0, is the control function, and equals

$$\varphi_{ux}(t) = \int_0^t v_c \gamma \, dt. \tag{114}$$

In view of the fact that when the dynamic errors have been found, it is possible to utilize approximate expressions for the kinematic trajectories, we make use of the fact that when the missile speed v_s is substantially greater than the target speed v_{ts}, as happens in many cases encountered in practice, $\gamma + \gamma_0 < \beta + \beta_0 \leq \pi/2$ [Formula (113)].

We may thus assume, in approximation, that

$$\gamma = \frac{v_u}{v_c} \sin(\beta + \beta_0) - \gamma_0. \tag{115}$$

Thus,

$$\varphi_{ux}(t) \approx \int_0^t [v_u \sin(\beta + \beta_0) - v_c \gamma_0] \, dt. \tag{116}$$

If the target moves at a constant speed $v_{ts} = \rho\Omega$ along a circle of radius ρ, angle $\beta = \Omega t$, and as a result

$$\varphi_{ux}(t) = \rho\Omega \int_0^t [\sin(\Omega t + \beta_0) - \sin\beta_0] \, dt = \\ = \rho [\cos\beta_0 - \cos\beta_0 \cos\Omega t + \sin\beta_0 \sin\Omega t - \Omega t \sin\beta_0]. \tag{117}$$

A comparison of this expression with (106) and (110) shows that controlling missile motion toward an instantaneously predicted point coincides, when the target takes evasive action, with the three-point method, provided that the distance to the target R_0 is much greater than the radius of curvature of the target path, ρ. Thus, in order to calculate errors when the missile is controlled by the method of parallel approach, it is possible to make use of Formulas (109), (110),

(111), and (112).

2. HOMING GUIDANCE

General considerations

Homing guidance is that method of controlling missile motion in which all of the data required is obtained on board the missile, with no aid from any external units measuring target or missile coordinates or developing the control commands. In view of the limited size of the equipment that can be carried on board a missile, homing, as a rule, provides a considerably shorter range than does guidance with the aid of a separate unit for measuring coordinates and for control. In addition, homing guidance, which makes it possible to measure target-motion parameters at small distances from the target, as we approach the target makes it possible to provide great accuracy in guidance to the target. This positive feature of homing guidance occasionally causes it to be used in combination with external guidance; here at great distances from the target, the missile is controlled from a separate control point, and it is only when the missile approaches sufficiently close to the target that it goes over to the homing mode. Naturally, this results in a considerable complication of the control apparatus.

The need to minimize the weight and size of the homing-guidance instruments, as well as the fact that this apparatus is designed for a single mission and will be destroyed with the missile, leads to a choice of homing control methods that require the simplest measurements of target-motion parameters. In addition, frequently only a single integrating element is employed in the control loop.

In certain cases, the commands may be developed as a function of the angle between the missile axis or a fixed direction in space and the target direction. Thus, the control function $\varphi_{vkh}(t)$ contains angular magnitudes, rather than the linear quantities involved in exter-

nal missile guidance methods.

As for the case in which the function $\varphi_{vkh}(t)$ contains linear quantities, it may be represented for the homing case as a power series with a limited number of terms, whose number is a function of the length of the time interval considered.

The transfer function Y(p) in homing guidance characterizes the ratio of the input and output angular magnitudes in an open control loop. Thus, $\varphi_{vkh}(t)$ will represent, for homing guidance, the change in the angle formed by the tangent to the kinematic missile-motion curve, depending upon time, while $\varphi_{vykh}(t)$ will be the time dependence of the same angle for the actual path.*

The equivalent transfer function $Y_e(p)$ can be obtained for homing by applying to the missile control system commands that change its direction of motion in sudden – step – fashion, and observing the errors $\varepsilon_1(t)$, which consist in a change in time of the difference between the given new missile course, and the actual direction.

The transient process that appears when a step-type command is applied may be aperiodic or a damped oscillation. In the first case, where there is a single integrating element, the equivalent transfer function can be represented by Formula (75), and in the second case, in the presence of two integrating elements, by Formula (77). If the transient process is a damped oscillation, and the control loop contains only a single integrating element, the open-loop equivalent transfer function can be represented as

$$Y_e(p) = \frac{\omega_0^2}{p(p + 2\alpha)}. \qquad (118)$$

The numerical coefficients of this expression can be found with the aid of an experimentally derived curve for $\varepsilon_1(t)$ representing the change in the magnitude of the error when $\varphi_{vkh}(t)$ acts on the system

in the form of a single step.

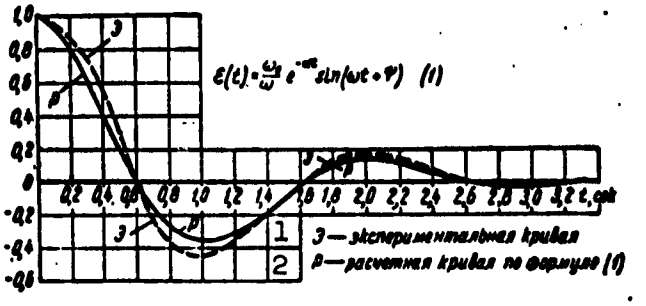

Fig. 31. 1) E – experimental curve; 2) r – curve calculated from Formula (1).

The transform of this error takes the form

$$\varepsilon_1(p)=\frac{1}{p}\,\frac{1}{1+Y(p)}$$

while in the limit, where $Y_e(p)$ is expressed by Function (118)

$$\lim_{t\to\infty}\varepsilon_1(t)=\lim_{p\to 0}\frac{p}{p+\dfrac{\omega_0^2}{p+2\alpha}}=0.$$

The integral of $\varepsilon_1(t)$ represents the error appearing at the output when the system is acted upon by $\varphi_{vkh}(t) = t$ having a transform

$$\varphi_{вх}(p)=\frac{1}{p^2}.$$

In this case

$$\lim_{t\to\infty}\int_0^t\varepsilon_1(\tau)\,d\tau=\lim_{p\to 0}\left(\frac{p}{p^2}\,\frac{p}{1+\dfrac{\omega^2}{p+2\alpha}}\right)=\frac{2\alpha}{\omega_0^2}. \qquad (119)$$

It is possible to separate the quantities 2α and ω_0^2 by making use of the fact that when $Y_e(p)$ is expressed by Formula (118), the error $\varepsilon_1(t)$, when a single-step process is applied to the system, is expressed by the formula

$$\varepsilon_1(t)=\frac{\omega_0}{\omega}e^{-\alpha t}\sin(\omega t+\varphi), \qquad (120)$$

where

$$\psi = \operatorname{arctg}\frac{\omega}{\alpha}\ ;\ \omega^2 = \omega_0^2 - \alpha^2.$$

Then when the curve $\varepsilon_1(t)$ passes through zero at time t_1 for the first time

$$\omega t_1 + \psi = \pi,$$

from which we find ω for the measured value of t_1 and, further, on the basis of Formula (119) and the fact that $\omega^2 = \omega_0^2 - \alpha^2$, we find α.

When the control function $\varphi_{vkh}(t)$ acting upon the system is a power series with a limited number of terms, the limiting value of error is expressed by Formula (66), in which

$$\frac{a_0}{b_0} = \frac{2\alpha}{\omega_0^2}.$$

Figure 31 shows an example of experimental and calculated curves for $\varepsilon_1(t)$ with the coefficients α and ω_0^2 found for the formula for the equivalent transfer function.

There are many different homing-guidance methods.

The simplest is the method in which the axis of the missile or, more accurately, its velocity vector is pointed toward the target at any given instant. The missile kinematic trajectory thus obtained is called the "pure pursuit curve." Equipment design considerations in the control system when the "pure pursuit" method is used are relatively uncomplicated, since the problem reduces to creating a device that will measure the angles formed by the missile axis or its velocity vector with the line-of-sight to the target.

It is extremely unfavorable, however, to have the missile approach the target along a pursuit curve from the viewpoint of the dynamic errors appearing at the end of the trajectory just at the target. Thus, several versions of this method are employed, "fixed-lead

navigation" and "proportional navigation."

In addition, in homing guidance it is also possible to use the constant-bearing navigation method, in which the direction in space of the line connecting the missile and target at any given moment is maintained constant. Equipment designed with this method is more complicated than with the pure pursuit method.

Let us commence our examination of dynamic errors in homing guidance with the constant-bearing method, since it is simpler from the point of view of the mathematical analysis.

Constant-bearing navigation

For homing guidance, constant-bearing navigation is carried out by maintaining constant the angle between the line joining the missile and the target, and any fixed bearing in space. When this is done, the condition (Fig. 30)

$$v_c \sin(\gamma + \gamma_0) = v_u \sin(\beta + \beta_0). \qquad (113)$$

is automatically satisfied.

Introducing the same simplification as was used when the constant-bearing method was considered as a guidance method, i.e., assuming that $v_s \gg v_{ts}$ and, thus, $\sin \gamma + \gamma_0 \approx \gamma + \gamma_0$, we find the control function, which in the homing case is the time dependence of the angle γ,

$$\varphi_{ex}(t) = \frac{v_u}{v_c} \sin(\beta + \beta_u) - \gamma_0. \qquad (121)$$

The angular homing-guidance error $\varepsilon_\gamma(t)$ is found in this case from its transform

$$\varepsilon_\gamma(p) = \varphi_{ex}(p) \frac{1}{1 + Y_e(p)},$$

where $Y_e(p)$ is the equivalent transfer function, found from experimental data.

From the practical viewpoint, we are interested not in the angular error, which is the difference in the angles formed by the tangents to the kinematic and actual paths at the instant of impact with the target, but with the linear error $\varepsilon_1(t)$, which shows the distance by which the missile missed the target.

If at time $t_0 = 0$, the missile moved along the kinematic trajectory, then the linear error at time t will be expressed in terms of the angular error as follows:

$$\varepsilon_л(t) = \int_0^t \varepsilon_1(t) v_c \, dt, \tag{122}$$

where v_s is the rate at which the missile moves along its path.

Thus, the transform of the linear error for homing guidance will equal

$$\varepsilon_л(p) = \frac{v_c \varphi_{вх}(p)}{p} \frac{1}{1 + Y_л(p)}. \tag{123}$$

Let us compare the expression for the linear error with constant-bearing navigation of the missile to the target by means of external guidance and homing.

For external guidance, the control function will be the integral

$$\varphi_{вх}(t) = \int_0^t v_c \gamma \, dt. \tag{114}$$

For homing guidance, the integral will be the linear error (122).

Thus, where the angle γ depends upon the time in the same way, and with identical control-loop transfer functions, constant-bearing navigation will give identical errors with external guidance and homing guidance, which is what we might expect.

In practice, however, the loop control function for a system with homing guidance differs substantially from the transfer function for an

external-guidance system.

As an illustration, let us find the error in a homing-guidance system for which the transient process upon application to the system of a single-step process $\varepsilon_1(t)$ takes the form shown in Fig. 31. We shall assume that the dashed curve of Fig. 31 has been obtained experimentally.

Let the target move in a circle of radius $\rho = 10$ km at speed of $v_{ts} = \rho\Omega = 0.5$ km/sec, i.e., $\Omega = 5 \cdot 10^{-2}$ rad/sec.

Let us find the error $\varepsilon_1(t)$ at time $t = 10$ sec.

Integration of the curve of Fig. 31 yields

$$\int_0^t \varepsilon_1(\tau)\,d\tau = \frac{2a}{\omega_0^2} \approx 0{,}2;\ \omega = \pi = 3{,}14,$$

thus it follows from the equation $\alpha/(\omega^2 + \alpha^2) = 0.1$ that $\alpha = 1.09$;

$$\psi = \arccos\frac{1{,}09}{3{,}14} = 70°;\ \omega_0^2 = 10{,}9;\ \omega_0 = 3{,}3 \text{ rad/sec}.$$

Let us assume for simplicity that at time $t = 0$, the missile moved toward the target, i.e., that $\beta_0 = \gamma_0 = 0$. Then

$$\varphi_{ts}(t) = \frac{v_t}{v_c}\sin\Omega t = 0{,}5\sin(0{,}05\,t);$$

$$\varphi_{ts}(p) = 0{,}5\frac{0{,}05}{p^2 + 2{,}5\cdot 10^{-3}};$$

$$\varepsilon_1(p) = \frac{2{,}5\cdot 10^{-3}}{p(p^2 + 2{,}5\cdot 10^{-3})}\cdot\frac{p + 2{,}18}{p^2 + 2{,}18p + 10{,}9}.$$

In view of the fact that $e^{-\alpha t}$ is very small where $\alpha = 1$ and $t = 10$ sec, we select from the table of originals and transforms only a term characterizing a steady-state error.

In such case

$$\varepsilon(t) = \frac{k}{\Omega}\sqrt{\frac{\Omega^2 + 4a^2}{(\omega_0^2 - \Omega^2) + 4a^2\Omega^2}}\sin(\Omega t + \psi_1),$$

where

$$\psi_1 = \operatorname{arc\,tg}\frac{\Omega}{2n} - \operatorname{arc\,tg}\frac{2n\Omega}{\omega_0^2 - \Omega^2};\ k = 2{,}5 \cdot 10^{-2},$$

while the remaining quantities are given. Substituting them into the expression for $\varepsilon(t)$, we find

$$\varepsilon(t) = 0{,}1 \sin(\Omega t + 1^\circ)$$

or, where t = 10 sec, the error proves to equal

$$\varepsilon(t) = 0{,}0454 \text{ км, i.e. } 45{,}4 \text{ м.}$$
$$t=10\text{sec}$$

Homing guidance: pure pursuit method

. The pure-pursuit method is a type of homing guidance in which the control system attempts to keep the missile axis aimed at the target. The control function $\varphi_{vkh}(t)$ in this case is the time dependence of the angle formed by the missile axis with its bearing at the initial time (Fig. 32). If the missile moves so as to pursue the target, then

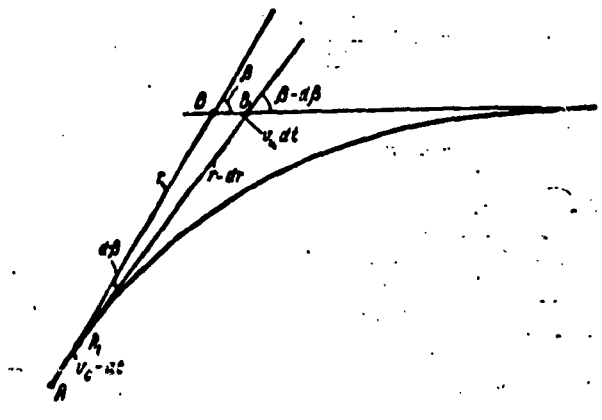

Fig. 32

from Fig. 32 it follows that

$$dr = -v_c\,dt + v_u \cos\beta\,dt; \qquad (124)$$
$$r\,d\beta = -v_u \sin\beta\,dt.$$

It follows from Eqs. (124), that

$$\frac{1}{r}\frac{dr}{dt}=\left(\frac{v_s}{v_u}\cdot\frac{1}{\sin\beta}-\operatorname{cot}\beta\right)\cdot\frac{d\beta}{dt}. \qquad (125)$$

The solution to Eq. (125) is

$$r=k\frac{(\sin\beta)^{s-1}}{(1+\cos\beta)^s}, \qquad (126)$$

where $s = v_s/v_{ts}$,

$$k=r_0\frac{(1+\cos\beta_0)^s}{(\sin\beta_0)^{s-1}},$$

r_0 is the distance, β_0 is the angle β at the initial instant of time.

If the missile moves to meet the target, then

$$r=k_1\frac{(1+\cos\beta_0)^s}{(\sin\beta_0)^{s+1}}, \qquad (127)$$

where

$$k_1=r_0\frac{(\sin\beta_0)^{s+1}}{(1+\cos\beta_0)^s}.$$

Expressions (126) and (127) determine the connection between the distance r and the angle β.

In order to express the angle β, the control function $\varphi_{vkh}(t)$, as a function of time, we multiply the first equation of (124) by cos β, and the second by sin β, and find their difference

$$\frac{dr}{dt}\cos\beta=v_u\cos^2\beta-v_c\cos\beta=$$

$$=v_u\cos^2\beta-\frac{v_c}{v_u}\left(\frac{dr}{dt}+v_c\right);$$

$$r\frac{d\beta}{dt}\sin\beta=-v_u\sin^2\beta;$$

$$\frac{dr}{dt}\left(\cos\beta+\frac{v_c}{v_u}\right)-r\sin\beta\frac{d\beta}{dt}=v_u-\frac{v_c}{v_u}v_c.$$

The left-hand portion of the last equation is

$$\frac{d\,|r(\cos\beta+s)|}{dt}=v_u-\frac{v_c}{v_u}v_c.$$

Thus

$$\int_{r_0,\beta_0}^{r,\beta} d[r(\cos\beta+s)] = \int_{r_0,\beta_0}^{r,\beta} (v_a - s v_c)\, dt.$$

Whence

$$t = \frac{r_0(\cos\beta_0 + s) - r(\cos\beta + s)}{s v_c - v_a}. \qquad (128)$$

Where the missile moves toward the target

$$t = \frac{r(\cos\beta - s) - r_0(\cos\beta_0 - s)}{s v_c - v_a}. \qquad (129)$$

Equations (128) and (129), together with (126) and (127) make it possible to plot a graph showing the way in which the angle β depends upon the time t. To do this, using Formulas (126) or (127), and having successive values of β, we find the values of r corresponding to them. Substituting into Formula (128) or (129) the values of β and r, we are able to find the times t corresponding to the chosen values of the angle β.

Thus, it is not possible for the pure-pursuit case to express the function $\beta = \varphi(t)$ in a form convenient for determining the error $\varepsilon(t)$, making use of the Laplace transformation, or some other method.

It is necessary to express the function $\varphi_{vkh}(t) = \beta(t)$, computed point-by-point, roughly as a power series over a limited time interval, and then to find, in accordance with this approximate value of the control function $\varphi_{vkh}(t)$, in accordance with the equivalent value of the transfer function $Y_e(p)$, the error $\varepsilon(t)$.

The function $\varphi_{vkh\ \gamma}(t)$ represents the angular magnitude as a function of time.

In order to find the linear error $\varepsilon_1(t)$, we make use of Formula (123), and introduce the auxiliary function $\varphi_{vkh\ 1}(t)$, connected with $\varphi_{vkh\ \gamma}(t)$ by the function

$$\varepsilon_a(p) = \frac{v_c}{p}\varphi_{ex\,1}(p)\frac{1}{1+Y(p)} = \varphi_{ex\,a}(p)\frac{1}{1+Y(p)}. \qquad (130)$$

It follows from Formula (130), that

$$\varphi_{ex\,a}(t) = \int_0^t v_c\,\varphi_{ex\,1}(t)\,dt.$$

Thus, if

$$\varphi_{ex\,1}(t) = a_0 + a_1 t + a_2 t^2 + \ldots a_n t^n,$$

then

$$\varphi_{ex\,a}(t) = A_0 + A_1(t) + A_2(t) + \ldots A_{n+1}t^{n+1} =$$
$$= v_c\left[a_0 t + \frac{1}{2}a_1 t^2 + \frac{1}{3}a_2 t^3 + \ldots \frac{a_n}{n+1}t^{n+1}\right].$$

Substitution of the values of the coefficients A_k into Formula (65) and (66) shows that in the presence of two integrating elements in the control loop, the linear error will equal

$$\varepsilon_a(t) = \frac{a_0 v_c}{b_0}[a_1 + 3a_2 t + 3!a_3 t^2 + \ldots n!a_n t^{n-1}]. \qquad (131)$$

If the control loop contains only a single integrating element, then

$$\varepsilon_a(t) = \frac{a_0 v_c}{b_0}[a_0 + a_1 t + a_2 t^2 + \ldots a_n t^n] = \frac{a_0 v_c}{b_0}\varphi_{ex\,1}(t). \qquad (132)$$

For the sake of illustration let us give the following example.

A missile, controlled by the pure-pursuit method, moves toward the target. The missile speed is v_s = 1 km/sec, the target speed is v_{ts} = 0.5 km/sec, i.e., s = v_s/v_{ts} = 2.

At the initial instant, t = 0, r_0 = 20 km, $\beta_0 = 30^\circ$.

The equivalent missile-loop transfer function $Y_e(p)$ is determined by the transient process for a single-step process of the type shown in Fig. 31.

TABLE 1

Angle β and distance r as functions of time t.

deg	30	35	40	45	50	60	100
r,km	20	12,5	8,4	5,9	4,31	2,46	0
t,sec	0	5,2	8,2	10	11,2	12,6	15,15

Making use of Formula (127), we calculate the relationship between the distance r and the angle β, and find from the values of r and β, by Formula (129), the corresponding times t.

Table 1 and Fig. 33 show the results of the calculation.

It is clear from Table 1 and the curve of Fig. 33 that the angle β rises extremely rapidly as the missile approaches the target. Here

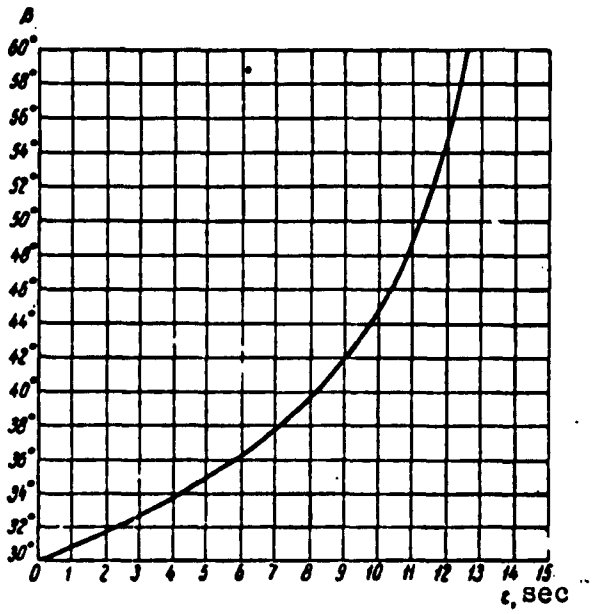

Fig. 33

there is a sharp increase in lateral accelerations, i.e., the acceleration force on the missile.

Thus, for example, using the curve of Fig. 33 to find $d\beta/dt = \Omega_s$ for time t = 8.2 sec, i.e., in the region $\beta = 40^\circ$, we find

$$\Omega_s \approx 20^\circ/\text{sec} = 0{,}333 \text{ rad/sec}.$$

As we know, the acceleration $w_s = v_s\Omega_s$, i.e., when $v_s = 10^3$ m/sec,

w_s = 333 m/sec^2 = 33.3 g, where g are the gravitational acceleration forces.

A homing missile using the pure-pursuit method when aimed along the last section of the path to the target will move by inertia, and be almost uncontrolled, i.e., its control surfaces or devices cannot provide such great angular velocities or load factors. This leads to very wide misses even where the strength of the missile is adequate, and it is able to withstand the g factors appearing close to the target.

TABLE 2

Angle β and Distance r as Functions of Time t.

deg	30	25	20	15	10	5	0
r, km	20	16.2	12.6	9.3	6.1	3.0	0.0
t, sec	0	6.7	13.5	19.8	25.9	32.2	38.2

The data of Table 1 and the curve of Fig. 33 for angles ranging from $\beta_0 = 30^\circ$ to $\beta = 50^\circ$, i.e., in the time interval from t = = 0 to t = 11.2 sec, can be represented approximately by the function

$$\varphi_{\text{опт}}(t) = \beta - \beta_0 = a_1 t + a_4 t^4.$$

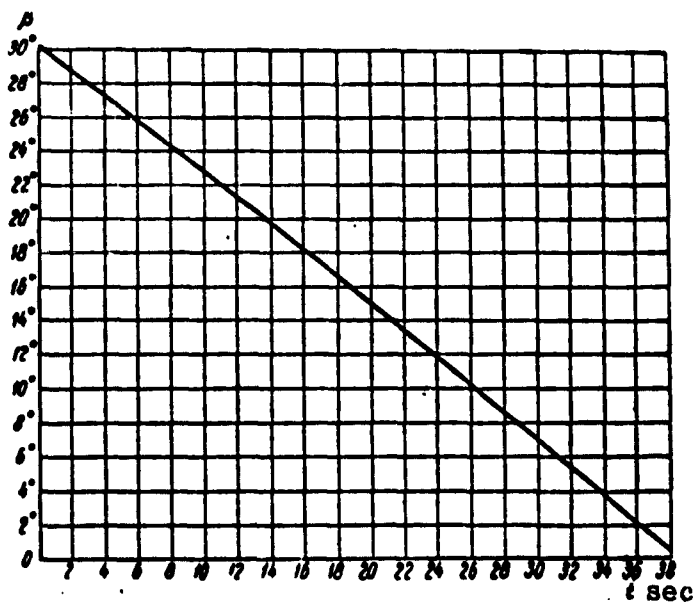

Fig. 34

where

$$a_1 = 0{,}865 \text{ deg/sec or } 1{,}51 \cdot 10^{-2} \text{ rad/sec};$$

$$a_4 = 6{,}5 \cdot 10^{-4} \text{ deg/sec}^4 \text{ or } 1{,}13 \cdot 10^{-5} \text{ rad/sec}^4.$$

If we assume that the control loop is characterized by the transient process of Fig. 31, and contains a single integrating element, we find from Formula (132) the steady-state error after the transient process has ended

$$\varepsilon_s(t) = \frac{a_y}{b_0} v_c (a_1 t + a_4 t^4),$$

or, substituting the values $a_0/b_0 = 2\alpha/\omega_0^2 = 0.2$, found from the curve of Fig. 29, as well as v_s, a_1, and a_4, we obtain

$$\varepsilon_s(t) = 0{,}2(1{,}51 \cdot 10^{-2} t + 1{,}13 \cdot 10^{-5} t^4) \text{ км}.$$

For example, where t_1 = 10 sec

$$\varepsilon_s(t)_{t=10\text{sec}} = 0{,}2\,(0{,}151 + 0{,}113) \text{ км}, \text{ i. e. } 52{,}6 \text{ м}.$$

For the pursuit course with the same missile and target speeds, the same initial distance and angle β_0 as we used in the preceding example, a calculation by Formula (126) and (128) for the angle β and distance r as functions of time leads to the results shown in Table 2 and illustrated by the curve of Fig. 34.

The curve of Fig. 34 shows that in the example under consideration, there is an almost precisely linear relationship between the angle β and the time

$$\varphi_{\text{зад}}(t) = \beta_0 - a_1 t,$$

where

$$a_1 = 0{,}765 \text{ deg/sec or } 1{,}33 \cdot 10^{-2} \text{ rad/sec}.$$

Substitution of a_1 into Formula (132) yields

$$\varepsilon_{\Delta}(t) = 2{,}66 \cdot 10^{-3} t$$

where

$$\frac{a_n}{b_0} = 0{,}2 \text{ и } v_c = 1 \text{ km/sec}.$$

It follows from Table 2 that collision of missile and target should occur on the kinematic trajectory at time t_v = 38.2 sec. At this instant, the error will equal

$$\varepsilon_{\Delta}(t)_{t=38.2\text{sec}} = 102 \text{ м}.$$

Pure pursuit with target evasive action

Where the target is in evasive action, for example, moving along a circle with a constant angular velocity, the expression for the kinematic trajectory in pure pursuit cannot be represented by formulas convenient for calculation. In this case, as in many others, calculation and plotting of the kinematic trajectory and control function $\varphi_{vkh}(t)$ must be carried out by numerical integration of the initial differential equations.

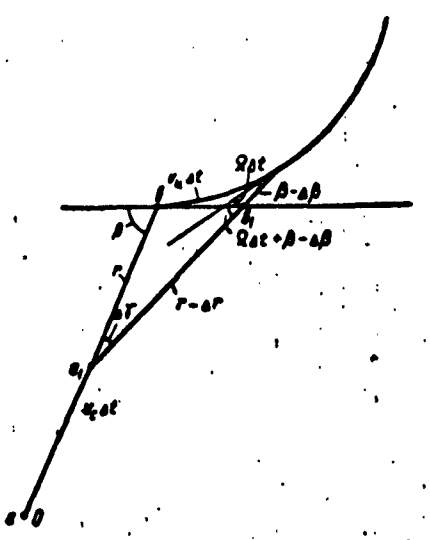

Fig. 35

Let us show by an example the method of solving a problem of this

type concerning a pure pursuit course with the target moving in a circle at constant speed.

Let the target move in a circle with a constant linear velocity v_{ts} and an angular velocity Ω. The missile speed equals v_s. Figure 35 shows the positions of the target ($\underline{b}$ and b_1) and missile ($\underline{a}$ and a_1) for two consecutive times $\underline{t}$ and $t + \Delta t$.

The control function for the closed missile control loop is the angle γ.

In order to find the way in which this angle depends upon time, and to plot $\varphi_{vkh}(t)$, we write equations for two infinitely close times $\underline{t}$ and $t + \Delta t$.

We see from Fig. 35 that at $\Delta t \to 0$

$$\Delta\gamma = \Delta\beta - \Omega\Delta t; \tag{133}$$

$$\Delta r = (v_c - v_a\cos\beta)\Delta t; \tag{134}$$

$$\Delta\beta = \frac{v_a\sin\beta + r\Omega}{r}\Delta t. \tag{135}$$

Taking a sufficiently small time interval Δt, we can find values of β, $\underline{r}$ and γ for successive times Δt, $2\Delta t$, $3\Delta t$, etc., substituting into the expressions for $\Delta\beta$, Δr, and $\Delta\gamma$ the values of β and $\underline{r}$ calculated for the preceding instants in time; we thus can plot $\varphi_{vkh}(t) = \gamma(t)$ point-by-point.

Let us show this in an example.

$$v_a = 0{,}5 \text{ km/sec } \Omega = 0{,}05 \text{ rad/sec } v_c = 1 \text{ km/sec}$$
$$\text{where } t = 0,\ r_0 = 20 \text{ km};\ \beta_0 = 30°;\ \gamma_0 = 0.$$

Then for $t_1 = \Delta t = 2$ sec

$$\Delta\beta = 2\frac{0{,}25 + 1}{20} = 0{,}125 \text{ rad or } 7{,}15°;$$
$$\Delta r = 2(1 - 0{,}433) = 1{,}134 \text{ km};$$
$$\Delta\gamma = 0{,}025 \text{ rad}.$$

For $t_2 = t_1 + \Delta t = 4$ sec

$$\Delta\beta = 2\frac{0{,}5\sin(30^\circ - 7{,}15^\circ) + (20 - 1{,}134)\cdot 0{,}05}{20 - 1{,}134} =$$
$$= 0{,}121\,\text{rad or } 7^\circ;$$
$$\Delta r = 2[1 - 0{,}5\cos(30^\circ - 7{,}15^\circ)] = 1{,}074\ км;$$
$$\Delta\gamma = 0{,}021\,\text{rad};\ \gamma = 0{,}025 + 0{,}021 = 0{,}046\ \text{rad}.$$

Continuing these calculations, we obtain Table 3.

TABLE 3

Values of Control Function $\varphi_{vkh}(t) = \gamma(t)$ and Distance r Between Target and Missile for Successive Times t.

sec	deg	sin β	cos β	r, км	Δr	Δr, км	Δβ, rad	Δγ rad	γ − φ_вх(t), rad
0	30	0,500	0,866	20	1	1,134	0,125	0,025	0,00
2	23	0,388	0,925	18,8	0,943	1,074	0,121	0,021	0,025
4	16	0,276	0,961	17,6	0,880	1,04	0,116	0,016	0,046
6	9,2	0,161	0,985	16,5	0,827	1,01	0,109	0,009	0,062
8	3	0,052	0,999	15,5	0,776	1,00	0,103	0,003	0,071
10	−3	−0,052	0,999	14,5	0,726	1,00	0,096	−0,004	0,074
12	−8,5	−0,148	0,989	13,5	0,676	1,01	0,089	−0,011	0,070
14	−13,5	−0,233	0,968	12,5	0,625	1,03	0,081	−0,019	0,059
16	−18,3	−0,314	0,944	11,5	0,574	1,06	0,073	−0,028	0,040
18	−22,5	−0,383	0,924	10,4	0,521	1,08	0,063	−0,037	0,012
20	−26,1	−0,440	0,898	9,34	0,467	1,10	0,053	−0,047	0,025
22	−29,2	−0,488	0,874	8,24	0,412	1,13	0,041	−0,059	−0,072
24	−31,5	−0,522	0,853	7,12	0,356	1,15	0,027	−0,073	−0,131
26	33	−0,545	0,839	5,97	0,298	1,16	0,008	−0,092	−0,204
28	33,5	−0,552	0,834	4,81	0,241	1,17	−0,114	−0,114	−0,296
30	32,7	−0,541	0,841	3,65	0,182	1,16	−0,049	−0,149	−0,410
32	30	−0,500	0,860	2,50	0,125	1,13	−0,100	−0,200	−0,558
34	24,75	−0,419	0,908	1,37	0,068	1,09	−0,200	−0,300	−0,778

Figure 36 gives a curve showing the time dependence of $\varphi_{vkh}\ \gamma(t) = \gamma(t)$.

With sufficient accuracy for practical purposes, this curve can be represented by the equation

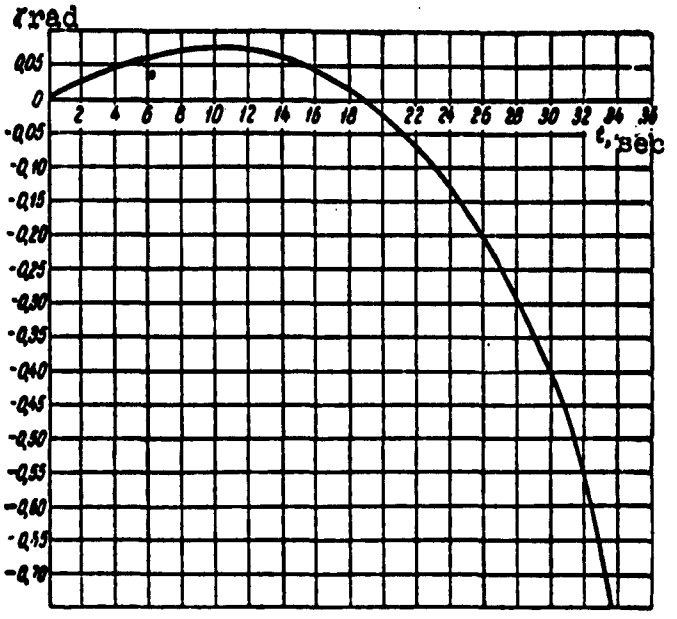

Fig. 36

$$\varphi_{\text{ос }1}(t) = a_0 + a_2 t_1^2 + a_4 t_1^4 = 0{,}081 - 1{,}055 \cdot 10^{-3} t_1^2 - \\ - 3{,}52 \cdot 10^{-7} t_1^4, \qquad (136)$$

where $t_1 = t - 10$.

Using the same value of the coefficient a_0/b_0 as in the preceding examples, we find by Formula (132) the value of the error

$$\varepsilon_1(t) = \frac{a_0}{b_0} v_c (a_0 + a_2 t_1^2 + a_4 t_1^4) = \\ = 0{,}2\,(0{,}081 - 1{,}055 \cdot 10^{-3} \cdot t_1^2 - 3{,}52 \cdot 10^{-7} \cdot t_1^4).$$

For example, in order to find the error at time t = 36 sec, we find $t_1 = t - 10 = 26$ sec, and thus $\varepsilon_1(t) \approx 160$ m.

$\underline{t=36\text{sec}}$

Deviated-pursuit course

The calculations and examples given show that "pure pursuit" leads to very great errors due to the large g factors on the missile as it approaches the target, especially when aimed headon.

In order to make the kinematic trajectories flatter, decrease acceleration forces on the missile near the target, and decrease the error, it is possible to employ several different guidance methods and, in particular, the deviated pursuit course method.

With the deviated-pursuit course, the missile axis is at each given moment directed not toward the target but in a direction that forms a constant angle δ with the missile-target line, toward the direction of target motion. In this case, the required sign for the angle δ is selected automatically depending upon which side of the missile axis the target is on, and in which direction it is moving.

Let us examine the deviated-pursuit course method where the missile is aimed at a target flying in a straight line at constant speed v_{ts}.

In this case (Fig. 37)

$$-\frac{dr}{dt} = v_c \cos\delta + v_u \cos\beta;$$

$$r\frac{d\beta}{dt} = v_u \sin\beta - v_c \sin\delta.$$

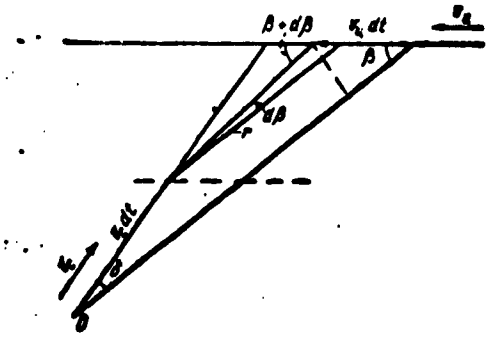

Fig. 37

Division of the first equation by the second yields

$$\frac{dr}{r} = \frac{v_c \cos\delta + v_u \cos\beta}{v_u \sin\beta - v_c \sin\delta} d\beta. \qquad (137)$$

Expression (137) is integrated in finite form. In practice, however, it is more convenient to solve such a problem by numerical integration in accordance with the formulas

$$\Delta r = -(v_c \cos\delta + v_u \cos\beta)\Delta t; \qquad (138)$$

$$\Delta\beta = \frac{1}{r}(v_u \sin\beta - v_c \sin\delta)\Delta t. \qquad (139)$$

Let us consider an example for the case in which

TABLE 4

Distance r and Angle β as Functions of Time for Deviated-Pursuit Course

t, sec	β	sin β	cos β	Δr, км	r, км	Δβ, rad
0	30°00′	0,500	0,866	— 1,418	20,00	3,8 ·10⁻³
1	30°20′	0,505	0,863	— 1,417	18,582	3,9 ·10⁻³
2	30°40′	0,510	0,860	— 1,415	17,165	4,0 ·10⁻³
3	31°10′	0,515	0,857	— 1,413	15,750	5,33·10⁻³
4	31°40′	0,525	0,851	— 1,411	14,337	6,0 ·10⁻³
5	32°00′	0,530	0,848	— 1,409	12,926	7,0 ·10⁻³
6	32°30′	0,537	0,843	— 1,406	11,517	8,1 ·10⁻³
7	33°00′	0,546	0,839	— 1,404	10,111	9,8 ·10⁻³
8	33°30′	0,552	0,834	— 1,402	8,707	1,17·10⁻²
9	34°10′	0,562	0,827	— 1,396	7,305	1,47·10⁻²
10	35°00′	0,574	0,819	— 1,394	5,907	1,92·10⁻²
11	36°10′	0,590	0,807	— 1,388	4,513	2,68·10⁻²
12	37°40′	0,611	0,792	— 1,381	3,125	4,23·10⁻²
13	40°00′	0,643	0,766	— 1,368	1,744	8,5 ·10⁻²

$$v_c = 1\,\text{km/sec};\ v_u = 0{,}5\,\text{km/sec};$$
$$r_0 = 20\ км;\ \beta_0 = 30°;\ \delta = 10°.$$

We use Formulas (138) and (139) to calculate a table of values for the distance r and the angle β as a function of the time at intervals Δt = = 2 sec.

The results of the calculation are shown in Table 4 and in the curve of Fig. 38.

Processing of the data of Table 3 indicates that the time dependence of the angle can be expressed approximately as

$$\beta - \beta_0 = \varphi_{вз1}(t) = a_1 t + a_2 t^2 + a_4 t^4,$$

where

$$a_1 = 0{,}34\,\text{deg/sec} \text{ or } 5{,}94\cdot10^{-3}\,\text{rad/sec};$$
$$a_2 = 10^{-2}\,\text{deg/sec}^2 \text{ or } 1{,}745\cdot10^{-4}\,\text{rad/sec}^2;$$
$$a_4 = 10^{-4}\,\text{deg/sec}^4 \text{ or } 1{,}745\cdot10^{-6}\,\text{rad/sec}^4.$$

Then, using the same control-loop data as in the preceding homing-guidance examples, we use Formula (132) to find an expression for

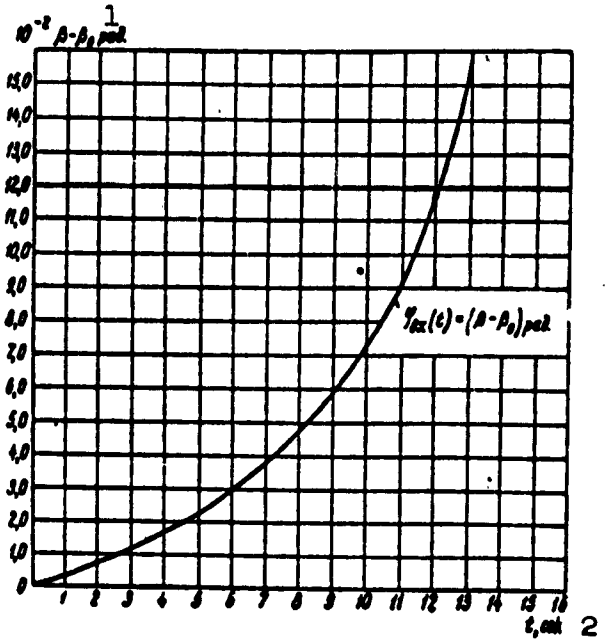

Fig. 38. 1) Rad; 2) sec.

the linear error

$$\varepsilon_s(t) = \frac{a_0}{b_0} v_c (a_1 t + a_2 t^2 + a_4 t^4),$$

i.e.,

$$\varepsilon_s(t) = \frac{a_0}{b_0} v_c \varphi_{вых}(t).$$

Thus, for example, where t = 13 sec, from the curve of Fig. 38 and Table 3, $\varphi_{vkh\ \gamma}(t) = \beta - \beta_0 = 0.163$ rad, owing to which the error is

$$\underset{t=13\,сек}{\varepsilon_s(t)} = 0{,}2 \cdot 0{,}163 = 0{,}0325\ км \text{ or } 32{,}5\ м.$$

The given calculation was carried out on the assumption that the missile moved at constant speed. We must note, however, that decelerated or accelerated motion of the missile introduces only slight changes in the error. Let us assume, for example, that the missile moves with deceleration, and that its speed is $v_s = (1 - 0.02\ t)\ \frac{km}{sec}$; we find that at t = 13 sec, $\varepsilon(t) \approx 0.028$ km, i.e., about 28 m instead

of 32.5 m in the constant-speed case.

Proportional Navigation

The proportional-navigation method consists in keeping the missile angular velocity along the path proportional to the angular velocity of the missile-target line-of-sight (Fig. 39).

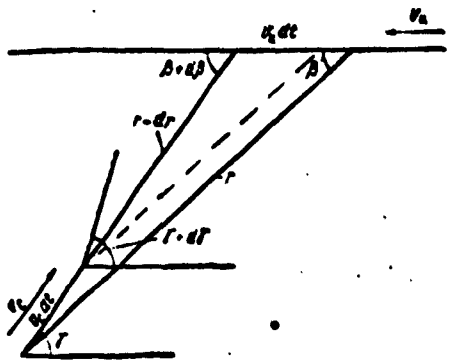

Fig. 39

From the very essence of the method

$$\frac{d\gamma}{dt} = a\frac{d\beta}{dt}, \tag{140}$$

whence

$$\gamma = \gamma_0 + a\beta - a\beta_0. \tag{141}$$

In addition, it follows from Formula

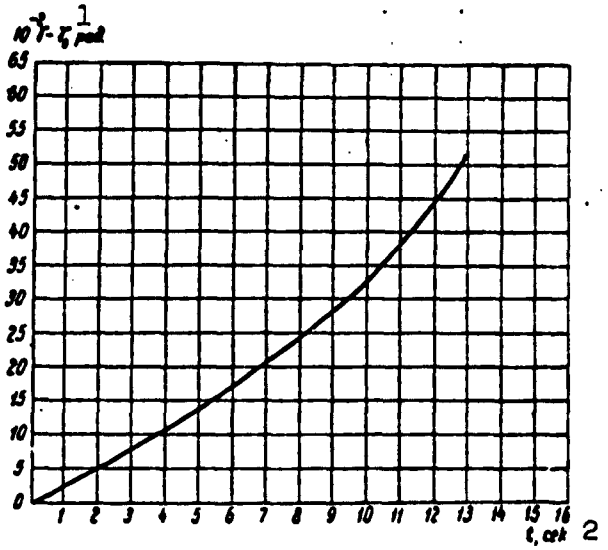

Fig. 40. 1) Rad; 2) sec.

(141) and Fig. 39 that

$$\Delta r = \{v_u \cos\beta + v_c \cos[\gamma_0 - a\beta_0 + (a-1)\beta]\}\Delta t = \tag{142}$$
$$= \{v_u \cos\beta + v_c \cos(\gamma - \beta)\}\Delta t,$$
$$\Delta\beta = \{v_u \sin\beta - v_c \sin[\gamma_0 - a\beta_0 + (a-1)\beta]\}. \tag{143}$$

Formulas (142) and (143) do not permit us to carry out integra-

tion and to obtain formulas associating r, β, γ, and t in a form convenient for computation. Thus, actual problems in homing guidance using proportional navigation are solved by a numerical integration method.

Let us carry out the appropriate calculations for the case

$$v_a = 0{,}5 \text{ km/sec}; v_c = 1 \text{ km/sec}; r_0 = 20 \text{ km}; \beta_0 = 30°;$$
$$a = 2; \gamma_0 = \beta_0 = 30°.$$

The results of the calculation are shown in Table 5 and illustrated in Fig. 40.

TABLE 5

Angles γ and β as Function of Time for Proportional Navigation

t, sec	β°	sin β	cos β	Δr, km	r, km	Δβ°	γ°
0	30°00'	0,500	0,866	1,433	20,00	40'	30°00'
1	30°40'	0,510	0,860	1,430	18,57	50'	31°20'
2	31°30'	0,522	0,853	1,427	17,14	50'	33°00'
3	32°20'	0,535	0,845	1,423	15,71	50'	34°40'
4	33°10'	0,547	0,837	1,418	14,29	50'	36°20'
5	34°00'	0,559	0,829	1,413	12,86	1°00'	38°00'
6	35°00'	0,574	0,819	1,405	11,46	1°00'	40°00'
7	36°00'	0,588	0,809	1,401	10,05	1°00'	42°00'
8	37°00'	0,602	0,799	1,392	8,65	1°15'	44°00'
9	38°15'	0,619	0,785	1,381	7,26	1°20'	46°30'
10	39°35'	0,637	0,771	1,372	5,88	1°40'	52°10'
11	41°05'	0,644	0,754	1,356	4,51	1°40'	52°10'
12	42°45'	0,679	0,734	1,342	3,15	2°10'	55°30'
13	44°55'	0,706	0,708	1,320	1,81	3°00'	65°50'

Using Formula (132)

$$\varepsilon_1(t) = \frac{a_0}{b_0} v_c \varphi_{a_0 T}(t)$$

and the data of Table 5, we can find the error $\varepsilon_1(t)$ at time t.

It is clear from Table 5, for example, that at t = 13 sec

$$\varphi_{\text{вых}}(t)_{t=13\text{сек}} = \gamma - \gamma_0 \approx 36^\circ, \text{ i.e. } 0{,}27 \text{ rad.}$$

Thus, the error at time t = 13 sec will equal

$$\dot{s}_{\text{г}}(t)_{t=13\text{сек}} = 0{,}2 \cdot 0{,}27 = 0{,}054 \text{ км}, \text{ i.e., } 54 \text{ м}.$$

In conclusion, it is necessary to make a few comments.

1. The control and homing-guidance methods presented above are extremely simple. In addition to these, there are several other possible control and homing-guidance methods available that differ from the ones listed in individual details, or that represent combinations of these methods. The derivation of the expressions for the control function $\varphi_{vkh}(t)$ and calculation of errors in these control methods may be carried out by the same methods as were used in the cases discussed.

2. The cases discussed relate, for the most part, to conditions of constant missile and target speed. In actuality, the speeds, especially the missile speed, are time-dependent magnitudes. We showed, in certain very simple examples, how to find the control function in such cases. In other cases that may be quite different, the calculation of the control function under conditions of changing missile and target speeds very frequently necessitates numerical integration, calculation of the control function point-by-point, and where necessary, the selection of coefficients for the power series that represents approximately $\varphi_{vkh}(t)$.

All of the preceding analysis refers to motion of missile and target in the same plane. As we have already said at the beginning, in order to calculate errors for three-dimensional missile and target paths, it is necessary to use the assumption that it is possible to consider missile and target motion as two independent movements in mutually perpendicular planes. Applying to each of these motions the method of error calculation presented above, it is possible to find the

magnitude of the resultant error as the square root of the sum of the squared errors in these two mutually perpendicular planes.

Manuscript Page No.

[Footnote]

103 Here and henceforth, in examining homing guidance it shall be assumed that the magnitude of the control command depends solely upon the magnitude of the angular error, and that it is independent of the distance between the missile and the target.

Manuscript Page No.

[List of Transliterated Symbols]

89 вх = vkh = vkhod = input

89 ц = ts = tsel' = target

89 н = n = navstrechu = collision

90 в = v = vstrecha = impact

90 с = s = snaryad = missile

96 э = e = ekvivalentnyy = equivalent

107 л = l = lineynyy = linear

112 к = k = kontur = loop

Chapter 6

ERRORS DUE TO DISCONTINUOUS INFORMATION

In many cases, a control function $\varphi_{vkh}(t)$ acting on a control loop is discontinuous rather than continuous. If, for example, data on target position are obtained with a radar antenna that rotates at N revolutions in unit time, the control function will be a series of individual signals or commands received at a frequency N in unit time. Circular antenna rotation may be replaced with periodic scanning of a narrower sector of space. If the radar antenna is not constantly pointed at the target, or does not continuously track it, however, information about target position is received only when the target falls within the field of view of the moving antenna, and information as to the angular position of the target will be discontinuous. This type of discontinuous target-range information is produced by a pulse radar which, using $\underline{n}$ pulses per second, permits us to obtain the same number of discrete data per second as to the target distance.

As long as the frequency of the individual signals or commands is sufficiently high, the control loop smooths the individual pulses, filtering out the high frequencies, and extracting the slowly varying component that corresponds to the variation in target angular position or range.

If, however, information on the position of the target, missile, or both is received infrequently, and the frequency of these signals lies within the control-loop passband, additional errors will appear owing to the fact that in the gaps preceding the arrival of fresh

data, the missile is controlled by the "inertia" or "memory" of the control loop, which does not always correspond to control that continuously accounts for the actual motion of target and missile.

Much work and research has been devoted to the problem of discontinuous pulse regulation and automatic control. A special mathematical apparatus has been developed to solve pulse-control problems and, in particular, a special theory of Laplace transformations for pulse functions, the theory of stability in discontinuous control, and for many other problems.

Rather than involving ourselves in an exhaustive and thorough examination of the way in which discontinuous reception of information as to missile and target motion affects the control loop, we shall examine the basic features of this influence, using the same physical concepts and the same mathematical apparatus as were used in the discussion of the preceding sections.

In a closed loop, discrete continuous control must be represented as a series of successive jolts or "steps," each corresponding to a change in the control function that is stored during the information gap. As a result, the control function changes from a smooth function to a step function (Fig. 41). Here, the characteristic feature is the fact that with discontinuous control, information as to the actual target position is always delayed, and gives the true data only at isolated instants in time.

The application to the loop input of a step control function $\varphi_{vkh\ st}(t)$ that includes only the uppermost points on the smooth control function $\varphi_{vkh\ gl}(t)$ causes the average smoothed value of $\varphi_{vkh\ st}(t)$ to be shifted by (a/2) with respect to the true function $\varphi_{vkh\ gl}(t)$. In other words, the average value of $\varphi_{vkh\ st}(t)$ will always lag behind the correct value by the change in information during

half the time interval between two applications of information to the loop, no matter what the step-smoothing properties of the loop. Thus, discontinuous pulsed information leads first of all to the appearance of a systematic delay error ε_{sz}, on which the periodic fluctuations resulting from the individual steps are superimposed.

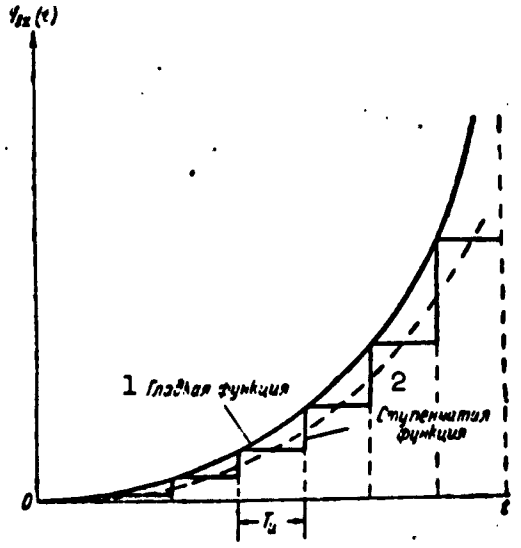

Fig. 41. 1) Smooth function; 2) step function.

The magnitude of the systematic delay error can be calculated easily for every actual case. If the control function is a linear variable that characterizes target motion, the systematic error will equal the rate of change in $\varphi_{vkh}(t)$ multiplied by half the information-arrival period T_i:

$$\varepsilon_{sz} = \frac{d\varphi_{vkh}(t)}{dt}\frac{T_i}{2}. \qquad (144)$$

Thus, for example, if the information for a target that has a velocity component v_n = 0.5 km/sec normal to the target-control point line is received with a period T_p [sic] = 0.1 sec, the systematic error will equal ε_{sz} = 0.025 km, or 25 m.

The systematic information-delay error can be compensated in those cases in which the target does not take evasive action, or executes a minor maneuver. If, however, the quantity $d\varphi_{vkh}(t)/dt$ changes abruptly, the delay error cannot be compensated.

In a properly designed control loop, the errors caused by the discrete nature of the information are, as a rule, considerably smaller than the other errors. In this case, the information-arrival

frequency is normally taken considerably higher than the maximum frequency of the control-loop passband.

There are cases, however, in which this condition is not satisfied, and it is necessary to evaluate the errors appearing owing to the discontinuous application of information at a relatively low frequency. The magnitude of this type of error may be found on the basis of the following considerations.

Each piece of information creates a pulse at the control-loop input in the form of a step of height a (Fig. 41). If the open-loop control transfer function is Y(p), the transform of the function that will appear at the output of a closed control loop owing to the action of each step, will be [Formula (48)]

$$L[\Delta\varphi_{вых}] = \frac{a}{p} \cdot \frac{Y(p)}{1 + Y(p)}. \qquad (145)$$

The waveform spectrum in the closed control loop, by (23), will in this case be [Formula (51)]

$$\varphi(\omega) = F(j\omega) = \frac{a}{j\omega} \cdot \frac{Y(j\omega)}{1 + Y(j\omega)}. \qquad (146)$$

The spectrum of Function (146), corresponding to the action upon the closed loop of the unit step of height a will be continuous. In actuality, the "steps" follow each other at the information-application frequency F.

In order to approximate the errors due to discontinuous information, let us assume identical step heights equal to the average value obtained for the time interval of interest to us when the step function replaces the smooth function (Fig. 41). As we know, when identical pulses are repeated at a frequency F, and each pulse has a continuous spectrum, the pulse train will have a line spectrum consisting of waveforms with frequencies F, 2F, 3F, etc., where the rela-

tive amplitudes and phase angles of the waveforms in the spectrum correspond to those produced at the same frequencies in the continuous spectrum of a single pulse.

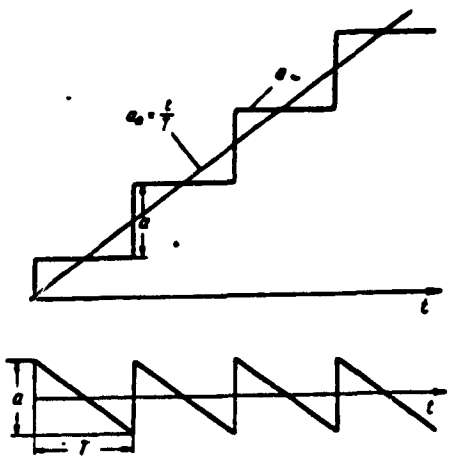

Fig. 42

The continuous spectrum is transformed into a line spectrum when the pulses repeat periodically because all the wave forms that make up a single pulse, with the exception of waveforms of frequency F and their harmonics cancel each other. For waveforms with frequencies that are not multiples of F, the initial phase angles corresponding to the individual pulses will differ, so that these waveforms will add up to zero. At the frequency F and its harmonics, however, the initial phase angles of the waveform constituents of the individual pulses are identical, and thus the amplitudes of these waveforms add algebraically.

A step function, all of whose steps have the same height a, can be thought of as the resultant of a continuously rising component $a_0 = a(t/T)$ and a sawtooth component (Fig. 42)

$$a_\sim = a\left(0{,}5 - \frac{t}{T}\right).$$

For a step height a, expansion of the component $a_\sim$ into a Fourier series yields

$$a_\sim = \frac{a}{\pi}\left(\sin \omega t + \frac{1}{2}\sin 2\omega t - \frac{1}{3}\sin 3\omega t + \ldots \frac{(-1)^k}{k}\sin k\omega t\right), \qquad (147)$$

where $\omega = 2\pi/T$.

If we use the values of the coefficients in Series (147), and we know the frequency characteristic for the open-control loop $Y(j\omega)$, we can find the alternating component at the closed-loop output as

$$a_{\sim \text{вых}} = \frac{a}{k\pi}\left|\frac{Y\left(j\frac{2\pi k}{T}\right)}{1+Y\left(j\frac{2\pi k}{T}\right)}\right|\sin\left[\left(\frac{2\pi k}{T}t\right)+\psi\right], \qquad (148)$$

where the angle ψ is the argument of the closed-loop frequency characteristic $Y(j\omega)/[1 + Y(j\omega)]$ at the frequencies $F = 2\pi/T$, $F_2 = 4\pi/T$, ..., $F_k = 2\pi k/T$.

If, however, experimental data is available as to the reaction of the closed loop to a unit step, the alternating component a~ is found by relatively simple calculation or by graphical means. In order to do this, it is necessary to form the sums of the unit-error values $\varepsilon_1(t)$, equal to $\varphi_{vkh}(t) - 1$ for the case in which a unit step acts upon the closed loop.

$$\sigma_0 = \sum_{k=0}^{k=m} \varepsilon_1(kT); \qquad \sigma_1 = \sum_{k=0}^{k=m} \varepsilon_1\left(kT+\frac{T}{n}\right);$$

$$\sigma_2 = \sum_{k=0}^{k=m} \varepsilon_1\left(kT+\frac{2T}{n}\right); \quad \sigma_{n-1} = \sum_{k=0}^{k=m} \varepsilon_1\left(kT+\frac{n-1}{n}T\right)$$

We then use the points obtained to plot the curve. This curve will be the step function at the output $\varphi_{vykh\ st}(t)$, when a step function with step height unity acts at the input.

As an example, Table 6 gives calculated data for σ_1, σ_2, ..., σ_{n-1} for the system in which a unit step excites the transient process shown in Fig. 21. In this case, the information-arrival period is taken as $T = 6$ sec, while the sums σ_1, σ_2, etc. are calculated for successive instants in time 0.2 sec apart, i.e., for $n = 30$. In view of the fact that the transient on the curve of Fig. 21 ends, for all

TABLE 6

Effect of Unit Step Function on System with Transient Process of Fig. 21. T = 6, n = 30, m = 5

q	0	1	2	3	4	5	6	7	8	9	10	11	12	13	14
$\varepsilon_1\left(\frac{qT}{n}\right)$	−1,00	−0,99	−0,97	−0,95	−0,93	−0,90	−0,87	−0,83	−0,79	−0,72	−0,65	−0,06	−0,53	−0,46	−0,37
$\varepsilon_1\left(T+\frac{qT}{n}\right)$	+0,43	+0,44	+0,46	+0,46	+0,47	+0,47	+0,47	+0,47	+0,47	+0,47	+0,47	+0,46	+0,45	+0,45	+0,44
$\varepsilon_1\left(2T+\frac{qT}{n}\right)$	+0,18	+0,17	+0,15	+0,13	+0,12	+0,10	+0,09	+0,08	+0,06	+0,05	+0,03	+0,02	+0,01	0,00	−0,01
$\varepsilon_1\left(3T+\frac{qT}{n}\right)$	−0,09	−0,09	−0,09	−0,09	−0,09	−0,09	−0,09	−0,09	−0,09	−0,09	−0,08	−0,08	−0,08	−0,08	−0,07
$\varepsilon_1\left(4T+\frac{qT}{n}\right)$	−0,03	−0,03	−0,03	−0,03	−0,03	−0,02	−0,02	−0,02	−0,02	−0,02	−0,02	−0,02	−0,02	−0,02	−0,02
ε_q	−0,51	−0,50	−0,49	−0,48	−0,47	−0,46	−0,43	−0,40	−0,37	−0,31	−0,25	−0,22	−0,17	−0,11	−0,03
q	15	16	17	18	19	20	21	22	23	24	25	26	27	28	29
$\varepsilon_1\left(\frac{qT}{n}\right)$	−0,30	−0,25	−0,16	−0,10	−0,05	−0,00	+0,04	+0,09	+0,14	+0,19	+0,23	+0,28	+0,32	+0,38	+0,40
$\varepsilon_1\left(T+\frac{qT}{n}\right)$	+0,43	+0,41	+0,40	+0,38	+0,37	+0,35	+0,33	+0,32	+0,30	+0,29	+0,27	+0,25	+0,24	+0,22	+0,20
$\varepsilon_1\left(2T+\frac{qT}{n}\right)$	−0,02	−0,03	−0,04	−0,04	−0,05	−0,06	−0,06	−0,07	−0,07	−0,08	−0,08	−0,08	−0,08	−0,09	−0,09
$\varepsilon_1\left(3T+\frac{qT}{n}\right)$	−0,07	−0,07	−0,07	−0,06	−0,06	−0,06	−0,05	−0,05	−0,05	−0,05	−0,04	−0,04	−0,04	−0,03	−0,03
$\varepsilon_1\left(4T+\frac{qT}{n}\right)$	−0,01	−0,01	−0,01	−0,01	−0,01	−0,01	−0,01	−0,01	−0,01	−0,01	−0,01	−0,00	0,00	0,00	0,00
ε_q	+0,03	+0,05	+0,12	+0,17	+0,20	+0,22	+0,25	+0,28	+0,31	+0,34	+0,37	+0,41	+0,44	+0,48	+0,48

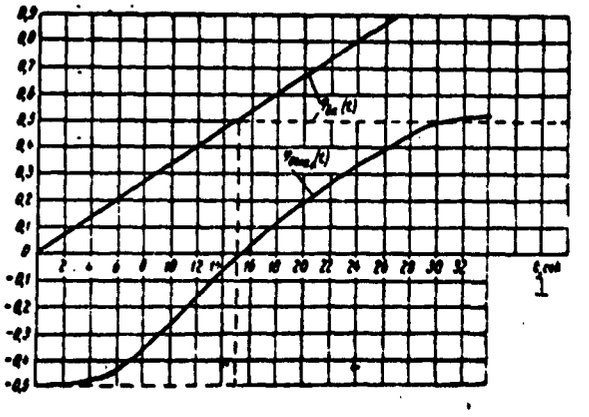

Fig. 43. 1) t, sec.

practical purposes, in 30 sec, the value of "m" was taken as m = = 30/T = 5.

Figure 43 shows the curve constructed from the data of Table 6 for the output function produced by a unit step function applied to the system input.

To go from the unit functions to actual values, we assume that the target moves so that $\varphi_{vkh}(t) = 0.3\ t$, i.e., it moves in a direction normal to the tracking radar beam at a speed of $v_n = 300$ m/sec.

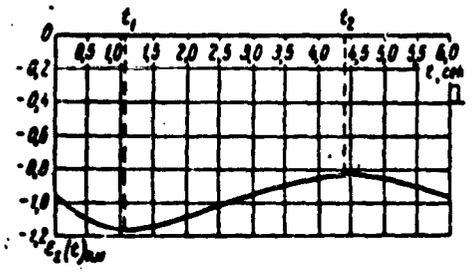

Fig. 44. 1) t, sec.

In view of the fact that the information-arrival period is $T = 6$ sec, the magnitude of the step or the information discreteness is $a = v_n T = 1.8$ km. Thus, the systematic shift or systematic error owing to the discontinuous nature of the information will be

$$\varepsilon_{t_1} = \frac{d\varphi_{vkh}(t)}{dt} = \frac{v_n T}{2} = 0{,}9\ км.$$

The systematic error will produce a displacement of the target to the right of its true position if the target moves from right to left, or to the left of the true position where the target moves in the opposite direction.

From Fig. 43, we find the periodic error component by multiplying the corresponding coordinates by $a = 1.8$ km. The resultant error is shown in Fig. 44, from which it is clear that the greatest deviation from the true target position will equal 1.16 km at time $t = nT + 1.1$ sec, and the minimum deviation will be 0.84 km at time $t = nT + 4.4$ sec.

Manuscript Page No.	[List of Transliterated Symbols]
127	вх = vkh = vkhod = input
128	ст = st = stupen'chatyy = step
128	гл = gl = gladkiy = smooth
129	сз = sz = sistematicheskoye zapazdyvaniye = systematic delay
129	и = i = informatsiya = information
129	н = n = normal'nyy = normal
129	п = p = period = period
132	к = k = kontur = loop
132	вых = vykh = vykhod = output

Chapter 7

FLUCTUATION NOISE AND ITS EFFECT UPON ERRORS IN DETERMINING COORDINATES OF AN OBJECT

As we have already noted, the basic type of fluctuation noise that acts upon radio receiving devices in missile-control systems is the thermal fluctuation of charges in resistors, and fluctuations of thermal-emission current in electron-current and ion-current devices. The structure of these fluctuations, which consist of a tremendous number of very small and short pulses following each other in disorderly fashion, makes it possible to discuss their resultant action at a receiver input as a random function whose instantaneous values follow the normal Gaussian distribution. As a result, the fluctuation spectrum is uniform over a broad frequency band covering, in practice, the entire bandwidth employed in radio-control systems.

Fluctuation signals at the input of any radio device result from the action of an ensemble of random electric pulses. Consequently, they follow a normal probability distribution and the probability that the random instantaneous absolute value of these signals will exceed a given level equals, as we know,

$$P(y \geq y_0) = \Phi(y) = \sqrt{\frac{2}{\pi}} \int_{y_0}^{\infty} e^{-\frac{y^2}{2}} dy, \qquad (36)$$

where $y_0 = x_0/\sigma$, x_0 is the magnitude of the given level, and σ is the RMS noise fluctuation at the system output; the square of σ is proportional to the fluctuation power $\sigma^2 P_p$.

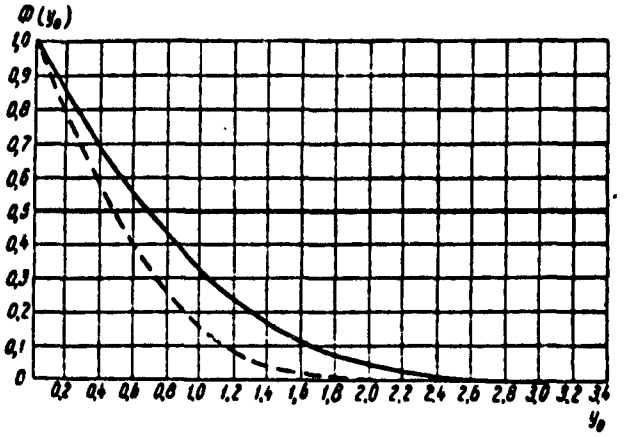

Fig. 45

Figure 45 shows the integral curve $\Phi(y_0)$ for a normal distribution. Numerical values of $\Phi(y_0)$ for various values of y_0 are given in Appendix 2.

The instantaneous current and voltage values exist in time. The greater the probability for some given current or voltage value, the greater the relative time interval during which they will be observed. Thus, Formula (36), which gives the probability that deviations of currents or voltages will exceed given values, at the same time gives the ratio of the time interval Δt during which these current or voltage deviations will occur to the total observation time $\underline{t}$.

For example, the probability that instantaneous fluctuations from the mean values will exceed the RMS deviation σ equals, according to Table 2 and Fig. 45

$$P(\sigma) = \Phi(y_0 = 1) = 0{,}3173.$$

Thus, for a sufficiently large observation time $\underline{t}$, the ratio between the total time Δt during which the instantaneous fluctuation values are larger than σ, and the entire observation time $\underline{t}$ has a limiting value

$$\frac{\Delta t}{t} = \Phi(y_0) = 0{,}3173.$$

The physical structure of fluctuation noise, which is made up of an enormous number of individual very short pulses following each other irregularly, is responsible for many of its properties.

When the results of reception at two different devices are combined, the fluctuation noise power is additive. Consequently, if the noise power due to both receivers is the same, the RMS value of the resultant noise signal equals the RMS value of the fluctuations in each channel, multiplied by $\sqrt{2}$.

When noise from two or more sources is combined, the sign or phase with which these signals are added has no effect upon the result. The noise power due to several sources will always equal the sum of the powers of the individual sources.

Of greatest importance is the fluctuation noise appearing at the input or in the early stages of receiving and measuring devices. This is due to the fact that, as a rule, the noise power due to each element or stage in a receiving-amplifying system is of nearly the same order of magnitude, and the fluctuation noise due to each amplifier stage is applied to the input of the next stage already amplified, and as a result the internal noise of the second and succeeding amplifier stages of a receiver can, as a rule, be neglected.

From the point of view of the magnitude of errors due to fluctuation noise, the ordinary noise spectrum is of great importance. For all practical purposes, this spectrum is completely specified by the frequency response of the elements in which the fluctuations appear, and through which these fluctuations pass.

The duration of a random pulse generating fluctuation noise is of the order of the electron transit time within an electronic vacuum de-

vice or the duration of a fluctuation charge on a resistance.

As is known, the spectral amplitude density distribution for a rectangular pulse of length τ can be represented by the formula

$$|\varphi_\omega| = \frac{2A\tau \sin\left(\frac{\omega\tau}{2}\right)}{\omega\tau}. \qquad (30)$$

For all frequencies ω that satisfy the condition $\omega\tau \ll \pi$ or $f \ll 1/2\tau$, the spectral distribution of noise amplitude and power will be uniform, i.e.,

$$|\varphi_\omega| = A\tau; \quad |\varphi_\omega|^2 = A^2\tau^2. \qquad (31)$$
$$\omega < \frac{\pi}{\tau}$$

Formula (31) is valid for a rectangular pulse alone. The uniform density distribution for noise amplitude and power holds not only for a rectangular pulse, however, but for any other type of pulse, provided that the region of frequencies f within which the uniform distribution is maintained satisfies the condition

$$f \ll \frac{1}{2\tau},$$

where τ is the pulse length.

Actually, by the Fourier transformation

$$\varphi(\omega) = \int_{-\infty}^{+\infty} \varphi(t)\, e^{-j\omega t}\, dt. \qquad (25)$$

If $\varphi(t)$ is zero everywhere except within the time interval from 0 to τ, and is either positive only or negative only within this time interval, we can assume that when $\varphi(\omega)$ is found for those frequencies for which $\omega\tau \ll \pi$ or $f \ll 1/2\tau$, that $e^{-j\omega\tau} \approx 1$, and then

$$\varphi(\omega) = \int_0^\tau \varphi(t)\, dt = Q,$$

where Q is the pulse area $\varphi(t)$.

For a square pulse, $\varphi(\omega) = A\tau$. For a triangular pulse, $\varphi(\omega) = A\tau/2$,

where A is the maximum amplitude of the pulse. For a cosine-wave pulse, $\varphi(\omega)$ is $2A\tau/\pi$, and so forth.

In view of the fact that fluctuation noise is the result of an irregular succession of an ensemble of individual short pulses, the spectral energy distribution for such noise will be the same as for each individual pulse forming the noise. Consequently, the noise power in the frequency region $\Delta\omega$ (expressed in radians) equals

$$P_n = \overline{A^2}\tau^2 \Delta\omega = 2\pi \overline{A^2}\tau^2 \Delta f \qquad (149)$$

or

$$P_n = U_n \Delta f,$$

where U_p is the noise-fluctuation power per unit spectrum bandwidth, or the noise energy.

At a given moment in time, the value of the fluctuation noise at the noise source (for example, across the ends of a resistor, or at the electrodes of a tube) is independent of the values existing at the preceding or subsequent instants of time, as if the time intervals over which the fluctuation noise was measured were small, practically speaking. This is completely natural, since the number of individual noise pulses within the time interval under consideration is independent of the number of pulses in the preceding or subsequent time intervals.

Under actual conditions, a fluctuation-noise source never exists independently, with no relationship to other circuit elements. Together with these elements, it forms a system of loops having specific amplitude and phase characteristics. Practically speaking, such systems of loops have limited frequency passbands, and thus the fluctuation-noise spectra at their outputs are neither uniform nor of unlimited width. At the output of such a system, each noise fluctuation

pulse produces not an instantaneous burst, but an extended process which lasts longer the narrower the passband of the system. Thus, the values of fluctuation noise at the system output, taken within adjacent brief time intervals are no longer mutually independent. It is impossible for the fluctuation noise at the output of a narrowband system to change in value by an instantaneous jump. This is impossible owing to the fact that a very narrowband system cannot pass the frequencies required to produce a steep transient. The system smooths sharp fluctuations in noise appearing across the source terminals.

Fluctuation waveforms in a narrow frequency band $f_2 - f_1 \ll f_1$ can be represented conveniently as waveforms having some mean frequency ω_0 such that $2\pi f_1 < \omega_0 < 2\pi_2$, with a slowly varying amplitude and phase, i.e.,

$$\varphi(t) = x(t)\cos\omega_0 t - y(t)\sin\omega_0 t = \\ = \rho(t)\cos[\omega_0 t + \psi(t)], \tag{150}$$

where $\rho(t)$ is the slowly changing amplitude and $\psi(t)$ is the slowly changing phase angle of the waveforms.

In this case, the RMS values of x(t) and y(t) and $\varphi(t)$, will all be equal, while the random values of these quantities will follow a normal distribution.

The function $\rho(t)$, which is the envelope of the fluctuation waveforms at the output, can be found from the condition

$$x(t) = \rho(t)\cos\psi(t);\ y(t) = \rho(t)\sin\psi(t).$$

Thus, the variables x(t) and y(t), whose random values follow a normal distribution with identical variance σ^2, are the projections of the random variable $\rho(t)$ on the rectangular axes. Here, as we know, the random values of the quantity $\rho(t)$ have a circular probability density distribution (Rayleigh distribution), and the probability that

a random value of $\rho(t)$ will exceed a given level r_0 is

$$P(r>y_0\sigma)=\int_{y_0}^{\infty} y e^{-\frac{y^2}{2}}\,dy=e^{-\frac{y_0^2}{2}}, \qquad (151)$$

where $y_0 = r_0/\sigma$.

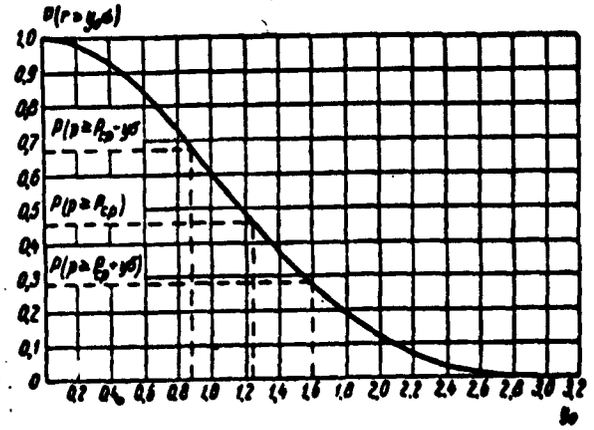

Fig. 46

In this case, the average value of the function $\rho(t)$ will equal

$$\rho_{cp}=\sqrt{\frac{\pi}{2}}\,\sigma\approx 1{,}25\,\sigma. \qquad (152)$$

If waveforms with slowly varying amplitude are subjected to linear rectification and sent through a low-pass filter, there will appear at the output of this filter a DC component proportional to ρ_{sr}, and a low-frequency AC component with random values $r = y\sigma$ proportional to the corresponding values of the function $\rho(t)$ and following the Rayleigh distribution (Fig. 46).

The noise power due to thermal fluctuations of charges in a system not containing an energy source, and having a passband Δf will be

$$\Delta P_ш = 4kT\Delta f, \qquad (153)$$

where k is the Boltzmann constant, equaling $1.38\cdot 10^{-23}$, T is the absolute temperature, Δf is the bandwidth in cycles per second.

In addition to resistances, the input circuits of all receiving

devices contain electronic devices associated with energy sources. The noise appearing in these devices resembles the noise in resistors. The equivalent temperature of the resistor that, from the noise point of view, can replace the electronic device supplied from an external source is greater, however, than the ambient temperature.

The higher equivalent temperature of the electronic device is accounted for by introducing the factor $\underline{h}$ into Formula (153); this quantity is called the noise factor or noise coefficient. The noise factor normally has a value less than ten, and depends upon the characteristics of the electronic device and its operating point. The noise figure is normally given as a characteristic of the receiving device.

In real circuits, the bandwidth Δf is not sharply limited. In order to consider the effects of noise upon a real circuit, it can be characterized by an equivalent frequency bandwidth F_e or Ω_e.

The equivalent bandwidth equals

$$\Omega_e = \frac{1}{|Y(j\omega_c)|^2} \int_0^\infty |Y(j\omega)|^2 d\omega, \qquad (154)$$

where $Y(j\omega)$ is the amplitude-frequency characteristic of the circuit, and $Y(j\omega_s)$ its value at the useful-signal frequency ω_s.

When both fluctuation-noise waveforms and a signal in the form of undamped waveforms $A \cos \omega_s t$, with an amplitude considerably exceeding the RMS value of the fluctuation noise, appear at the input, the resultant due to superposition of the signal and fluctuations may be represented as

$$\varphi(t) = A\cos\omega_c t + x(t)\cos\omega_c t - y(t)\sin\omega_c t = \\ = \rho(t)\cos[\omega_c t + \psi(t)]. \qquad (155)$$

In this case, where $A^2 \gg \overline{x(t)^2}$,

$$\rho(t) = \sqrt{[A + x(t)]^2 + y(t)^2} \approx A + x(t). \qquad (156)$$

Thus, the average value of the signal envelope $\rho(t)$ will equal A; the momentary random $\rho(t)$ will be normally distributed about this mean value [Eq. (36)]. Thus after the signal has been rectified linearly, and passed through a low-pass filter there will appear at the output: a DC component proportional to the amplitude of the signal at the input, A, and an AC low-frequency component proportional to $x(t)$.

The random values of the low-frequency component (distributed normally with a variance σ^2) are proportional to P_p, the power of the fluctuations at the input.

Linear rectification is not the only method of "linearly" converting high-frequency signals and extracting the signal envelope appearing at the input of a receiver.

One possible method for extracting signal envelopes is the so-called homodyne detection method. It consists in using, as a rectifier or detector, a nonlinear element, whose gain varies identically in time and in phase with the frequency of the incoming signal. In practice, this element is an electron tube having a variable gain that is controlled by a local oscillator locked to the frequency of the incoming signal.

Passage of waveforms through a homodyne detector is equivalent to multiplying them by the gain $k \cos \omega_s t$, where $\underline{k}$ is a constant, and ω_s is the frequency of the incoming signal.

Writing the fluctuation noise at the input in the form

$$\varphi(t) = x(t)\cos \omega_c t - y(t)\sin \omega_c t,$$

we obtain

$$k\cos \omega_c t\,\varphi(t) = k\left[x(t)\cos^2 \omega_c t - y(t)\sin \omega_c t\cos \omega_c t\right] = \\ = \frac{k}{2}\left[x(t) + x(t)\cos 2\omega_c t - y(t)\sin 2\omega_c t\right]. \qquad (157)$$

after the signal has passed through the homodyne detector.

If we pass these signals through a filter that eliminates the high-frequency components, we obtain at the filter output the low-frequency component, which is proportional to x(t), i.e., a random quantity following the normal probability distribution law [Formula (36)].

When both a signal A cos $\omega_s t$ and fluctuation noise are present at the input, we obtain at the output of the homodyne detector

$$k\cos\omega_c t\varphi(t) = k[(A + x(t))\cos^2\omega_c t - y(t)\sin\omega_c t\cos\omega_c t] = \\ = \frac{k}{2}[A + x(t) + (A + x(t))\cos 2\omega_c t - y(t)\sin 2\omega_c t]. \quad (158)$$

When these waveforms are passed through a filter that removes the high frequencies, we obtain at the output the sum (k/2)[A + x(t)], which consists of the DC component kA/2 and the superposed random quantity (k/2)x(t) which is normally distributed, and is the same as the random quantity appearing at the output in the absence of signal.

Thus, with homodyne detection, in contrast to linear amplitude detection, the random fluctuation quantity at the output of the low-pass filter is independent of the presence or absence of signal, and in either case, its value follows a normal probability distribution law.

Manuscript Page No.

[List of Transliterated Symbols]

135 п = p = pomekha = noise

141 ср = sr = srednyy = average

141 ш = sh = shum = noise

142 э = e = ekvivalentnyy = equivalent

142 с = s = signal = signal

Chapter 8

FLUCTUATION ERRORS IN BEARING DETERMINATION

1. AREA-COMPARISON METHOD

Fluctuation noise causes errors in determining the position of an object, as well as errors in homing or external guidance owing to the fact that it creates chaotically random deviations in the measured coordinates of objects from their true values.

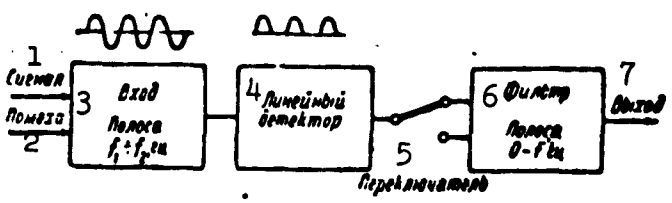

Fig. 47. 1) Signal; 2) noise; 3) input band, f_1-f_2, cps; 4) linear detector; 5) switch; 6) filter, bandwidth, 0-F cps; 7) output.

In order to clarify the basic relationships connecting the angular accuracy of coordinate determination with fluctuation-noise intensity, we shall discuss the following simplified circuit for a receiving-measuring device (Fig. 47) and direction-finding method (Fig. 48).

In the simplified circuit (Fig. 47), the input frequency bandwidth is limited sharply to values lying between f_1 and f_2, so that $f_2 - f_1 \ll f_1$, while at the output, the bandwidth runs from 0 to F cps. The filters at the input and at the output are ideal, i.e., they have a rectangular response curve within these frequency bands. We shall assume that rectification is linear. This is valid for the case under discussion, since in the majority of devices amplification prior to

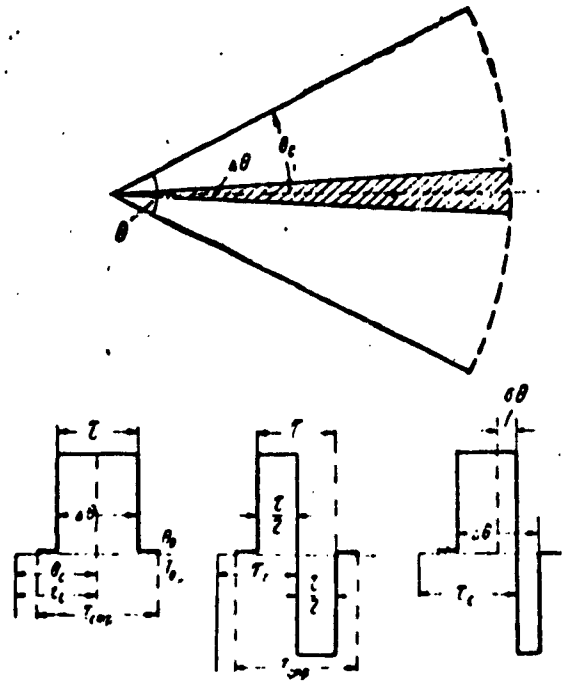

Fig. 48

the final detection stages is so great that the final rectification takes place in the linear region.

We shall assume that frequency conversion, which is almost always used in modern receiver circuits, occurs without distortion of the signal or noise amplitude and phase characteristics in the limited frequency band that is necessary for nearly undistorted signal transmission.

We represent the direction-finding circuit in the following manner.

In rectangular coordinates, let the receiving-device radiation pattern have a width $\Delta\theta$. The pattern periodically sweeps a sector θ degrees wide, with a scanning time of T sec for the sector θ, and a time τ sec required to sweep the angle $\Delta\theta$.

In synchronism with the sector scanning, the direction of the rectified signal is switched (the switch of Fig. 47); the instant of

switching τ_s is so set that it occurs precisely at the center of the angular signal $\Delta\theta$ arriving from the source (Fig. 48).

When there is no fluctuation noise at the input, and when the time t_s coincides precisely with the center of the angular signal, the DC component at the output will be zero. In this case

$$\theta_c = \frac{t_c}{T}\theta.$$

If, however, the switching time is shifted by an angle $\delta\theta$ with respect to the center of the angular signal, the DC signal at the output will equal

$$\delta a_- = kA\frac{\Delta\theta}{\theta}2\frac{\delta\theta}{\theta} = k_1\sqrt{2P_c}\,2\frac{\delta\theta}{\theta}, \qquad (159)$$

where A is the amplitude of the signal waveforms at the input to the receiver circuit, P_s is the signal power at the input, and $\underline{k}$ and k_1 are constants.

When both signal and fluctuation noise are present simultaneously at the input, the receiving circuit is in receiving condition only during the time interval τ, and, as before, the direction of the rectified current is switched at the center of the angular signal, there will be no DC component at the output, but there will be a low-frequency AC output proportional to x(t) [Formula (156)].

In view of the fact that the fluctuation-spectrum bandwidth at the input is considerably wider than the filter bandwidth at the output and that there is practically no correlation between fluctuations at the input in two adjacent time intervals $\tau/2$ (Fig. 48), the switching of the rectified current has no effect upon the power or nature of the low-frequency component appearing at the filter output. Thus, the average power of the low-frequency fluctuation component at the filter output proves equal to

$$P_{n\sim} = k_2^2 P_n \frac{\tau}{T} = k_2^2 P_n \frac{\Delta\theta}{\theta}, \qquad (160)$$

while the RMS value of the low-frequency fluctuation-noise component at the output will be

$$|a_{n\sim}| = k_1 \sqrt{P_{n\sim}} = k_1 \sqrt{P_n \frac{\Delta\theta}{\theta}}. \qquad (161)$$

In this case, the random instantaneous values of $a_{n\sim}$ will be normally distributed, and will have a variance $\sigma_n^2 = k_1^2 P_n(\Delta\theta/\theta)$.

If follows from Formula (159) that to an instantaneous current δa at the filter output there corresponds a deviation of the angle θ_s from the target bearing by an amount

$$\delta\theta = \frac{\delta a}{k_1} \frac{\theta}{2} \sqrt{\frac{1}{2P_c}}.$$

Consequently, the RMS value of the AC component $|a_{n\sim}|$ corresponds to a RMS value of the deviation angle or error

$$|\delta\theta| = \sigma_\theta = \frac{\Delta\theta}{2} \sqrt{\frac{P_n \theta}{2P_c \Delta\theta}} = \frac{\Delta\theta}{2} \sqrt{\frac{P_n}{2P_c} \cdot \frac{T}{\tau}}. \qquad (162)$$

Thus, when there is a Watson noise flux at the input, the signal-source bearing is measured with a random error following a normal law with a RMS value of σ_θ [Formula (162)].

The expression for σ_θ can be written in a more obvious form.

The noise power equals $P_p = U_p F$, where U_p is the mean noise power per unit bandwidth or the fluctuation-noise energy, while F is the bandwidth.

The quantity F is connected with the output-filter time constant so that

$$\frac{1}{F} \approx T_v$$

where T_v is the duration of the transient at the output (Fig. 49). In other words, T_v characterizes the observation or storage time.

Then

$$2P_c\frac{\tau}{T}T_n = 2U_{cr}, \qquad (163)$$

where U_{st} is the signal energy stored during the observation time, and the factor τ/T allows for the discontinuity of the signal energy arriving at the receiving device.

Thus, the RMS error in the angular measurement will equal

$$\sigma_\theta = \frac{\Delta\theta}{2}\sqrt{\frac{U_n}{2U_{cr}}}. \qquad (164)$$

where the random bearing errors $\delta\theta$ are normally distributed, with a variance σ_θ^2.

As Formulas (162) and (164) show, the RMS error in bearing determinations σ_θ is proportional to $\sqrt{(P_p/2P_s)(T/\tau)}$, or $\sqrt{U_p/2U_{st}}$. It will be clear later that in certain other cases (where a different bearing determination method is used, or where a different type of detection is used), the coefficient 2 in the denominator will disappear, and the error proves to be proportional to $\sqrt{U_p/U_{st}}$. The coefficient 2 characterizes the suppression of fluctuation noise by a more powerful signal, since it was assumed earlier that $U_p \ll U_{st}$.

To clarify this, let us consider the effect upon a linear detector of two signals $A_1 \cos \omega_1 t$ and $A_2 \cos(\omega_2 t + \varphi)$, where $A_1 \gg A_2$.

The sum of these signals may be represented, in approximation, as

$$A_1\cos\omega_1 t + A_2\cos(\omega_2 t + \varphi) =$$
$$= \sqrt{|A_1 + A_2\cos(\Delta\omega t + \varphi)|^2 + A_2^2\sin^2(\Delta\omega t + \varphi)}\cos(\omega_1 t + \psi) \approx$$
$$\approx |A_1 + A_2\cos(\Delta\omega t + \varphi)|\cos(\omega_1 t + \psi),$$

where

$$\Delta\omega = \omega_2 - \omega_1, \quad \psi = \operatorname{arctg}\frac{A_2\sin(\Delta\omega t + \varphi)}{A_1 + A_2\cos(\Delta\omega t + \varphi)}.$$

With linear halfwave detection of a signal with amplitude A_1 +

+ $A_2 \cos(\Delta\omega t + \varphi)$ there will appear at the output a DC component proportional to A_1/π, and a low-frequency AC component with an amplitude proportional to A_2/π, and RMS values proportional to $A_2/\pi\sqrt{2}$. Thus, the ratio of the RMS value for the AC component σ_n and the DC component a_- will be

$$\frac{\sigma_n}{a_-} = \frac{A_2}{\sqrt{2}A_1} = \sqrt{\frac{P_2}{2P_1}}.$$

where P_1 is the power of the signal having amplitude A_1 at the input, and P_2 is the power of the signal with amplitude A_2.

If, in addition to a powerful signal with amplitude A_1 there are at the input many signals with amplitudes A_2, A_3, etc., such that their total power P_Σ is considerably less than the power of the first signal, P_1, then by means of considerations similar to those cited above, it is possible to show that in this case as well

$$\frac{\sigma_n}{a_-} = \sqrt{\frac{P_\Sigma}{2P_1}}.$$

When the fluctuation-noise spectrum is continuous, and there is a sufficiently strong signal at the input, this will lead in the limit to Formulas (162) and (164).

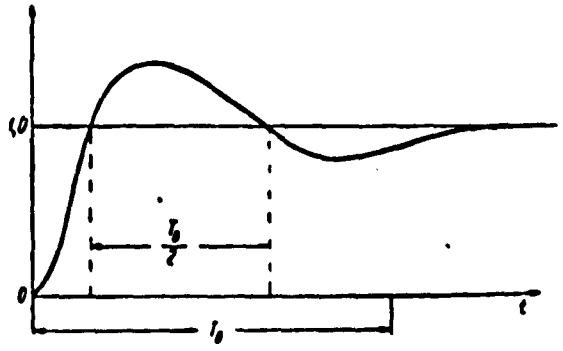

Fig. 49

Formula (164) indicates that the greater the resolution $\Delta\theta$ of the device, and the longer the observation time T_v, the smaller the RMS

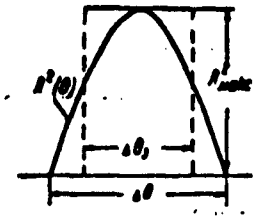

Fig. 50

error and the variance for bearing determination.

The time T_v is a characteristic of the receiving-measuring device. An increase in the time T_v requires a contraction of the device's passband. An increase in reading accuracy can also be gained by automatic recording of individual readings followed by averaging. Then the averaging device or the observer, where the readings are recorded by a human, itself becomes an output filter with a narrow passband and long time constant.

Formula (164) for the RMS angular error σ_θ has been derived for a particular case of measurement; it can be extended, however, to other angular-coordinate measurement cases.

If the antenna pattern is not rectangular, but has some other shape (Fig. 50), the angle $\Delta\theta$ can be replaced by an equivalent angle $\Delta\theta_e$, which is found from the condition

$$P_{\text{макс}}\,\Delta\theta_e = \int_{-\frac{\Delta\theta}{2}}^{+\frac{\Delta\theta}{2}} P_n(\theta)\,d\theta. \quad \text{or} \quad \Delta\theta_e = \varkappa\,\Delta\theta, \tag{165}$$

where

$$\varkappa = \frac{1}{A^2_{\text{макс}}\,\Delta\theta}\int_{-\frac{\Delta\theta}{2}}^{+\frac{\Delta\theta}{2}} A^2(\theta)\,d\theta = \frac{P_{\text{ср}}}{P_{\text{макс}}}. \tag{166}$$

In Expressions (165) and (166), $P(\theta) \sim A^2(\theta)$ is the relationship between the received power and the angle, $P_{maks} \sim A^2_{maks}$ is the maximum received power and P_{sr} is the average received power.

For example, where

$$A^2(\theta) = A^2_{макс} \frac{\sin^2\left(\frac{\pi D}{\lambda}\sin\theta\right)}{\left(\frac{\pi D}{\lambda}\sin\theta\right)^2},$$

$$\int_{-\frac{\Delta\theta}{2}}^{+\frac{\Delta\theta}{2}} A^2(\theta)\,d\theta = A^2_{макс} \int_{-\frac{\Delta\theta}{2}}^{+\frac{\Delta\theta}{2}} \frac{\sin^2\left(\frac{\pi D}{\lambda}\sin\theta\right)}{\left(\frac{\pi D}{\lambda}\sin\theta\right)^2} d\theta.$$

If we assume that $D/\lambda = m$, where m is a sufficiently large integer, while

$$\frac{\pi D}{\lambda}\cdot\frac{\Delta\theta}{2} \approx \pi;\ \frac{\Delta\theta}{2} = \frac{1}{m}.$$

Then

$$\int_{-\frac{\Delta\theta}{2}}^{+\frac{\Delta\theta}{2}} \frac{\sin^2\left(\frac{\pi D}{\lambda}\sin\theta\right)}{\left(\frac{\pi D}{\lambda}\sin\theta\right)^2} d\theta \approx \int_{-\frac{\Delta\theta}{2}}^{+\frac{\Delta\theta}{2}} \frac{\sin^2(a\theta)}{(a\theta)^2} d\theta,$$

where

$$a = \frac{\pi D}{\lambda} = m\pi.$$

$$\int_{-\frac{\Delta\theta}{2}}^{+\frac{\Delta\theta}{2}} \frac{\sin^2(a\theta)}{(a\theta)^2} d\theta = \frac{1}{a}\int_{-\frac{a\Delta\theta}{2}}^{+\frac{a\Delta\theta}{2}} \frac{\sin^2 x}{x^2} dx =$$

$$= -\frac{1}{a}\left|\frac{\sin^2(\pi m\theta)}{\pi m\theta}\right|_{-\frac{1}{m}}^{+\frac{1}{m}} + \frac{1}{a}\int_{-\frac{a\Delta\theta}{2}}^{+\frac{a\Delta\theta}{2}} \frac{\sin 2x}{2x} d(2x) = \frac{2}{a}\,\mathrm{Si}(2\pi),$$

where Si is the sign of the sine integral.

Finding from tables Si (2π) = 1.435, and substituting a = $2\pi/\Delta\theta$, we find

$$\varkappa = 0{,}458$$

for

$\Delta\theta_0 = 0{,}458\,\Delta\theta.$

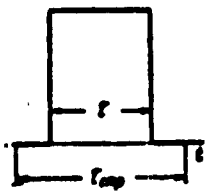

Fig. 51

If the receiving device is turned on during each cycle not for a time τ, but for a longer interval τ_{str} (Fig. 51), then the fluctuation noise power will increase.

As we have already shown, the fluctuation-noise envelope $\rho(t)$ is governed by a Rayleigh distribution in the absence of signal [Formulas (151) and (152)], and has an average value $\rho_{sr} = \sqrt{\pi/2}\sigma$. For a Rayleigh distribution, the probability that a random value $\rho(t)$ will be found between 0 and $y_0\sigma$ equals

$$P(\rho < y_0\sigma) = \int_0^{y_0} y e^{-\frac{y^2}{2}} dy. \qquad (152)$$

With linear amplitude detection, the DC component is proportional to ρ_{sr}. The probability that a random value $\rho(t)$ will be greater than the mean value by an amount $y\sigma$ equals (Fig. 46)

$$P(\rho < \rho_{cp} + y\sigma) - P(\rho < \rho_{cp}) = \int_0^{\rho_{cp}+y\sigma} ye^{-\frac{y^2}{2}} dy - \int_0^{\rho_{cp}} ye^{-\frac{y^2}{2}} dy.$$

The probability that a random value $\rho(t)$ will be less than ρ_{sr} by an amount $y\sigma$ equals

$$P(\rho < \rho_{cp}) - P(\rho < \rho_{cp} - y\sigma) = \int_0^{\rho_{cp}} ye^{-\frac{y^2}{2}} dy - \int_0^{\rho_{cp}-y\sigma} ye^{-\frac{y^2}{2}} dy.$$

When the sign of the rectified signal is switched at the center of time interval τ_{str} (Figs. 47 and 48), the DC component, proportional to ρ_{sr}, will be zero, while the random values of the low-fre-

quency AC component will be determined by the integral curve

$$0{,}5[P(\rho \leqslant \rho_{cp} + y\sigma) - P(\rho < \rho_{cp} - y\sigma)]. \qquad (167)$$

Graphical determination of this probability is shown by the curve in Fig. 46, while curve (167) itself is shown by the dashed line of Fig. 45. Calculation shows that the integral curve (167) is extremely close to the curve that corresponds to a normal probability distribution having double the variance $\sigma_1^2 = 2\sigma^2$. Consequently, if the signal and noise were to act alternately over equal time intervals, then with linear amplitude detection, the RMS angular error would be

$$\sigma'_\theta = \frac{\Delta\theta}{2}\sqrt{\frac{U_n}{U_{cr}}} \qquad \text{rather than} \qquad \sigma_\theta = \frac{\Delta\theta}{2}\sqrt{\frac{U_n}{2U_{cr}}}.$$

When there is no signal, actually, the fluctuation noise acts not for τ_{str} sec during each cycle, but for $\tau_{str} - \tau$ sec. As a result, the RMS angular error equals

$$\sigma_{\theta_0} = \frac{\Delta\theta_0}{2}\sqrt{\frac{U_n}{2U_{cr}}\frac{1}{\tau_k}}, \qquad \text{where} \qquad \tau_k = \frac{\tau}{2(\tau_{cp} - \tau) + \tau} \qquad (168)$$

for linear amplitude detection, and

$$\sigma_{\theta_0} = \frac{\Delta\theta_0}{2}\sqrt{\frac{U_n}{U_{cr}}\frac{\tau_{cp}}{\tau}}.$$

for homodyne detection.

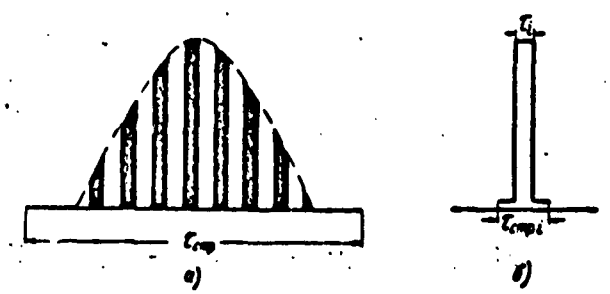

Fig. 52

Where the signal received is not continuous but pulsed (Fig. 52a, b), and the receiving device is switched on for a time $\tau_{str\,i}$ with

each pulse, and the pulse length is τ_1 (we assume that the receiver is turned on within the total time interval τ_{str}), then considerations similar to those given above in examining the effect of various τ_{str} and τ [Formula (168)] with a continuous signal can be used to show that in this case

$$\sigma_\theta = \frac{\Delta\theta_0}{2}\sqrt{\frac{U_ш}{2U_{ст}}\frac{1}{\tau_к}\frac{1}{\tau_ш}}, \qquad (169)$$

where

$$\tau_ш = \frac{\tau_1}{2(\tau_{стр1}-\tau_1)+\tau_1}$$

for linear amplitude detection and

$$\sigma_\theta = \frac{\Delta\theta_0}{2}\sqrt{\frac{U_ш}{U_{ст}}\frac{\tau_{стр}}{\tau}\frac{\tau_{стр1}}{\tau_1}} \qquad (169a)$$

for homodyne detection.

Expressions (169) and (169a) are also general expressions for the RMS angular error due to fluctuation noise. They hold not only for the above-considered method of determining bearing by comparing two halves of the angular signal (Fig. 48), but for other methods as well.

2. THE EQUISIGNAL METHOD

In determining bearing by the equisignal-zone method (Fig. 53), a deviation in the direction of arriving signals from the equisignal line causes a low-frequency harmonic component to appear in the envelope of the signal at the input, on the linear portion of the antenna-directivity curve, while an alternating current with amplitude

$$a_{с-} = \frac{dA(\theta)}{d\theta}\delta\theta = A_{макс}\frac{d\frac{A(\theta)}{A_{макс}}}{d\theta}\delta\theta = \qquad (170)$$
$$= k_1\sqrt{2P_с}\frac{d\frac{A(\theta)}{A_{макс}}}{d\theta}\delta\theta.$$

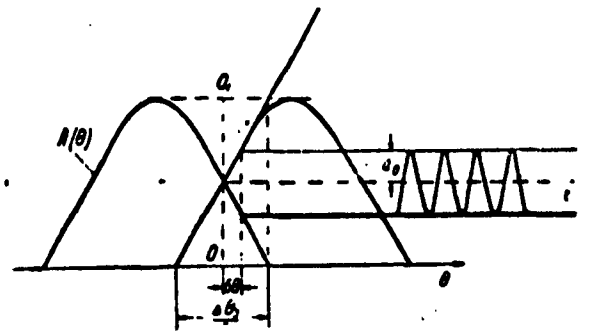

Fig. 53

is produced at the output.

As a result, the RMS value of the low-frequency signal component at the output filter (Fig. 47), which in this case is tuned for a bandwidth that includes the pattern-rotation frequency, equals

$$|a_{c\sim}| = \frac{a_{c\sim}}{\sqrt{2}} = k_1 \sqrt{P_c} \frac{d\frac{A(\theta)}{A_{макс}}}{d\theta} \delta\theta. \qquad (171)$$

At the same time, the RMS value of the low-frequency fluctuation component at the output filter will equal

$$|a_{-n}| = k_1 \sqrt{P_n} = k_1 \sqrt{U_n F}, \qquad (172)$$

where F is the output-filter passband.

The RMS fluctuation error in bearing will in this case be

$$\sigma_\theta = \frac{d\theta}{d\frac{A(\theta)}{A_{макс}}} \sqrt{\frac{U_n}{U_{ст}}}. \qquad (173)$$

The expression $d\theta/(dA\theta/A_{maks})$ represents the angle $\Delta\theta_e/2$ shown in Fig. 53. Thus, the RMS bearing error σ can be represented as

$$\sigma_\theta = \frac{\Delta\theta_э}{2} \sqrt{\frac{U_n}{U_{ст}}}, \qquad (174)$$

where

$$\Delta\theta_э = \sqrt{2}\,\Delta\theta_э',$$

for linear amplitude detection, and $\Delta\theta_e = \Delta\theta_0$ for homodyne detec-

tion.

The effect of the pulse nature of the signal, where the signal is a pulse train, can be allowed for by the very same factor used in Formulas (169) and (169a).

3. PHASE METHOD OF BEARING DETERMINATION

This method consists in the reception of signals by two identical spatially separated input devices I and II (Fig. 54). The outputs of the devices are connected in opposition, and the signals, after being combined in this fashion, are amplified and converted by subsequent stages. If both signals arriving at the input devices are identical in phase, then the added (or more accurately, subtracted) signals will have a zero resultant. In this case, the direction of the incoming signals will be perpendicular to the base D. If, however, the bearing of the signal source differs from the normal to the base by the angle $\delta\theta$, then the difference

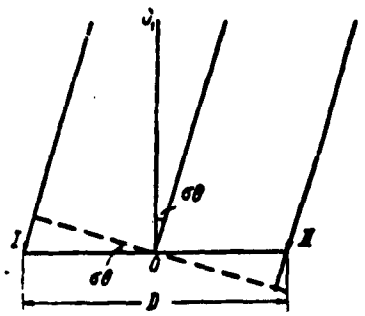

Fig. 54

$$k_1\sqrt{2P_c}\cos\left(\omega_c t-\frac{\pi D}{\lambda}\sin\delta\theta\right)-k_1\sqrt{2P_c}\cos\left(\omega_c t+\frac{\pi D}{\lambda}\sin\delta\theta\right)=k_1 2\sqrt{2P_c}\sin\left(\frac{\pi D}{\lambda}\sin\delta\theta\right)\sin\omega_c t, \quad (175)$$

will be applied to the common stages of the receiver; here P_s is the signal power at the input of one receiving device, D is the separation of the input devices, and λ is the wavelength of the received signal.

The RMS value of the fluctuation noise applied to the common stages of the receiver by the two input devices results, after rectification, in low-frequency oscillations having a RMS value of

$$|a_{n\sim}|=k_1\sqrt{2P_n},$$

where P_p is the fluctuation noise power at the input of one device.

The DC component set up by the rectified signal at the filter output (Fig. 47) equals

$$a_{c-} = k_1 2\sqrt{2P_c}\frac{\pi D}{\lambda}\delta\theta, \qquad (176)$$

when the angles $\delta\theta$ are small. Thus, the RMS fluctuation error in the bearing σ_θ will equal

$$|\delta\theta| = \sigma_\theta = \frac{\lambda}{2\pi D}\sqrt{\frac{U_n}{U_{cr}}} = \frac{\Delta\theta_e}{2}\sqrt{\frac{U_n}{U_{cr}}}. \qquad (177)$$

where $\Delta\theta_e$ is the equivalent angle, equal numerically to $\lambda/\pi D$, i.e., equal to the angle between two successive values of the angle θ for which the signal at the output of the receiver vanishes, divided by π.

A phase detector can also be used for bearing determination by the phase method.

A phase detector is a circuit element that contains an electronic device passing current of constant magnitude and sign only when positive voltage is applied simultaneously to the two control electrodes.

When harmonic waveforms having the same frequency, but differing in phase by an angle $\pi-\varphi$ are applied to the control electrodes of such a device, a series of DC pulses of length proportional to the phase shift φ, appears at the output of the device. In view of the fact that the pulse height is constant and independent of the control-voltage amplitude, the DC component at the output of such a phase detector will always be proportional to the phase-shift angle φ (Fig. 55a).

Figure 55a gives a diagram for the two voltages $A_1 \sin \omega t$ and $A_2 \sin (\omega t - \pi + \varphi)$, while Fig. 55b shows pulses of current with a constant amplitude A passing through the phase detector only in the time interval $\tau = \varphi/\omega$; the pulses are proportional to the phase-shift angle between the voltages on the first and second control electrodes.

In the phase method of bearing determination, the signal voltage

on one control electrode of the phase detector equals $k_1 A \cos [\omega t - (\pi D/\lambda) \sin \delta\theta)]$, while the voltage on the second control electrode will be $k_2 A \cos [\omega t + (\pi D/\lambda) \sin \delta\theta - \pi]$ [Fig. 54 and Formula (175)]. In addition, there will appear on the control electrodes fluctuation-noise voltages equal respectively to

$$k_1 [x(t) \cos \omega t_1 - y(t) \sin \omega t_1]$$

and

$$k_2 [x(t) \cos \omega t_2 - y(t) \sin \omega t_2],$$

where

$$t_1 = t - \frac{\pi D}{\lambda \omega} \sin \delta\theta;$$

$$t_2 = t + \frac{\pi D}{\lambda \omega} \sin \delta\theta.$$

Thus, the resultant voltages on the first and second control electrodes can be written as

$$k_1 A_{o1} \cos \left(\omega t - \frac{\pi D}{\lambda} \sin \delta\theta + \psi_1\right) =$$

$$= k_1 \sqrt{[A + x(t)]^2 + [y(t)]^2} \cos \left(\omega t - \right.$$

$$\left. - \frac{\pi D}{\lambda} \sin \delta\theta + \psi_1\right).$$

where

$$\operatorname{tg} \psi_1 = \frac{k_1 y(t)}{k_1 [A + x(t)]} \approx \frac{y(t)}{A}, \text{ or } \psi_1 \approx \frac{y(t)}{A},$$

and

$$k_2 A_{o2} \cos \left(\omega t + \frac{\pi D}{\lambda} \sin \delta\theta - \pi + \psi_2\right).$$

where

$$A_{o2} = \sqrt{[A + x(t)]^2 + [y(t)]^2} \text{ \& } \psi_2 \approx \frac{y(t)}{A}.$$

Thus, the phase shift between the voltages on the electrodes will be equal, approximately, to

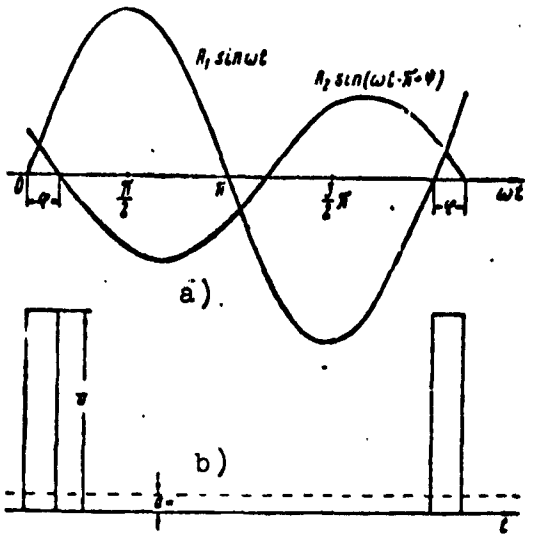

Fig. 55

$$\varphi = \frac{2\pi D}{\lambda}\delta\theta + \psi_1 + \psi_2.$$

Since following the detector the current will be proportional to the phase-shift angle φ, at the filter output there will be DC component

$$a_- = k\frac{2\pi D}{\lambda}\delta\theta$$

and a random low-frequency AC component

$$a_{n\sim} = k(\psi_1 + \psi_2).$$

The quantities ψ_1 and ψ_2 follow the normal probability distribution for random values. Consequently, the variance of the sum of these quantities will equal the sum of the variances

$$\sigma_\Sigma^2 = \sigma_{\psi 1}^2 + \sigma_{\psi 2}^2.$$

As a result, the RMS value of the low-frequency component will be

$$|a_{n\sim}| = k\sqrt{2}|y(t)|.$$

Or, if we express the signal amplitude A ~ $\sqrt{2P_s}$ in terms of the signal power at input P_s, and y(t) ~ $\sqrt{2P_p}$ in terms of the mean noise

power P_p, we will obtain

$$|a_{n\sim}| = k\sqrt{\frac{P_n}{P_c}}.$$

Comparison of the expressions for $a_{\sim}$ and $|a_{n\sim}|$ shows that the RMS error in bearing determination by the phase method, when there is a linear phase detector in the circuit, will be

$$|\delta\theta| = \sigma_\theta = \frac{\lambda}{2\pi D}\sqrt{\frac{P_n}{P_c}} = \frac{\lambda}{2\pi D}\sqrt{\frac{U_n}{U_{cr}}}. \qquad (177)$$

This agrees with the expression for the RMS error (177) with the same bearing-determination method and a linear amplitude detector.

As an illustration, we will give some examples of fluctuation-error calculations.

1. Let us find the fluctuation error in bearing determination by a PPI radar unit with the following characteristics:

scanning angle, $\theta = 360^\circ$;

scanning time, $T_0 = 5$ sec;

observation (storage) time, $T_v = 10$ sec;

antenna area, $S_a = 40$ m^2;

antenna gain, $\bar{g} = 30{,}000$;

equivalent resolution, $\Delta\theta_e = 3.7 \cdot 10^{-2}$;

efficiency of receiving-transmitting system, $\eta_a = 0.5$;

pulse power, $P_i = 5 \cdot 10^6$ watts;

pulse duty factor, $1/\mu_i = 1/1000$;

angle gate utilization factor [Formula (156)], $\eta_s = 0.5$;

pulse gate utilization factor [Formula (157)], $\eta_i = 0.5$;

noise energy, $U_p = 10^{-19}$ watt/cps.

Linear amplitude detection is used.

It is required to find the magnitude of the RMS error in determining the bearing of an object having a reflecting surface $S_{ts} = 1$ m^2,

located at a distance R = 200 km from the radar unit.

We find the peak signal power

$$P_c = \frac{P_i \bar{g} S_a S_u \eta_{ip}}{(4\pi R^2)^2} = \frac{5 \cdot 10^6 \cdot 3 \cdot 10^4 \cdot 40 \cdot 1 \cdot 0{,}5}{(12{,}56 \cdot 4 \cdot 10^{10})^2} =$$
$$= 1{,}19 \cdot 10^{-11} \text{ watt.}$$

The signal energy stored during the observation time is

$$U_{cr} = \frac{P_c}{\mu_i} \frac{\Delta\theta}{\theta} \frac{T_a}{T_0} = \frac{1{,}19 \cdot 10^{-11}}{10^3} \times$$
$$\times \frac{3{,}7 \cdot 10^{-2}}{6{,}28} \frac{10}{5} = 1{,}4 \cdot 10^{-16} \text{ watt/cps.}$$

The RMS error in bearing determination is

$$\sigma_\theta = \frac{\Delta\theta_a}{2} \sqrt{\frac{U_n}{2U_{cr}} \frac{1}{\eta_k} \frac{1}{\eta_u}} =$$
$$= 1{,}85 \cdot 10^{-2} \sqrt{\frac{10^{-19} \cdot 4}{2 \cdot 1{,}4 \cdot 10^{-16}}} = 6{,}95 \cdot 10^{-4} \text{ radians,}$$

i.e., $\sigma_\theta \approx 0.04^\circ$ or an angle of 2.4 minutes.

Manuscript Page No.

[List of Transliterated Symbols]

147 с = s = signal = signal

148 н = n = nizkochastotnyy = low-frequency

148 п = p = pomekha = noise

148 в = v = vykhod = output

151 э = e = ekvivalentnyy = equivalent

151 макс = maks = max = maximum

151 ср = sr = srednyy = average

161 ц = ts = tsel' = target

Chapter 9

FLUCTUATION-NOISE ERRORS IN RANGING

1. PULSE METHOD

The determination of distance by comparison of two halves of a pulse (Fig. 56) is carried out as in the determination of direction by the same method (Fig. 48). Thus, the expression for the RMS fluctuation error in bearing σ_r is identical with the expression for the angular error σ_θ with the angular resolution being replaced by the range resolution $\Delta r = c\tau_1/2$, where c is the speed of light,

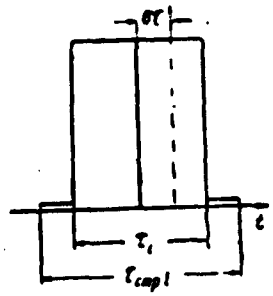

Fig. 56

$$\sigma_r = \frac{\Delta r}{2}\sqrt{\frac{U_n}{2U_{cr}}\frac{1}{\gamma_{ic}}\frac{1}{\gamma_{ii}}}, \text{ where } \gamma_{ii} = \frac{\tau_i}{2(\tau_{cmp\,i} - \tau_i) + \tau_i} \qquad (178)$$

for linear amplitude detection, or

$$\sigma_r = \frac{\Delta r}{2}\sqrt{\frac{U_n}{U_{cr}}\frac{\tau_{cmp\,i}}{\tau_i}} \qquad (178a)$$

for homodyne detection.

2. CONTINUOUS-WAVE METHOD

We now consider a method of measuring distance with the aid of a continuous-wave frequency-modulated signal. In this case, the range is measured by comparing the frequency of the signal radiated by the transmitter at a given instant with the frequency of the reflected signal. If the transmitter frequency is varied linearly at a rate f', beats with frequency

$$F_r = f' \frac{2r}{c}.$$

are formed between the emitted and received signals.

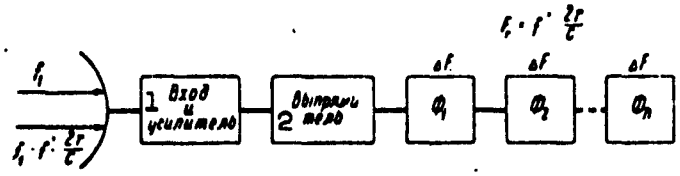

Fig. 57. 1) Input and amplifier; 2) rectifier.

If at the output of the receiving device, following the rectifier, there is a bank of filters (57), each having a passband ΔF (we assume that these are ideal filters), it is possible to determine the distance in terms of the presence of a discrete number of oscillations in one of the filters of this bank, with a range resolution

$$\frac{\Delta r}{2} = \frac{c\Delta F}{2f'}. \qquad (179)$$

In those filter sections in which there is no signal, the RMS value of the low-frequency signals due to fluctuation noise will equal, as we have already shown,

$$|a_{n\sim}| = k_1 \sqrt{P_n} = k_1 \sqrt{U_n \Delta F}.$$

Both signal and noise will be present in that section within whose passband the frequency F_r corresponding to the target range falls; as a result, the amplitude of the resultant signal will change slowly.

As in the very first case considered by us of superposition of fluctuation noise on a continuous signal, the envelopes of these waveforms will be [Formula (156)]

$$\rho(t) = A + x(t), \qquad (156)$$

where A is the amplitude of the waveforms of the signal, and x(t) is a

random quantity characterizing the probability that the envelope will deviate from the mean value A.

The random values of the quantity x(t) follow a normal distribution, and if the signal amplitude A is expressed in terms of the input signal power P_s as $A = k\ 2P_s$, then the RMS value of |x(t)| will be

$$\sigma = k\sqrt{P_n} = |a_{n-}|.$$

The interaction of the signal and fluctuation noise leads to the appearance of a probability that within a certain time interval, the random value of the envelope [Formula (156)] will be equal to or less than the RMS value of the waveforms in those filter sections where fluctuation noise alone is present. For this to happen, the random value of the quantity x(t) must be negative and must approach A. Since the RMS value of |x(t)| equals $k\sqrt{P_p}$, this is equivalent to having the random value of x(t) exceed the RMS value by

$$\frac{A}{|a_{n-}|} = \sqrt{\frac{2P_c}{P_n}} = y_0 \text{ times.}$$

The probability of this event is

$$0{,}5\,\Phi(y_0) = \frac{1}{\sqrt{2\pi}}\int_{y_0}^{\infty} e^{-\frac{y^2}{2}}\,dy.$$

We have the same probability for the event in which the random value of the range fluctuation exceeds the RMS σ_r by $\Delta r/2\sigma_r = y_0$ times.

Thus, the RMS value of fluctuations or errors in distance measured with the aid of a FM-CW signal is the same as that for the pulse ranging method,

$$\sigma_r = \frac{\Delta r}{2y_0} = \frac{\Delta r}{2}\sqrt{\frac{P_n}{2P_c}} = \frac{\Delta r}{2}\sqrt{\frac{U_n}{2U_{cr}}}, \qquad (180)$$

where $\Delta r/2$ is given by Formula (179).

As an illustration for the determination of range-measurement er-

ror, we will use the data of the first example of angular-error calculation on page 162. We will assume the duration of the pulse to be $\tau_1 = 4 \cdot 10^{-6}$ sec.

Then the resolution distance is $\Delta r = c\tau_1/2 = 0.6$ km. Consequently, the RMS range-measurement error is

$$\sigma_r = \frac{\Delta r}{2}\sqrt{\frac{U_n}{2U_{cr}}\frac{1}{\tau_u}\frac{1}{\tau_c}} = 0{,}3\sqrt{\frac{4\cdot 10^{-10}}{2{,}8\cdot 10^{-10}}} = 0{,}011 \text{ км},$$

i.e., $\sigma_r = 11$ m.

Manuscript Page No.

[List of Transliterated Symbols]

164	н = n = nizkochastotnyy = low-frequency
164	Ф = F = fil'tr = filter
165	с = s = signal = signal

Chapter 10

PROBABLE VALUES OF COORDINATES, VELOCITIES, AND ACCELERATIONS

1. PROBABLE VALUES OF OBJECT COORDINATES IN THE PRESENCE OF FLUCTUATION NOISE

The considerations given above showed that with linear detection, the RMS value of coordinate fluctuations due to fluctuation noise equals

$$\sigma_\xi = \frac{\Delta\xi}{2}\sqrt{\frac{U_ш}{U_{сг}}}. \qquad (181)$$

where ξ is the coordinate (angular or linear), and $\Delta\xi$ is the system resolution for this coordinate.

The random errors in determining coordinates (angles and distances) are normally distributed with variances equal, respectively, to σ_θ^2 and σ_r^2. This makes it possible to find the probability that the object is located within a given volume of space. In polar coordinates, the volume of space is determined by the range, azimuth, and elevation resolutions Δr, $\Delta\theta$, and $\Delta\varphi$ (Fig. 58). We let the variances of the corresponding coordinates be σ_r^2, σ_θ^2, and σ_φ^2.

Let us go from the coordinates $\underline{r}$, θ, and φ to the dimensionless quantities

$$x = \frac{\delta\theta}{\Delta\theta/2}; \quad y = \frac{\delta\varphi}{\Delta\varphi/2}; \quad z = \frac{\delta r}{\Delta r/2}.$$

The magnitudes $\delta\theta$, $\delta\varphi$, and δr are measured from the center of the volume (Fig. 58) formed by segments $\Delta\theta$, $\Delta\varphi$, and Δr. The RMS value of fluctuations in the ($\underline{x}$, $\underline{y}$, $\underline{z}$) coordinate system will be constant and

equal to

$$\sigma_{x,y,z} = \sqrt{\frac{U_n}{2U_{cr}}}, \qquad (182)$$

so that the random values of $\underline{x}$, $\underline{y}$ and $\underline{z}$ will have a normal probability distribution.

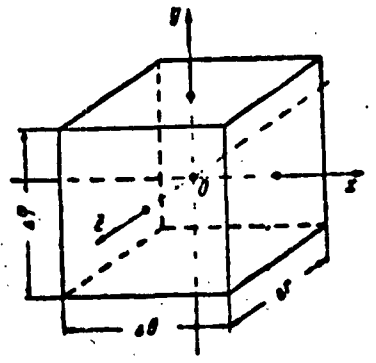

Fig. 58

If the projections of the vector ρ on the three mutually perpendicular axes are random quantities, normally distributed, and with identical variances σ^2 then, as we know, the magnitude of the vector ρ is also a random quantity with a spherical probability distribution. In this case, the probability $P(\rho \leq \rho_0)$ that a point with coordinates $\underline{x}$, $\underline{y}$, and $\underline{z}$ lies within a sphere of radius ρ_0 equals

$$P(\rho < \rho_0) = \sqrt{\frac{2}{\pi}} \int_0^{\rho_0} \frac{\rho^2}{\sigma^3} e^{-\frac{\rho^2}{2\sigma^2}} d\rho = 1 - \Phi(y_0) - \sqrt{\frac{2}{\pi}}\, y_0\, e^{-\frac{y_0^2}{2}},$$

where

$$y_0 = \frac{\rho_0}{\sigma}; \quad \Phi(y_0) = \sqrt{\frac{2}{\pi}} \int_{y_0}^{\infty} e^{-\frac{y^2}{2}} dy; \quad \sigma = \sqrt{\frac{U_n}{2U_{cr}}}. \qquad (183)$$

Thus, the smaller the fluctuation-noise energy in comparison with the signal energy, and the greater the signal power and observation time T_v, the greater the probability that a target will be located within a given volume having a common center with the resolution cell formed by the coordinate segments Δr, $\Delta\theta$, and $\Delta\varphi$.

When we go from the $\underline{x}$, $\underline{y}$, $\underline{z}$ coordinates to θ, φ, and $\underline{r}$ coordinates, the spherical distribution becomes an ellipsoidal distribution,

and the geometric locus of points forming the surface of equal target-detection probability changes from a sphere to an ellipsoid with axes δr, $\delta\theta$, and $\delta\varphi$.

For example, when $U_p/2U_{st} = 0.16$ and $\sigma_{x,y,z} = 0.4$, the probability that there is a target within the ellipsoid with semiaxes $\delta r_0 = \Delta r/2$, $\delta\theta_0 = \Delta\theta/2$, and $\delta\varphi_0 = \Delta\varphi_2$, i.e., for $\rho = 1$, $y_0 = 2.5$, will equal

$$P(\rho < 1) = 1 - \Phi(2,5) - \sqrt{\frac{2}{\pi}} 2,5 e^{-3,125} =$$
$$= 1 - 0,0124 - 0,0137 = 0,974.$$

When only two coordinates are being measured, for example, the azimuth θ and the elevation φ, the spherical distribution will be replaced by a circular distribution of the random coordinate values

$$x = \frac{\delta\theta}{\Delta\theta/2} \quad \text{and} \quad y = \frac{\delta\varphi}{\Delta\varphi/2}.$$

In accordance with the circular distribution, the probability of finding a point with coordinates x and y within a circle of radius ρ equals

$$P = (\rho < \rho_0) = \frac{1}{\sigma^2}\int_0^{\rho_0} \rho e^{-\frac{\rho^2}{2\sigma^2}} d\rho = 1 - e^{-\frac{y_0^2}{2}}. \qquad (184)$$

where

$$y_0 = \frac{\rho_0}{\sigma}.$$

Formula (181) makes it possible to draw certain general conclusions.

1. Consider a volume of space scanned by a radar station within the angle θ in one plane, within the angle φ in a second plane perpendicular to the first, and within a range of 0 to r (Fig. 59).

We let the equivalent angular resolution in one plane be $\Delta\theta_e$, and in the other plane, $\Delta\varphi_e$, while the range resolution is Δr_e. With the

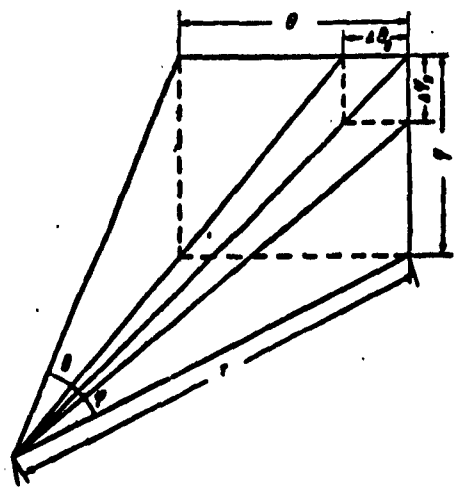

Fig. 59

available mean radar power P_{sr}, it is possible to use various methods in searching for a target.

Angle scanning can be carried out continuously, dividing the power P_{sr} among $(\theta/\Delta\theta_e)(\varphi/\Delta\varphi_e) = mn$ installations, each scanning a solid angle $\Delta\theta_e \times \Delta\varphi_e$. Then each such solid angle will receive a power $P_{sr}(1/m)(1/n)$.

It is possible to scan the solid angle $\theta \cdot \varphi$ sequentially by a beam measuring $\Delta\theta_e \times \Delta\varphi_e$, in which the entire power P_{sr} is concentrated, using continuous emission, but employing a receiver having mn identical output filters each connected in turn to the rectifier for a time equal precisely to 1/mn of the entire time T that the solid angle $\theta\varphi$ is scanned. Thus, each output filter stores energy from a solid angle $\Delta\theta_e\Delta\varphi_e$ assigned specifically to it.

From the formula

$$q_t = \frac{\Delta\xi}{2}\sqrt{\frac{U_s}{2U_{cr}}} \qquad (181)$$

it follows that for the same observation time T_v, the probability of finding a target within a given solid angle will be the same with both scanning methods.

Actually, in the first case, the signal energy stored over time T_v by an output filter of an individual receiver scanning the angle $\Delta\theta_e\Delta\varphi_e$ will equal the power P_{sr}/mn, multiplied by the total time T_v, i.e.,

$$U_{cr} = P_{cp}\frac{\Delta\theta_e\Delta\varphi_e}{\theta\varphi}T_v.$$

In the second case, the energy U_{st} entering the appropriate filter during one scan of the angle will equal the product of the power P_{sr} and the time $(1/N)(\Delta\theta_e/\theta)(\Delta\varphi_e/\varphi)$, where N is the number of times the angle is scanned in one second. As in the first case, over a time

T_v sec during which the angle $\theta\varphi$ will be scanned T_vN times, each output filter will store an amount of energy

$$U_{cr} = P_{cp}\frac{T_n N}{N}\frac{\Delta\theta_0\Delta\varphi_0}{\theta\varphi}$$

As we have already noted, the RMS error in range measurement for a given resolution Δr, given total observation time T_v, and mean signal power P_{sr} is independent of whether the signal is continuous or pulsed.

This permits us to formulate the following statement. For given receiver-transmitter parameters, distance r and observation time T_v, the probability of detecting a target in a given volume is determined completely by the energy supplied to unit volume of space, and does not depend upon the scanning method.

2. For range measurements

$$\sigma_r = \frac{\Delta r}{2}\sqrt{\frac{U_s}{2U_{cr}}} \qquad (181)$$

Thus, the probability of finding an object within a given volume of space for a given pulse energy becomes greater the shorter the pulse. This follows from the fact that when the pulse energy is constant, i.e., with U_{st} = const, σ_r is directly proportional to Δr, i.e., to the pulse length.

3. Using Formula (181) let us determine the effect of frequency on the accuracy with which object coordinates are determined when all other system parameters remain unchanged, including the antenna dimensions.

An n-fold decrease in wavelength leads to an n^2-fold increase in antenna power gain. Thus, the power incident upon an object within the field of view of the antenna will also increase by a factor of n^2. When a solid angle $\theta\varphi$ is sequentially scanned with the same number of

scanning cycles per unit time, but the wavelength is shortened by a factor of n, the object will be located within the field of view for $1/n^2$ less time, since the beam area $\Delta\theta \cdot \Delta\varphi$ decreases by a factor of n^2 for an n-fold decrease in wavelength. Thus, the energy stored in each output filter over the observation time T_v will be precisely the same. But, since the lengths $\Delta\theta$ and $\Delta\varphi$ are reduced by a factor of n when the wavelength is divided by the same factor, the RMS error in determining the angular coordinates θ and φ will be decreased by a factor of n at the shorter wavelength.

The conclusions drawn from the examples just given are naturally valid only when the output filter is opened only during the time in which a signal pulse is arriving. If the output filter is affected by rectified waveforms during the entire scanning period T, we must use Formula (168) in place of Formula (181), and introduce the factor $1/\eta_s$, which substantially changes the results.

The basic limitation on all of the considerations given is that of linear amplification and linear rectification in the receiving device. The presence of extremely nonlinear elements in the receiver (such as limiters) substantially changes the expressions for the RMS error and the probability of detecting an object within a given volume of space.

The utilization of nonlinear elements in the receiving device prior to the final rectifier causes operation of the entire system to depend strongly upon the signal power, which complicates the device. Thus, it is permissible to use the simplified circuit shown in Fig. 47 for a large class of very common devices designed to operate over a broad range of received-signal powers.

2. FLUCTUATION ERRORS IN DETERMINING VELOCITY AND ACCELERATION

The presence of fluctuation noise causes uncertainty in measure-

ment of target coordinates, as we have seen. There is a similar uncertainty in measuring the speed of an object in the presence of fluctuation noise.

As an illustration, we shall discuss an example pertaining to measurement of angular velocity.

Let an antenna with a pattern $\Delta\theta$ wide track a target moving with an angular velocity θ'.

If the angular velocity with which the target moves differs from θ' by an amount $\Delta\theta'$, and the observation time (system time constant), which is the reciprocal of the system bandwidth F, equals T_v, the average angular displacement of the antenna-pattern axis relative to the target bearing in time T_v will be $\Delta\theta' T_v = \delta\theta$.

It was shown earlier, in our discussion of the question of the divergence of the antenna-pattern center line from the target bearing that the DC component of the rectified signal will in this case equal [Formula (159)]

$$\delta a_{-} = k_{11}\sqrt{2P_c}\frac{2\delta\theta}{\theta}. \qquad (159)$$

If the relative angular velocity of the target equals $\Delta\theta'$,

$$\delta a_{-} = k_{11}\sqrt{2P_c}\frac{2\Delta\theta' T_a}{\theta}. \qquad (182)$$

When fluctuation noise is present, the RMS value of the low-frequency component in the rectified signal will equal

$$a_{n-} = k_{11}\sqrt{P_n}\sqrt{\frac{\Delta\theta}{\theta}}. \qquad (161)$$

Looking at the random values of the low-frequency fluctuation component, we can assume that they appear as the DC component a_{-} and are generated by the divergence between the axis line of the antenna pattern and the target bearing, or by the fact that the target moves

at speed θ', but is located off the equisignal line by an angle $\delta\theta$, or by the fact that the target is moving with a relative speed $\Delta\theta'$ during the observation time.

In the first case, the presence of signal at the receiver output may be caused by uncertainty in target position measurement, expressed by the RMS value of the angular fluctuation

$$\sigma_\theta = \frac{\Delta\theta_0}{2}\sqrt{\frac{U_ш}{U_{сг}}}.$$

In the second case, we can explain the observational results by target motion with a RMS value of the fluctuation in the relative angular velocity $\Delta\theta'$

$$\sigma_{\Delta\theta'} = \frac{\Delta\theta_0}{2T_0}\sqrt{\frac{U_ш}{U_{сг}}}. \qquad (183)$$

Thus, in determining target bearing in the presence of fluctuation noise, we interpret the observation results either as an uncertainty in target position (expressed in terms of the RMS error σ), or as an uncertainty in target speed (expressed in terms of the RMS error $\sigma_{\Delta\theta'}$).

In precisely the same way, we can show that if the apparent variations in the angular velocity of an object due to fluctuations take on random values changing during the observation time in accordance with a normal law with variance $\sigma^2_{\Delta\theta'}$, the apparent acceleration values will also be random quantities, normally distributed, and the RMS acceleration will be

$$\sigma_{\Delta\theta'} = \frac{\Delta\theta_0}{2T_0^2}\sqrt{\frac{U_ш}{2U_{сг}}}. \qquad (184)$$

In discussing the effect of fluctuation noise on vehicle control, we must remember that control commands are usually functions of the coordinates, and contain both terms proportional to the coordinates,

and terms proportional to their derivatives.

Thus, not only fluctuations in target coordinates affect the motion of a guided vehicle, but fluctuations in the coordinate derivatives as well, i.e., random velocities and accelerations.

In order to find the random and RMS values of the apparent velocities, conditioned by fluctuation noise, we note that if the fluctuation spectrum is uniform with an amplitude density A and frequency range of from 0 to F, the instantaneous fluctuations can be represented as

$$\int_{f=0}^{F} A\cos(2\pi f t + \varphi_f)\,df,$$

where the values of φ_f are random. Then the mean fluctuation power is

$$P_{cp} = \sigma_t^2 = \frac{A^2}{2} F,$$

and the RMS value of the fluctuations is

$$|\xi| = \sigma_t = \frac{A}{\sqrt{2}}\sqrt{F}.$$

The random fluctuation values are normally distributed.

For a uniform spectrum in the frequency band from 0 to F, the amplitude density for the first derivative of a fluctuation at frequency F equals $2\pi fA$, since the instantaneous value of the fluctuation derivative is

$$\frac{d\int_0^F A\cos(2\pi f t + \varphi_f)\,df}{dt} = -\int_0^F A 2\pi f \sin(2\pi f t + \varphi_f)\,df.$$

Thus, the variance of the first derivative equals

$$\sigma_{t'}^2 = \int_0^F \frac{A^2 4\pi^2 f^2}{2}\,df = \frac{A^2 4\pi^2}{6} F^3, \qquad (185)$$

and the RMS value of the apparent velocity, due to fluctuations is

$$|\xi'| = \sigma_{\xi'} = \frac{2\pi FA}{\sqrt{6}}\sqrt{F} \,. \qquad (186)$$

The random values of the apparent velocity will also be normally distributed.

Comparing the RMS values of the coordinate fluctuations $|\xi|$ with the RMS velocity $|\xi'|$, we find that

$$|\xi'| = \sigma_{\xi'} = \frac{2\pi F}{\sqrt{3}}\sigma_{\xi}$$

or

$$\sigma_{\xi'} \approx \frac{2\pi\sigma_{\xi}}{\sqrt{3}\,T_0}. \qquad (187)$$

Applying the same considerations to the apparent acceleration ξ'', we find that

$$|\xi''| = \sigma_{\xi''} = \frac{4\pi^2F^2}{\sqrt{5}}\sigma_{\xi};$$

$$\sigma_{\xi''} = \frac{4\pi^2}{\sqrt{5}}\frac{\sigma_{\xi}}{T_0^2}. \qquad (188)$$

In the general case, where the amplitude density in the fluctuation spectrum is frequency-dependent, and the frequency spectrum at the output cannot be strictly limited by the frequency F, the variance of the coordinates ξ will equal

$$\sigma_{\xi}^2 = \frac{1}{2}\int_0^{\infty} A^2(f)\,df.$$

The variance of the first derivative is

$$\sigma_{\xi'}^2 = \frac{4\pi^2}{2}\int_0^{\infty} A^2(f)f^2 df.$$

The variance of the second derivative is

$$\sigma_{\xi''}^2 = \frac{16\pi^4}{2}\int_0^{\infty} A^2(f)f^4 df$$

etc.

The apparent target velocity and acceleration appearing when fluctuations are present lead to the production of commands for guided vehicles corresponding to these apparent changes in target-motion conditions. Such commands cause the guided vehicle to oscillate irregularly about the basic direction of motion. The object thus experiences, in addition to acceleration forces caused by the nature of the path, additional acceleration forces and mechanical stresses that can reach considerable magnitudes.

Let us show this with an example.

Let a guided vehicle move precisely toward the predicted point of impact with the target, and let it be located near this point, which is at a distance R = 200 km from the point at which the target coordinates are measured. In addition, let the RMS error in the determination of one of the angular target coordinates equal an angle of one minute, $\sigma_\xi = 1' = 2.9 \cdot 10^{-4}$ radians, and let the bandwidth of the vehicle closed control loop be F = 0.2 cps. Then the RMS linear acceleration of the vehicle due to the control commands caused by fluctuations will equal

$$|w| = R\sigma_{\dot{\omega}} = \frac{4\pi^2 \cdot 4 \cdot 10^{-2} \cdot 2{,}9 \cdot 10^{-4} \cdot 2 \cdot 10^{-6}}{\sqrt{5}} = 41{,}5\ \text{m/sec}^2,$$

i.e., the RMS acceleration force on the vehicle will be

$$\frac{|w|}{g} = \frac{41{,}5}{9{,}81} = 4{,}25.$$

Manuscript Page No.	[List of Transliterated Symbols]
168	в = v = vklyuchena = "on"
169	п = p = pomekha = noise
169	э = e = ekvivalentnyy = equivalent
170	ср = sr = srednyy = average
173	с = s = signal = signal
173	н = n = nizkochastotnyy = low-frequency

Chapter 11

ERRORS DUE TO SIGNAL FLUCTUATIONS

If the amplitude of a signal from a target is not constant, changes chaotically, and is a random quantity, it will also produce errors in determining target coordinates.

In many cases, the source of signal fluctuations is the existence of a set of radiation-scattering points on the object whose coordinates are being measured. When the object is moving, the phase angles of radio waves scattered from the different points vary randomly, and their sum, arriving at the receiver, will be a random quantity following a Rayleigh distribution. In this respect, the effect of a signal fluctuation is similar to that of thermal fluctuation noise. The signal-fluctuation spectrum, however, covers a considerably narrower frequency band than does the noise fluctuation spectrum. The intensity of a signal scattered from the target can also vary substantially if the target turns or oscillates about its center of mass.

When the signal-fluctuation spectrum is considerably broader than the reciprocal of the length τ of an angle-signal pulse in bearing measurement (Fig. 48), or than the length of a pulse τ_1 in ranging (Fig. 51), the errors in the determination of target coordinates due to signal fluctuations can be found as in the case of errors due to noise fluctuations.

A special case of signal fluctuations, observed at small distances from a target, is the wandering of the reflection center over the tar-

get surface.

It is convenient to discuss the influence of signal fluctuations on coordinate measurement in terms of the simplest example of bearing determination by the equal-area method with a rectangular antenna pattern (Fig. 48).

The noise power acting on the output filter when the equal-area method of bearing determination is used (Figs. 47 and 48) is proportional to the ratio between the passband F of this filter and the bandwidth f_f of the signal fluctuation spectrum.

Thus, the RMS fluctuation error will equal

$$\sigma_{\theta c} = \frac{\Delta\theta}{2}\sqrt{\frac{P_n}{P_c}\frac{F}{f_\phi}} = \frac{\Delta\theta}{2}\sqrt{\frac{F}{f_\phi}}. \qquad (189)$$

since in this case $P_p = P_s$, on the basis of the considerations that were used to derive Formula (168), allowing for the effect of fluctuations in the absence of signal.

When the signal fluctuations have a limited relative amplitude, as, for example, when the direct and scattered signals arrive simultaneously at the receiver input, the RMS error is

$$\sigma_{\theta c} = \frac{\Delta\theta}{2}\sqrt{\frac{\varkappa}{2}\frac{F}{f_\phi}}. \qquad (190)$$

where $\varkappa$ is a coefficient accounting for that portion of the input power due to the presence of the scattered signal. The factor 2, appearing in the denominator under the radical, is due to the fact that superposition of the fluctuating portion of the signal upon the nonfluctuating portion has the same effect (with linear amplitude detection) as the reception of fluctuation noise in the presence of a signal [derivation of Formula (162)].

The most frequently encountered case, in which the signal fluctuation spectrum is narrower than the reciprocal of τ or τ_1 may be

considered, in approximation, as follows (Fig. 60).

We assume that when there are fluctuations in the signal, the envelope varies in accordance with a cosine law. Then, if the bearing is measured by the equal-area method, and the antenna pattern is rectangular (Fig. 48), during each scanning cycle, there will act upon the low-frequency filter at the output a pulse equal to the difference of the difference of the neighboring areas, hatched on Fig. 60,

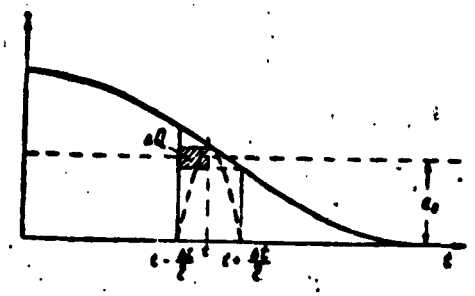

Fig. 60

$$\Delta Q = a_0 \int_{t-\frac{\Delta t}{2}}^{t} \cos \Omega \tau \, d\tau - a_0 \int_{t}^{t+\frac{\Delta t}{2}} \cos \Omega \tau \, d\tau \approx \frac{a_0 \Omega \Delta t^2}{4} \sin \Omega t .$$

If we assume equal probability for any time t, the RMS value of the pulse area will be

$$\Delta Q_0 = \frac{a_0 \Omega \Delta t^2}{4\sqrt{2}} ,$$

while the mean square area Q_e, with a uniform signal-fluctuation frequency spectrum over the range from 0 to Ω_0 will be

$$\overline{\Delta Q_0^2} = \frac{a_0^2 \Delta t^4}{32 \Omega_0} \int_0^{\Omega_0} \Omega^2 \, d\Omega = \frac{a_0^2 \Delta t^4 \Omega_0^2}{96} .$$

Thus, if we simplify the physical picture somewhat, we can assume that where there is signal fluctuation in the frequency band extending from 0 to Ω_0, pulses will arrive at the low-frequency filter input with a RMS area of

$$|\Delta Q_0| = \sqrt{\overline{\Delta Q_0^2}} = \frac{a_0 \Omega \Delta t^2}{\sqrt{96}} \approx 0{,}1 \, a_0 \Omega_0 \Delta t^2 . \qquad (191)$$

Since the pulse duration is $\Delta t/2$, as we see from Fig. 60, the RMS

pulse amplitude or height will be

$$|\Delta Q_0|\frac{2}{\Delta t} = |A| = 0{,}2\,a_0\Omega_0\Delta t.$$

The energy of such a pulse is proportional to the product of the square of the height, A^2, and the pulse length $\Delta t/2$, i.e.,

$$|A^2|\frac{\Delta t}{2} = 0{,}02\,a_0^2(\Omega_0\Delta t)^2\Delta t,$$

while the power is proportional to

$$0{,}02\,a_0^2(\Omega_0\Delta t)^2\Delta t\,N$$

where there are N pulses per second.

If all the pulses had the same sign, their energy and power would be distributed between the DC and AC components. Since the sign or direction of the pulse is random, however, the DC component equals zero and all of the pulse power goes into the AC components.

As we know, the energy in the spectrum of a single pulse of length τ is distributed in accordance with the law

$$\frac{\sin^2\left(\frac{\omega\tau}{2}\right)}{\left(\frac{\omega\tau}{2}\right)^2},$$

and thus

$$\int_0^{\infty}\frac{\sin^2\left(\frac{\omega\tau}{2}\right)}{\left(\frac{\omega\tau}{2}\right)^2}\,d\left(\frac{\omega\tau}{2}\right) = \frac{\pi}{2},$$

while for the region in which $\omega\tau/2$ is small, where $\omega\tau/2 \approx \sin(\omega\tau/2)$,

$$\int_0^{\frac{\omega\tau}{2}}\frac{\sin^2\left(\frac{\omega\tau}{2}\right)}{\left(\frac{\omega\tau}{2}\right)^2}\,d\left(\frac{\omega\tau}{2}\right) \approx \frac{\omega\tau}{2}.$$

Thus, only that portion of the power that is proportional to

$$\frac{\omega\tau}{2}\frac{2}{\pi} = \frac{4\pi F\Delta t}{4\pi} = F\Delta t.$$

is concentrated in the frequency region between 0 and F cps.

Thus, the low-frequency power at the filter output in the receiving device due to target fluctuations is proportional to

$$0{,}02\,a_0^2(\Omega_0\Delta t)^2 NF\Delta t^2,$$

while the RMS value of the low-frequency component is

$$|a_{n\sim}| = 0{,}141\,a_0\Omega_0\Delta t\sqrt{NF\Delta t}. \qquad (192)$$

If we equate $|a_{n\sim}|$ with the DC increment $\delta a_=$ that appears when the center line of the antenna pattern deviates by an angle $\delta\theta$ from the target bearing,

$$\delta a_= = 2a_0 N\Delta t\frac{\delta\theta}{\Delta\theta},$$

we find that the RMS bearing error $|\delta\theta|$ due to signal fluctuations equals

$$|\delta\theta| = \sigma_\theta = \frac{\Delta\theta}{2}\,0{,}141\,\Omega_0\Delta t\sqrt{\frac{F}{N}}. \qquad (193)$$

Owing to the fact that under actual conditions the directivity characteristic of the receiving device is not rectangular (dashed line on Fig. 60), the area $\Delta\theta_e$ is substantially reduced, and the RMS fluctuation error becomes several (up to 2-3) times smaller than the value calculated above.

In order to develop some idea of the effect that the shape of the angle signal has upon the magnitude of errors in the presence of signal fluctuations, we shall discuss the special case in which the antenna pattern has the form M cos $\omega_0 t$, and the angular signal has a cosine form.

If the angular signal were a rectangle, the area difference $Q_1 - Q_2$ would equal

$$Q_1 - Q_2 = -\frac{4A}{\Omega}\cos\varphi \sin^2\frac{\Omega\tau}{4}. \qquad (194)$$

If the angular signal were of the cosine type,

$$Q_1 = A\int_{-\frac{\tau}{2}}^{0}\sin(\Omega t+\varphi)\cos\omega_0 t\,dt =$$

$$= \frac{A}{2}\int_{-\frac{\tau}{2}}^{0}\{\sin[(\omega_0+\Omega)t+\varphi]-\sin[(\omega_0-\Omega)t-\varphi]\}\,dt;$$

$$Q_2 = A\int_{0}^{\frac{\tau}{2}}\sin(\Omega t+\varphi)\cos\omega_0 t\,dt = \frac{A}{2}\int_{0}^{\frac{\tau}{2}}\{\sin[(\omega_0+\Omega)t+\varphi]-$$

$$-\sin[(\omega_0-\Omega)t-\varphi]\}\,dt.$$

Then

$$Q_1-Q_2=\frac{2A\cos\varphi}{\omega_0^2-\Omega^2}\left(\Omega-\omega_0\sin\frac{\omega_0\tau}{2}\sin\frac{\Omega\tau}{2}-\Omega\cos\frac{\omega_0\tau}{2}\cos\frac{\Omega\tau}{2}\right).$$

Since $\omega_0\tau/2 = \pi/2$

$$Q_1 - Q_2 = \frac{2A\cos\varphi}{\omega_0^2-\Omega^2}\left(\Omega-\omega_0\sin\frac{\Omega\tau}{2}\right).$$

While if $(\Omega\tau/2) \ll (\pi/2)$,

$$Q_1 - Q_2 \approx \frac{2A\cos\varphi}{\omega_0^2-\Omega^2}\left(\Omega-\frac{\pi}{2}\Omega\right) = -1{,}14\frac{\Omega}{\omega_0^2-\Omega^2}A\cos\varphi. \qquad (195)$$

Comparing Expression (195) with the difference $(Q_1-Q_2)_1$ for the case in which the angular signal is rectangular (194), we find that

$$\frac{(Q_1-Q_2)_1}{(Q_1-Q_2)_2} = \frac{4A\cos\varphi}{\Omega}\sin^2\frac{\Omega\tau}{4}\frac{\omega_0^2-\Omega^2}{1{,}14\,A\,\Omega\cos\varphi} =$$

$$= \frac{4}{1{,}14}\frac{\omega_0^2-\Omega^2}{\Omega^2}\sin^2\frac{\Omega\tau}{4}. \qquad (196)$$

Or, in approximation, allowing for the fact that

$$\omega_0\tau=\pi;\ \sin\frac{\Omega\tau}{4}\approx\frac{\Omega\tau}{4};\ \omega_0^2>\Omega^2,$$

$$\frac{(Q_1-Q_2)_1}{(Q_1-Q_2)_2}\approx\frac{\pi^2}{4{,}6}=2{,}15.$$

In the limiting case, when the angular signal is triangular,

$$(Q_1 - Q_2)_3 = A\left[\int_{-\frac{\tau}{2}}^{0}\left(1-\frac{2t}{\tau}\right)\sin(\Omega t+\varphi)\,dt - \right.$$

$$\left. -\int_{0}^{\frac{\tau}{2}}\left(1-\frac{2t}{\tau}\right)\sin(\Omega t+\varphi)dt\right] = \frac{2A\cos\varphi}{\Omega}\left(\frac{2}{\Omega\tau}\sin\frac{\Omega\tau}{2}-1\right).$$

Expanding sin ($\Omega\tau/2$) in a series, and taking only the first two terms of the expansion, we obtain

$$(Q_1 - Q_2)_3 = \frac{2A\cos\varphi}{\Omega}\left[\frac{2}{\Omega\tau}\left(\frac{\Omega\tau}{2}-\frac{\Omega^3\tau^3}{2\cdot 3\cdot 8}\right)-1\right] =$$

$$= \frac{2A\cos\varphi}{\Omega}\frac{\Omega^2\tau^2}{24}.$$

Comparing this expression with the value of $(Q_1-Q_2)_1$ for the rectangular signal, we find

$$\frac{(Q_1-Q_2)_1}{(Q_1-Q_2)_3} = \frac{4A\cos\varphi}{\Omega}\sin^2\frac{\Omega\tau}{4}\frac{12}{A\cos\varphi\,\Omega\tau^2} \approx 3, \qquad (197)$$

i.e., a nonrectangular signal can decrease the value of $|\delta\theta| = \sigma_\theta$ [Formula (193)] by at most a factor of three.

We shall now determine the order of magnitude of errors due to signal fluctuations, and will compare their magnitude with the RMS noise error computed in the example of page 162. We shall assume that the data for the radar unit and the observation conditions are the same as those given for this example, and that the signal-fluctuation spectrum is uniform and occupies a band of frequencies F_0 ranging from 0 to 10 cps.

We find the ratio of $\sigma_{\theta sh}$, the noise error [Formula (169)], and $\sigma_{\theta s}$, the signal fluctuation error [Formula (193)], dividing the latter by two owing to the fact that the signal is not rectangular:

$$\frac{\sigma_{\theta sh}}{\sigma_{\theta s}} = \left(\frac{\Delta\theta_0}{2}\sqrt{\frac{U_n}{2U_{cr}}\frac{1}{\eta_k}\frac{1}{\eta_d}}\right):\left(\frac{\Delta\theta_0}{2}0{,}07\,\Omega_0\Delta t\sqrt{\frac{F}{N}}\right).$$

In this expression, $\Omega_0 = 2\pi F_0 = 20\pi$,

$$\Delta t = \frac{\overline{\Delta\theta_0}}{2\pi} N = \frac{\Delta\theta_0}{2\pi}\frac{1}{T_0}; \quad F = \frac{1}{T_0} = 0{,}1 \text{ cps}; N = \frac{1}{T_0} = 0{,}2 \text{ cps}.$$

Then

$$\sigma_{\theta c} = 1{,}85 \cdot 10^{-2} \cdot 1{,}4\pi \frac{3{,}7 \cdot 10^{-2}}{2\pi} 0{,}2 \sqrt{0{,}5} = 6{,}75 \cdot 10^{-5} \text{ radians}.$$

On page 165, it was found that $\sigma_{\theta sh} = 6.95 \cdot 10^{-4}$ radians.

Thus,

$$\frac{\sigma_{\theta sh}}{\sigma_{\theta c}} \approx 10.$$

This is the ratio where the target distance is R_1 = 200 km. If the target range is less, this ratio will decrease and, for example, at a distance R_2 = 100 km, it will be 2.5, at a distance R_3 = 50 km, it will be 0.6, etc. Thus, the noise fluctuation errors and the errors due to signal fluctuations are comparable in magnitude.

In determining bearing by the equisignal zone method (Fig. 53), these signal fluctuations pass into the receiving device in their entirety when the equisignal zone is pointed accurately toward the source. Thus, the RMS value of the low-frequency fluctuation-noise component at the receiver output equals, in this case,

$$|a_{n-}| = k_1 \sqrt{P_c \frac{F}{f_\phi}},$$

where F is the passband of the receiver output filter, f_f is the bandwidth of the spectrum of signal fluctuations, which we assume to be uniform over this band.

In discussing bearing errors caused by fluctuation noise, it was shown that deviation of the equisignal zone from the target bearing causes low-frequency signals to appear in the receiver with a RMS value of

$$|a_{c-}| = k_1 \sqrt{P_c} \frac{d\frac{A(\theta)}{A_{max}}}{d\theta} \delta\theta, \qquad (171)$$

where $\delta\theta$ is the angular error.

Thus, with the equisignal-zone method, the RMS angle fluctuation due to signal fluctuations proves to equal

$$|\delta\theta| = \sigma_\theta = \left| \frac{d\theta}{d\frac{A(\theta)}{A_{max}}} \right| \sqrt{\frac{F}{f_\Phi}} = \frac{\Delta\theta_0}{2} \sqrt{\frac{F}{f_\Phi}}. \qquad (198)$$

Bearing measurement by the phase method is not affected by errors associated with signal fluctuations for cases in which these fluctuations are purely amplitude changes, and involve no distortion of the arriving wave fronts owing to wandering of the radiation source over the target surface.

The effect of signal fluctuations on the magnitude of ranging errors with the equal-area method can be found by the same method used for bearing errors. The corresponding expression for the RMS bearing error takes the form

$$\sigma_r = \frac{\Delta r}{2} \frac{0{,}14\,\Omega_0 \Delta t \sqrt{F}}{\sqrt{N_i}}. \qquad (199)$$

where N_i is the number of pulses per second, Δt is the pulse length.

The remaining designations are the same as those used for the bearing error [Formula (193)].

Signal fluctuations also cause errors in ranging with the CW-FM method. The physical significance of their appearance lies in the fact that in place of the monochromatic waveforms with a beat frequency determining the distance to the source, a spectrum of waveforms appears, changing the beat frequency into a frequency band; this may lead to an uncertainty in range measurement with a narrow output-filter passband

ΔF.

In addition to fluctuations in the signal from a target, a substantial source of errors in determining distance by the CW method is oscillator fluctuation noise. Despite the low power carried by this noise in comparison with the oscillator power, it may cause substantial errors, since in converting the beat frequencies, the power of the oscillator signal appearing in the receiving device is far greater than the signal power. From the physical viewpoint, oscillator fluctuation noise has the same effect upon error magnitude in ranging as does thermal fluctuation noise, and if we know the energy U_p, the RMS error in determining the distance can be found from Formula (181).

Manuscript Page No.

[List of Transliterated Symbols]

179 Ф = f = flyuktuatsiya = fluctuation

179 с = s = signal = signal

180 э = e = ekvivalentnyy = equivalent

182 н = n = nizkochastotnyy = low-frequency

184 ш = sh = shum = noise

186 макс = maks = maximum = maximum

187 п = p = pomekha = noise

Chapter 12

EQUIVALENT CONTROL-LOOP BANDWIDTH

One of the chief characteristics of a linear system that determines the way in which it is affected by fluctuation noise is the width of the system passband. In analyzing the effect of fluctuation noise on a system, it is convenient to replace it with an ideal filter that is flat with respect to a limited passband. In actuality, however, the amplitude response of any system is nonuniform, and is not strictly limited, but is spread out over the spectrum with a gradual drop in amplitude, either in the high-frequency region alone, or in both directions from the maximum value.

In this connection, it becomes necessary to replace the actual characteristic by an ideal characteristic, and to determine the equivalent bandwidth for the ideal response curve that would cause noise to have an identical effect upon the actual and equivalent systems.

If the noise spectrum at the system input is uniform, then the distribution of the RMS amplitude values over the spectrum at the output is determined completely by the amplitude-frequency characteristic of the system

$$|Y(j\omega)| = \Phi(\omega),$$

where $|Y(j\omega)|$ is the modulus of the frequency characteristic $Y(j\omega)$. As far as the distribution of noise energy over the frequency spectrum at the output is concerned, if it is distributed uniformly at the input, it will be proportional to $\Phi^2(\omega) \cdot d\omega$, where $d\omega$ is an element of the

frequency spectrum, expressed in radians/sec.

Thus, in order to determine the fluctuation-noise energy at the system output, we must know the value of the integral

$$\int_0^{\infty} \Phi^2(\omega)\, d\omega.$$

It is a very cumbersome task to evaluate this integral on the basis of the complete characteristic of a complex system such as the

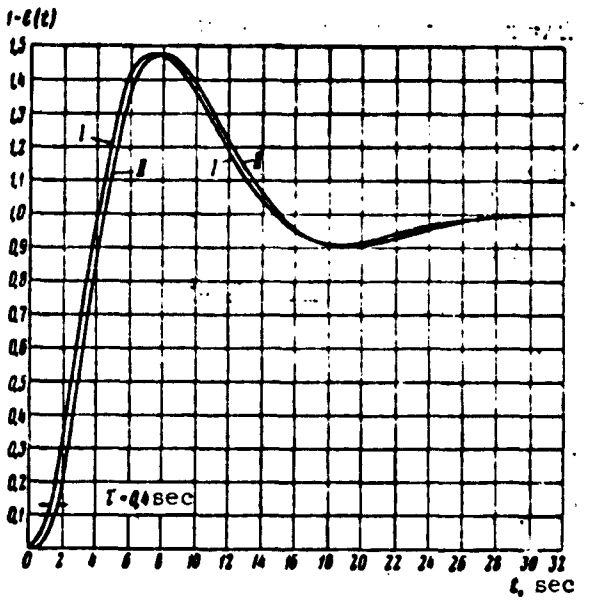

Fig. 61

closed control loop required by a sufficiently high order of control. In addition, the many coefficients that determine the frequency characteristics of actual systems cannot be determined beforehand with sufficient accuracy. The characteristic of a system that has already been designed, however, and the equivalent bandwidth, determining the way in which the system is affected by fluctuation noise, can be found rather simply from experimental data.

To do this, we may make use of the system reaction to a unit step function, found experimentally.

Let us consider the relationship between the energy of a process

occurring in time, and the expression for this energy in terms of the step function for this process.

A process occurring in time can be represented as a Fourier integral*

$$\varphi(t)=\frac{1}{2\pi}\int_{-\infty}^{\infty}\varphi_\omega\, e^{j\omega t}\,d\omega, \qquad (23)$$

where $\varphi(\omega)$ characterizes the distribution of amplitudes and phases over the spectrum of waveforms corresponding to the process $\varphi(t)$.

On the other hand, the function $\varphi(\omega)$ has a Fourier expression in terms of $\varphi(t)$:

$$\varphi_\omega=\int_{-\infty}^{+\infty}\varphi(t)e^{-j\omega t}\,dt. \qquad (24)$$

Formulas (23) and (24) enable us to find the integral of $\varphi^2(t)$

$$\int_{-\infty}^{+\infty}\varphi^2(t)\,dt=\frac{1}{\pi}\int_{0}^{\infty}|\varphi_\omega|^2\,d\omega. \qquad (37)$$

If we know the reaction of the loop to the unit step function, this reaction can be used as a basis for plotting loop reaction to a rectangular pulse of length τ and amplitude unity. Such a pulse takes the form of two unit steps of opposite sign, following each other by a time interval τ. Thus, if we have the experimentally obtained time dependence of the process in the closed loop when a single pulse acts on the loop, as shown in Curve I of Fig. 61, we will obtain the reaction of this loop to a rectangular pulse of length τ, as a function of the difference in ordinates of the two curves I and II of Fig. 61; the curves are shifted by the time τ with respect to each other. This construction is shown in Fig. 62.

The modulus of the spectral function for a rectangular pulse of length τ and unity amplitude, i.e., the spectral amplitude distribution vs. frequency relationship, will be

$$|\varphi(\omega)| = \frac{2\sin\frac{\omega\tau}{2}}{\omega} = \tau\frac{\sin\frac{\omega\tau}{2}}{\left(\frac{\omega\tau}{2}\right)}.$$

For sufficiently small values of τ and ω

$$\sin\frac{\omega\tau}{2} \approx \frac{\omega\tau}{2} \;\&\; |\varphi(\omega)| = \tau,$$

i.e., in the region of small ω, the spectrum is uniform.

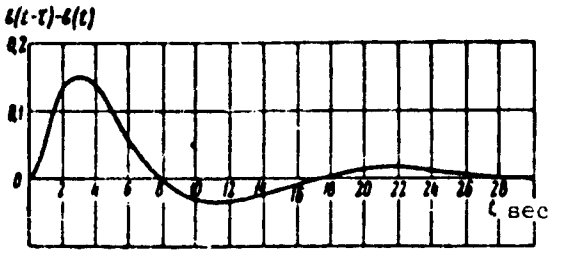

Fig. 62

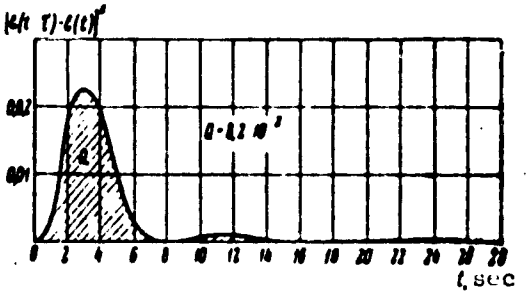

Fig. 63

If the amplitude-frequency characteristic of the system is limited, practically speaking, to the frequency band ranging from 0 to ω_{maks}, satisfying the condition

$$\sin\frac{\omega_{макс}\tau}{2} \approx \frac{\omega_{макс}\tau}{2},$$

then the area under the curve of Fig. 63, whose ordinates are the squares of the ordinates of the curve of Fig. 62, will represent the energy of the system under the influence of a uniform continuous waveform spectrum with a spectral amplitude density of τ.

Thus, if we have an experimentally derived relationship for the waveforms at the system output $\varphi(t)$ when a unit step function acts on the system, by completing the construction shown in Figs. 61, 62, and 63, we are able to find the system energy when it is acted upon by fluctuations having a uniform continuous waveform spectrum.

If the system or loop under consideration were an ideal filter with a passband ranging from 0 to ω_1, and a frequency response whose ordinates were unity within this passband, then when a rectangular pulse of length τ and a height of unity acted upon the loop, the energy in the loop would be, by (37)

$$\frac{1}{\pi}\int_0^{\omega_1} \tau^2 \frac{\sin^2\left(\frac{\omega\tau}{2}\right)}{\left(\frac{\omega\tau}{2}\right)^2} d\omega.$$

If the pulse length τ satisfies the condition

$$\frac{\omega_1\tau}{2} \approx \sin\frac{\omega_1\tau}{2},$$

then

$$\frac{1}{\pi}\int_0^{\omega_1} \tau^2 \frac{\sin^2\left(\frac{\omega\tau}{2}\right)}{\left(\frac{\omega\tau}{2}\right)^2} d\omega \approx \frac{\omega_1\tau^2}{\pi}. \qquad (200)$$

Let us select a value $\omega_1 = 2\pi$ (naturally, for a sufficiently small value of τ). Then by Formula (200), the quantity $2\tau^2$ will equal the energy in the ideal filter, having a passband from F = 0 to F = = 1 cps.

The ratio of the energy in an actual system studied to the energy in an ideal filter with a passband F equal to unity, when this system and the ideal filter are acted upon by a continuous uniform waveform spectrum with identical amplitude densities, will be equal numerically to the equivalent system passband F_{ekv}. In other words, this ratio

equals the passband of that ideal bandpass filter whose energy equals the energy in the system under consideration when there is a uniform waveform spectrum at the input.

Thus, if

$$Q = \tau^2 \int_{-\infty}^{+\infty} \varphi^2(t)\,dt = \frac{1}{\pi}\int_0^{\infty} \Phi^2(\omega)\,d\omega,$$

then

$$\frac{Q}{2\tau^2} = F_e = \frac{1}{2}\int_{-\infty}^{+\infty} \varphi^2(t)\,dt. \qquad (201)$$

Thus, if we have an experimentally derived curve for the reaction of a system to a unit step function (Fig. 61), we may use this curve as a basis for constructing the reaction of the same system to a pulse of unit height and length τ (Fig. 62); then, squaring the ordinates of this curve (Fig. 63), and determining the area Q under the curve (Fig. 63), we find the equivalent system passband,

$$F_{экв} = \frac{Q}{2\tau^2}.$$

For example, for the curves shown in Figs. 61, 62, and 63

$$Q = 8{,}2\cdot 10^{-2} \text{ at } \tau = 0{,}4 \text{ sec}.$$

Thus

$$F_e = \frac{Q}{2\tau^2} = \frac{8{,}2\cdot 10^{-2}}{0{,}32} = 0{,}26 \text{ cps}.$$

[Footnote]

Manuscript Page No.

190 We shall not dwell on the well-known limits of applicability of the Fourier integral.

Manuscript Page No.

[List of Transliterated Symbols]

191 макс = maks = maximum = maximum

192 экв = ekv = ekvivalentnyy = equivalent

193 э = e = ekvivalentnyy = equivalent

APPENDIX 1

Values of Probability Integral

$$\Phi(y) = \sqrt{\frac{2}{\pi}} \int_{y}^{\infty} e^{-\frac{y^2}{2}} dy \qquad (36)$$

y	Φ(y)	y	Φ(y)
0,00	1,0000	1,15	0,2501
0,05	0,9601	1,20	0,2301
0,10	0,9203	1,25	0,2113
0,15	0,8808	1,30	0,1936
0,20	0,8415	1,35	0,1770
0,25	0,8026	1,40	0,1615
0,30	0,7642	1,45	0,1471
0,35	0,7263	1,50	0,1336
0,40	0,6892	1,55	0,1211
0,45	0,6527	1,60	0,1096
0,50	0,6171	1,65	0,0989
0,55	0,5823	1,70	0,0891
0,60	0,5485	1,75	0,0801
0,65	0,5157	1,80	0,0719
0,70	0,4839	1,85	0,0643
0,75	0,4533	1,90	0,0574
0,80	0,4237	1,95	0,0512
0,85	0,3953	2,00	0,0455
0,90	0,3681	2,25	0,0244
0,95	0,3421	2,50	0,0124
1,00	0,3173	2,75	0,0060
1,05	0,2937	3,00	0,00270
1,10	0,2713	3,50	0,00047
		4,00	0,00006

APPENDIX 2

Table of Functions φ(t) and Their Laplace Transforms

$L[\varphi(t)] = \varphi(p)$

1 № пп.	2 Функция φ(t)	3 Изображение φ(p)
1	4 Единичная ступенька при $t = 0$	$\frac{1}{p}$
2	$e^{-\alpha t}$	$\frac{1}{p+\alpha}$
3	$\frac{e^{-\alpha t} - e^{-\gamma t}}{\gamma - \alpha}$	$\frac{1}{(p+\alpha)(p+\gamma)}$
4	$\frac{(a_0-\alpha)e^{-\alpha t} - (a_0-\gamma)e^{-\gamma t}}{\gamma-\alpha}$	$\frac{p+a_0}{(p+\alpha)(p+\gamma)}$
5	$\frac{1}{\alpha\gamma} + \frac{\gamma e^{-\alpha t} - \alpha e^{-\gamma t}}{\alpha\gamma(\alpha-\gamma)}$	$\frac{1}{p(p+\alpha)(p+\gamma)}$
6	$\frac{a_0}{\alpha\gamma} + \frac{(a_0-\alpha)e^{-\alpha t}}{\alpha(\alpha-\gamma)} + \frac{(a_0-\gamma)e^{-\gamma t}}{\gamma(\gamma-\alpha)}$	$\frac{p+a_0}{p(p+\alpha)(p+\gamma)}$
7	$\frac{a_0}{\alpha\gamma} + \frac{\alpha^2 - a_1\alpha + a_0}{\alpha(\alpha-\gamma)}e^{-\alpha t} - \frac{\gamma^2 - a_1\gamma + a_0}{\gamma(\alpha-\gamma)}e^{-\gamma t}$	$\frac{p^2+a_1p+a_0}{p(p+\alpha)(p+\gamma)}$
8	$\frac{e^{-\alpha t}}{(\gamma-\alpha)(\delta-\alpha)} + \frac{e^{-\gamma t}}{(\alpha-\gamma)\cdot(\delta-\gamma)} + \frac{e^{-\delta t}}{(\alpha-\delta)\cdot(\gamma-\delta)}$	$\frac{1}{(p+\alpha)(p+\gamma)(p+\delta)}$

5 Продолжение

№ пп.	Функция $\varphi(t)$	Изображение $\varphi(p)$
9	$\frac{a_0-\alpha}{(\gamma-\alpha)\cdot(\delta-\alpha)}e^{-\alpha t}+$ $+\frac{a_0-\gamma}{(\alpha-\gamma)\cdot(\delta-\gamma)}e^{-\gamma t}+$ $+\frac{a_0-\delta}{(\alpha-\delta)\cdot(\gamma-\delta)}e^{-\delta t}$	$\frac{p+a_0}{(p+\alpha)(p+\gamma)(p+\delta)}$
10	$\frac{\alpha^2-a_1\alpha+a_0}{(\gamma-\alpha)(\delta-\alpha)}e^{-\alpha t}+$ $+\frac{\gamma^2+a_1\gamma+a_0}{(\alpha-\gamma)(\delta-\gamma)}e^{-\gamma t}+$ $+\frac{\delta^2+a_1\delta+a_0}{(\alpha-\delta)(\gamma-\delta)}e^{-\delta t}$	$\frac{p^2+a_1p+a_0}{(p+\alpha)(p+\gamma)(p+\delta)}$
11	$\frac{1}{\omega}\sin\omega t$	$\frac{1}{p^2+\omega^2}$
12	$\frac{1}{\omega}\cdot\mathrm{sh}\,\omega t$	$\frac{1}{p^2-\omega^2}$
13	$\cos\omega t$	$\frac{p}{p^2+\omega^2}$
14	$\mathrm{ch}\,\omega t$	$\frac{p}{p^2-\omega^2}$
15	$\frac{1}{\omega}\sqrt{a_0^2+\omega^2}\sin(\omega t+\psi)$ $\psi=\mathrm{arctg}\frac{\omega}{a_0}$	$\frac{p+a_0}{p^2+\omega^2}$
16	$\frac{1}{\omega^2}(1-\cos\omega t)$	$\frac{1}{p(p^2+\omega^2)}$

5 Продолжение

№ пп.	Функция $\varphi(t)$	Изображение $\varphi(p)$
17	$\frac{a_0}{\omega^2}-\frac{1}{\omega^2}\sqrt{a_0^2+\omega^2}\cos(\omega t+\psi)$ $\psi=\mathrm{arctg}\frac{\omega}{a_0}$	$\frac{p+a_0}{p(p^2+\omega^2)}$
18	$\frac{a_0}{\omega^2}-\frac{1}{\omega^2}\sqrt{(a_0-\omega^2)^2+a_1^2\omega^2}\times$ $\times\cos(\omega t+\psi)$ $\psi=\mathrm{arctg}\frac{a_1\omega}{a_0-\omega^2}$	$\frac{p^2+a_1p+a_0}{p(p^2+\omega^2)}$
19	$\frac{1}{\omega}e^{-\alpha t}\sin\omega t$	$\frac{1}{(p+\alpha)^2+\omega^2}$
20	$\frac{1}{\omega}\sqrt{(a_0-\alpha)^2+\omega^2}\times$ $\times e^{-\alpha t}\sin(\omega t+\psi)$ $\psi=\mathrm{arctg}\frac{\omega}{a_0-\alpha}$	$\frac{p+a_0}{(p+\alpha)^2+\omega^2}$
21	$e^{-\alpha t}\cos\omega t$	$\frac{p+\alpha}{(p+\alpha)^2+\omega^2}$
22	$\frac{1}{\omega_0^2}+\frac{1}{\omega\cdot\omega_0}e^{-\alpha t}\sin(\omega t-\psi)$ $\psi=\mathrm{arctg}\frac{\omega}{-\alpha};\quad \omega_0^2=\alpha^2+\omega^2$	$\frac{1}{p[(p+\alpha)^2+\omega^2]}$
23	$\frac{a_0}{\omega_0^2}+\frac{1}{\omega\cdot\omega_0}\sqrt{(a_0-\alpha)^2+\omega^2}\times$ $\times e^{-\alpha t}\sin(\omega t+\psi)$ $\psi=\mathrm{arctg}\frac{\omega}{a_0-\alpha}-\mathrm{arctg}\frac{\omega}{-\alpha};$ $\omega_0^2=\alpha^2+\omega^2$	$\frac{p+a_0}{p[(p+\alpha)^2+\omega^2]}$

5 Продолжение

№ п/п	2 Функция $\varphi(t)$	3 Изображение $\varphi(p)$
24	$\frac{a_0}{a_0^2} + \frac{1}{\omega \cdot a_0}\sqrt{(\alpha^2-\omega^2-a_1\alpha+a_0)^2+\omega^2(a_1-2\alpha)^2}\times$ $\times e^{-\alpha t}\sin(\omega t+\psi)$ $\psi=\operatorname{arctg}\frac{\omega(a_1-2\alpha)}{\alpha^2-\omega^2-a_1\alpha+a_0}-$ $-\operatorname{arctg}\frac{\omega}{-\alpha}$; $\omega_0^2=\alpha^2+\omega^2$	$\frac{p^2+a_1p+a_0}{p[(p+\alpha)^2+\omega^2]}$
25	$\frac{e^{-\gamma t}}{(\gamma-\alpha)^2+\omega^2}+$ $+\frac{1}{\omega}\sqrt{(\gamma-\alpha)^2+\omega^2}\,e^{-\alpha t}\sin(\omega t-\psi)$ $\psi=\operatorname{arctg}\frac{\omega}{\gamma-\alpha}$	$\frac{1}{(p+\gamma)[(p+\alpha)^2+\omega^2]}$
26	$\frac{a_0-\gamma}{(\alpha-\gamma)^2+\omega^2}e^{-\gamma t}+$ $+\frac{1}{\omega}\sqrt{\frac{(a_0-\alpha)^2+\omega^2}{(\gamma-\alpha)^2+\omega^2}}\times$ $\times e^{-\alpha t}\sin(\omega t+\psi)$ $\psi=\operatorname{arctg}\frac{\omega}{a_0-\alpha}-\operatorname{arctg}\frac{\omega}{\gamma-\alpha}$	$\frac{p+a_0}{(p+\gamma)[(p+\alpha)^2+\omega^2]}$
27	$\frac{\gamma^2-a_1\gamma+a_0}{(\alpha-\gamma)^2+\omega^2}e^{-\gamma t}+$ $+\frac{1}{\omega}\sqrt{\frac{(\alpha^2-\omega^2-a_1\alpha+a_0)^2}{(\gamma-\alpha)^2+\omega^2}+\frac{\omega^2(a_1-2\alpha)^2}{(\gamma-\alpha)^2+\omega^2}}\times$ $\times e^{\alpha t}\sin(\omega t+\psi)$;	$\frac{p^2+a_1p+a_0}{(p+\gamma)[(p+\alpha)^2+\omega^2]}$

5 Продолжение

№ п/п	2 Функция $\varphi(t)$	3 Изображение $\varphi(p)$
	$\psi=\operatorname{arctg}\frac{\omega(a_1-2\alpha)}{\alpha^2-\omega^2-a_1\alpha+a_0}-$ $-\operatorname{arctg}\frac{\omega}{\gamma-\alpha}$	
28	$\frac{1}{\sqrt{(\omega_0^2-\Omega^2)^2+4\alpha^2\Omega^2}}\times$ $\times\left[\frac{1}{\Omega}\sin(\Omega t-\psi_1)+\right.$ $\left.+\frac{1}{\omega}e^{-\alpha t}\sin(\omega t-\psi_2)\right]$; $\psi_1=\operatorname{arctg}\frac{2\alpha\Omega}{\omega_0^2-\Omega^2}$; $\psi_2=\operatorname{arctg}\frac{-2\alpha\omega}{\alpha^2-\omega^2+\Omega^2}$; $\omega_0^2=\alpha^2+\omega^2$	$\frac{1}{(p^2+\Omega^2)[(p+\alpha)^2+\omega^2]}$
29	$\frac{1}{\Omega}\sqrt{\frac{a_0^2+\Omega^2}{(\omega_0^2-\Omega^2)^2+4\alpha^2\Omega^2}}\times$ $\times\sin(\Omega t+\psi_1)+$ $+\frac{1}{\omega}\sqrt{\frac{(a_0-\alpha)^2+\omega^2}{(\omega_0^2-\Omega^2)^2+4\alpha^2\Omega^2}}\times$ $\times e^{-\alpha t}\sin(\omega t+\psi_2)$; $\psi_1=\operatorname{arctg}\frac{\Omega}{a_0}-\operatorname{arctg}\frac{2\alpha\Omega}{\omega_0^2-\Omega^2}$; $\psi_2=\operatorname{arctg}\frac{\omega}{a_0-\alpha}-$ $-\operatorname{arctg}\frac{-2\alpha\omega}{\alpha^2-\omega^2+\Omega^2}$; $\omega_0^2=\alpha^2+\omega^2$	$\frac{p+a_0}{(p^2+\Omega^2)[(p+\alpha)^2+\omega^2]}$

5 Продолжение

№ пп.	2 Функция $\varphi(t)$	3 Изображение $\varphi(p)$
30	$\frac{1}{\Omega}\sqrt{\frac{(a_0-\Omega^2)^2+a_1\Omega^2}{(\omega_0^2-\Omega^2)+4\alpha^2\Omega^2}}\times$ $\times\sin(\Omega t+\psi_1)+$ $+\frac{1}{\omega}\sqrt{\frac{(\alpha^2-\omega^2-a_1\alpha+a_0)^2+}{(\omega_0^2-\Omega^2)^2+4\alpha^2\Omega^2}}$ $\overline{+\omega^2(a_1-2\alpha)^2}$ $\frac{}{(\omega_0^2-\Omega^2)^2+4\alpha^2\Omega^2}\,e^{-\alpha t}\sin(\omega t+\psi_2)$; $\psi_1=\operatorname{arctg}\frac{a_1\Omega}{a_0-\Omega^2}-$ $-\operatorname{arctg}\frac{2\alpha\Omega}{\omega_0^2-\Omega^2}$; $\psi_2=\operatorname{arctg}\frac{\omega(a_1-2\alpha)}{\alpha^2-\omega^2-a_1\alpha+a_0}-$ $-\operatorname{arctg}\frac{-2\alpha\omega}{\alpha^2-\omega^2+\Omega^2}$; $\omega_0^2=\alpha^2+\omega^2$	$\frac{p^2+a_1p+a_0}{(p^2+\Omega^2)[(p+\alpha)^2+\omega^2]}$
31	t	$\frac{1}{p^2}$
32	$\frac{1}{(n-1)!}t^{n-1}$, где n — целое положительное число	$\frac{1}{p^n}$
33	$\frac{e^{-\alpha t}+\alpha t-1}{\alpha^2}$	$\frac{1}{(p+\alpha)p^2}$
34	$\frac{a_0-\alpha}{\alpha^2}e^{-\alpha t}+\frac{a_0}{\alpha}t+\frac{\alpha-a_0}{\alpha^2}$	$\frac{p+a_0}{(p+\alpha)p^2}$
35	$\frac{\alpha^2-a_1\alpha+a_0}{\alpha^2}e^{-\alpha t}+$ $+\frac{a_0}{\alpha}t+\frac{a_1\alpha-a_0}{\alpha^2}$	$\frac{p^2+a_1p+a_0}{(p+\alpha)p^2}$

5 Продолжение

№ пп.	2 Функция $\varphi(t)$	3 Изображение $\varphi(p)$
36	$te^{-\alpha t}$	$\frac{1}{(p+\alpha)^2}$
37	$[(a_0-\alpha)t+1]e^{-\alpha t}$	$\frac{p+a_0}{(p+\alpha)^2}$
38	$\frac{1}{(n-1)!}t^{n-1}e^{-\alpha t}$, где n — целое положительное число	$\frac{1}{(p+\alpha)^n}$
39	$e^{-\alpha t}\sum_{k=0}^{n}\frac{n!(-\alpha)^k}{(n-k)!(k!)^2}t^k$, где n — целое положительное число	$\frac{p^n}{(p+\alpha)^{n+1}}$
40	$\frac{1}{\omega_0^2}\left[t-\frac{2\alpha}{\omega_0^2}+\right.$ $\left.+\frac{1}{\omega}\cdot e^{-\alpha t}\sin(\omega t-\psi)\right]$; $\psi=2\operatorname{arctg}\frac{\omega}{-\alpha}$; $\omega_0^2=\omega^2+\alpha^2$	$\frac{1}{[(p+\alpha)^2+\omega^2]\cdot p^2}$
41	$\frac{1}{(\alpha-\gamma)^2+\omega^2}\left[te^{-\gamma t}+\right.$ $+\frac{2(\gamma-\alpha)}{(\alpha-\gamma)^2+\omega^2}e^{-\gamma t}+$ $\left.+\frac{1}{\omega}e^{-\alpha t}\sin(\omega t-\psi)\right]$; $\psi=2\operatorname{arctg}\frac{\omega}{\gamma-\alpha}$	$\frac{1}{(p+\gamma)^2[(p+\alpha)^2+\omega^2]}$

5 Продолжение

1 № пп.	2 Функция $\varphi(t)$	3 Изображение $\psi(p)$
42	$\frac{\gamma^2 - a_1\gamma + a_0}{(\alpha-\gamma)^2+\omega^2} - t e^{-\gamma t} + \left[\frac{(\alpha-\gamma)^2+\omega^2](a_1-2\gamma)}{[(\alpha-\gamma)^2+\omega^2]^2} - \frac{2(\alpha-\gamma)(\gamma^2-a_1\gamma+a_0)}{[(\alpha-\gamma)^2+\omega^2]^2}\right] e^{-\gamma t} + \frac{\sqrt{(\alpha^2-a_1\alpha+a_0)^2+\omega^2(a_1-2\alpha)^2}}{\omega[(\gamma-\alpha)^2+\omega^2]} e^{-\alpha t}\sin(\omega t+\psi)$ $\psi = \operatorname{arctg}\frac{\omega(a_1-2\alpha)}{\alpha^2-\omega^2-a_1\alpha+a_0} - 2\operatorname{arctg}\frac{\omega}{\gamma-\alpha}$	$\frac{p^2+a_1p+a_0}{(p+\gamma)^2[(p+\alpha)^2+\omega^2]}$

[Key to Appendix 2]: 1) Number; 2) function $\varphi(t)$; 3) transform $\varphi(p)$; 4) unit step function at; 5) continuation; 6) where n is a positive integer.

More detailed tables of the functions and their Laplace transforms are given in the following books:

1. M.F. Gardner and Dzh.L. Berns, Transient Processes in Linear Systems, State Technical and Theoretical Press, 1951.

2. V.A. Ditkin and P.I. Kuznetsov, Handbook of Operational Calculus, State Technical and Theoretical Literature Press, 1951.

Note. In their handbook, V.A. Ditkin and P.I. Kuznetsov show functions f(t) appearing at the output of systems having as transfer function the expression F (p) when a unit step function acts on the systems. Thus, the functions f(t) given here have transforms F(p)/p, rather than F(p), which should be kept in mind when this handbook is used.

REFERENCES

1. Van der Pol', B. and Bremmer, Kh., Operatsionnoye ischisleniye na osnove dvustoronnego preobrazovaniya Laplasa [Operational Calculus Based on Inverse Laplace Transformation], IL [Foreign Literature Publishing House], 1952.
2. Osnovy avtomaticheskogo regulirovaniya [Fundamentals of Automatic Control], Kollektiv avtorov pod red. prof. Solodovnikova, V.V. [Collective of Authors, Edited by Prof. V.V. Solodovnikov], Mashgiz [State Scientific and Technical Publishing House of Literature on Machinery], 1954.
3. Kharkevich, A.A., Spektry i analiz [Spectra and Analysis], GITTL [State Publishing House of Technical and Theoretical Literature], 1957.
4. Kharkevich, A.A., Teoreticheskiye osnovy radiosvyazi [Theoretical Foundations of Radio Communication], GITTL, 1957.
5. Voronov, A.A., Elementy teorii avtomaticheskogo regulirovaniya [Elements of the Theory of Automatic Control], Voyenizdat [Military Publishing House], 1954.
6. Gardner, M.F. and Beris, Dzh. L., Perekhodnyye protsessy v lineynykh sistemakh s sosredotochennymi postoyannymi [Transient Processes in Linear Systems With Lumped Constants]. GITTL. 1951.
7. Dzheyms, Kh., Nikol's, N. and Filips, R., Teoriya sledyashchikh sistem [Theory of Follow-Up Systems], IL [Publishing House of Foreign Literature], 1951.
8. Lokk, A.S., Upravleniye snaryadami [Missile Guidance], GITTL. 1957.
9. Bunimovich, V.I., Flyuktuatsionnyye protsessy v radiopriyemnykh ustroystvakh [Fluctuation Processes in Radio Receivers], Sovetskoye radio [Soviet Radio], 1951.
10. Kotel'nikov, V.A., Teoriya potentsial'noy pomekhoustoychivosti

[Theory of Potential Noise Suppression], GEI [State Power Engineering Publishing House], 1956.

11. Bennet, U.R., Osnovnyye ponyatiya i metody teorii shumov v radiotekhnike [Basic Concepts and Methods of the Theory of Noise in Radio Engineering], Sovetskoye radio [Soviet Radio], 1957.
12. Vudvard, F.M., Teoriya veroyatnostey i teoriya informatsii s primeneniyem k radiolokatsii [Theory of Probability and Information Theory With Application to Radar], Sovetskoye radio, 1955.
13. Tsypkin, Ya.Z., Perekhodnyye i ustanovivshiyesya protsessy v impul'snykh skhemakh [Transient and Steady-State Processes in Pulse Circuits], GEI, 1951.